Dissertation zur Erlangung des Doktorgrades
der Fakultät für Chemie und Pharmazie
der Ludwig-Maximilians-Universität München

Controlled nucleation and heat flux measurements as innovative technologies for freeze-drying

Ilona Elisabeth Vollrath
geb. Konrad

aus Weißenhorn, Deutschland
2018

Erklärung

Diese Dissertation wurde im Sinne von § 7 der Promotionsordnung vom 28. November 2011 von Herrn Prof. Dr. Gerhard Winter betreut.

Eidesstattliche Versicherung

Diese Dissertation wurde eigenständig und ohne unerlaubte Hilfe erarbeitet.

München, den 29.10.2018

Ilona Elisabeth Vollrath

Dissertation eingereicht am: 29.10.2018

1. Gutachter: Prof. Dr. Gerhard Winter

2. Gutachter: Prof. Dr. Wolfgang Frieß

Mündliche Prüfung am: 06.12.2018

FOR MORITZ AND MY PARENTS

ACKNOWLEDGEMENTS

The presented thesis was prepared between March 2013 and June 2017 at the facilities of Coriolis Pharma in Martinsried in collaboration with the Department of Pharmacy, Pharmaceutical Technology and Biopharmaceutics at the Ludwig-Maximilians-University (LMU) Munich under the supervision of Dr. Andrea Hawe and Dr. Angelika Freitag from Coriolis Pharma and Prof. Dr. Gerhard Winter from the LMU.

First, I want to express my deepest gratitude to Prof. Dr. Gerhard Winter from the LMU and Dr. Andrea Hawe and Dr. Michael Wiggenhorn from Coriolis Pharma who gave me the opportunity to work on this project. I also want to thank you very much for the possibility to present my work at several conferences worldwide.

Additionally, I want to greatly thank Prof. Dr. Gerhard Winter, my first supervisor from the LMU, for his excellent and continuous scientific input and encouraging personal support throughout all phases of this work. I am deeply grateful for your guidance and the effort you put into my scientific and personal development.

My deepest gratitude goes to Dr. Andrea Hawe, my first supervisor from Coriolis Pharma, for her outstanding and reliable input and support. Thank you for always being personally available for any issues. I am very grateful for the valuable discussions your honest advice and your mentoring – scientifically and personally.

My second supervisor from the university, Prof. Dr. Wolfgang Frieß, is greatly acknowledged for his helpful suggestions and valuable contributions to our publications and the project. I also want to thank you for taking over the co-referee. Furthermore, I want to thank you and Prof. Dr. Winter for keeping up the great team spirit by various social activities.

Dr. Angelika Freitag, my second supervisor from Coriolis Pharma, is kindly acknowledged for her scientific and personal mentoring, for the interesting discussions and her guidance. Thank you for always motivating me especially in the challenging phases of this project.

I highly appreciate the collaboration with T.N. Thompson from Millrock Technologies. Thank you very much for all the exciting discussions and ideas and the great technical support. Additionally, Stefan Piatkowski from Piatkowski Forschungsgeräte is acknowledged for his technical support with the Millrock Magnum freeze-dryer and the FreezeBooster®. Futhermore, I would like to express my gratitude to Johann Kaltenegger from Linde AG, Eugen Wexler and Philippe Selsis from IMA Life for their technical help with the VERISEQ® nucleation system and the interesting discussions. I also want to thank Christian Minke for taking uncounted numbers of SEM images.

Victoria Pauli is kindly acknowledged for her outstanding work during her master thesis. It was a pleasure to work, discuss, laugh and sometimes even cry with you. Likewise, I want to thank Laura Benz and Martin Schubert for their work and contribution to this project.

It is all about people and a lot of people made the work on the project and my time at the university and at Coriolis Pharma memorable. At first, I want to express my deepest gratitude to my office mates: First and foremost, Daniel Weinbuch and Dr. Ariadna Martos, thank you so much for always having a motivating word, for the great discussions, thoughts and ideas and for becoming very good friends. Just as much, I want to thank Matthias Wurm, Dr. Wendelin Koch and Marco Carfagna. It was a great pleasure to share the “brain office” with you. Furthermore, I want to greatly thank Dr. Benjamin Werner, who was my lab mate at the LMU for always being helpful and keeping the lab organized.

Next, I want to thank all my colleagues from Coriolis Pharma and the LMU for creating a comfort zone that enabled the productive working atmosphere while having fun. The social events and all other coming togethers were great fun. It is difficult to mention someone in particular, but I want to express special thanks to my Coriolis colleagues Dr. Thomas Bosch, Franziska Scholbeck, Katharina Kolland, Orhan Causevic, Dr. Alexandra Kafka, Dr. Silke Reiffert, Dr Stefan Heindl, Dr. Julia Eckl, Mirjam Salazar, and Dr. Tim Menzen from Coriolis; thank you all for your help and support. In the same way, I am grateful to Dr. Raimund Geidobler, Randy Wanner, Kay Strüver, Dr. Matthias Lucke, Dr. Marie-Paule Even, Dr. Christoph Korpus, Dr. Robert Liebner, Dr. Roman Mathaes, Dr. Stefanie Funke, Dr. Elisa Agostini, Dr. Laura Engelke,

Dr. Ellen Köpf, Dr. Jacqueline Horn, Ayla Tekbudak, and Alice Hirschmann from the LMU; thank you all for the great “Doktoranden Stammtische”, barbecues, hiking and skiing trips.

Above all, I deeply thank my family and friends. Without your continuous encouragement, advice and motivation this work would not have been successful. Foremost, I want to thank my parents, Friederike and Alois, my brother, Michael, together with his wife Johanna, and my parents-in-law, Ulrike and Jürgen, for the support they gave me over all the years and for simply being my family. Just as much, I am deeply grateful to my closest friends Sonja, Julia, Nadja and Sandra for our continuous and precious friendship. At the end, I want to express my deepest gratitude to my husband, Moritz. Thank you for your motivating words, your patience, your continuous encouragement and above all, for your love.

TABLE OF CONTENTS

CHAPTER I

I. GENERAL INTRODUCTION AND OBJECTIVES OF THE THESIS

I.1 GENERAL INTRODUCTION

In 2002, the Food and Drug Administration (FDA) announced the “Pharmaceutical Current Good Manufacturing Practices (cGMP) for the 21st Century” initiative to modernize and coordinate the regulation of pharmaceutical manufacturing [1]. This cGMP initiative should create a regulatory framework that encourages and enables the pharmaceutical industry to early adopt modern tools and facilitate the implementation of robust manufacturing processes that ensure continuously high product quality. Furthermore, industry`s “application of modern quality management techniques, including implementation of quality system approaches” [1] should be facilitated. In context of this cGMP initiative, the FDA announced and published several “Guidance for Industry” papers, i.a. “PAT - A Framework for Innovative Pharmaceutical Development, Manufacturing, and Quality Assurance” [2] and “Quality Systems Approach to Pharmaceutical cGMP Regulations” [3]. Based on the cGMP initiative with its relating guidance documents and in line with ICH Q8 (2009) [4], “Quality by design” (QbD) for pharmaceuticals was introduced. In contrast to the traditionally applied end product testing approach, QbD promotes to build quality into the product by design rather than testing it at the end [5]. According to ICH Q8 (2009), QbD is defined as “A systematic approach to development that begins with predefined objectives and emphasizes product and process understanding and process control, based on sound science and quality risk management” [4]. This approach, based on scientific knowledge, thorough process and product understanding and control accompanied by appropriate quality risk management principles, can enhance pharmaceutical product development [5]. Two critical elements of QbD are the definition of a *Design Space* and the application of *Process Analytical Technology (PAT)* tools. According to ICH Q8 (R2), a Design Space is defined as “The multidimensional combination and interaction of input variables (e.g., material attributes) and process parameters that have been demonstrated to provide assurance of quality” [4]. Consequently, working in the ranges of the Design Space is not considered as a change by the authorities and does not require a post approval change request [4].

In 2005, a QbD pilot program for small molecules started, followed by a comparable pilot program for biologics. By mid 2011, 11 design space approvals were submitted for small molecules and none for biologics. The first biologic approved by the FDA with design space was Genentech`s Gazyva in 2013. The complexity of the manufacturing process for a biologic reflects the challenge of defining the predefined objectives and a design space. This might be one reason, why the implementation of QbD for biologics seems to require more time and discussion than for small molecules. For example, it is more straightforward to validate a chemical synthesis compared to a cell culture production process [6].

Biologics, e.g. proteins, require a unique 3-D structural conformation for their activity. Furthermore, proteins are prone to several degradation processes during manufacturing, e.g. deamidation, oxidation, hydrolysis, aggregation, and denaturation. Due to these physical and chemical instabilities, biological products need to be administered parenterally and pose challenges for adequate shelf life time of the final product. Thus, a lot of effort was put into formulation development [6]. However, if a biological product does not exhibit enough stability in liquid formulation, freeze-drying, also named as lyophilization, has become the method of choice to stabilize these temperature sensitive products [7, 8].

Freeze-drying is based on heat and mass transfer principles and fits well into the QbD concept [9]. During a freeze-drying process, comprising the freezing, primary and secondary drying step, primary drying is the longest and most critical step, which can result in compromised product quality, e.g. by collapse, resulting in higher residual moisture. As collapse occurs if the product temperature (T_p) exceeds the critical collapse temperature (T_c), freeze-drying requires process specific optimization to ensure that T_p does not exceed T_c during primary drying and that primary drying is completed [8]. Therefore, design spaces for primary drying intend to keep T_p below T_c by a safe margin [9]. However, one major challenge for this approach is that T_p cannot directly be controlled. T_p depends on various factors, mainly the set shelf temperature (T_s) and the chamber pressure (p_c), but also on the so-called vial heat transfer coefficient (K_v) and the mass flow resistance (e.g. cake resistance or stopper resistance). Both academia and industry have

been interested in understanding the correlation between T_s, p_c, K_v and the resulting T_p to optimize freeze-drying processes. With the above mentioned QbD initiative, the need for a thorough process understanding increased. Various studies and approaches to optimize and model freeze-drying cycles have been performed [10-15].

Besides maintaining product quality, the optimization of freeze-drying cycles with respect to economic drying times was another aim. This means that the safety margin between T_p and T_c should be as small as possible and primary drying as fast as possible. Thus, the accurate monitoring of T_p and the determination of the end of primary and secondary drying are crucial to assure product quality and process economy [8]. Consequently, the need for rigorous product monitoring and process analytical technology (PAT) tools during cycle development is high. In the field of PAT tools for freeze-drying, extensive research has been performed. Tools like thermocouples [16, 17], Manometric Temperature Measurement (MTM) [18-21], Near-Infrared spectroscopy [22-26], Raman spectroscopy [22, 27], Tunable diode laser absorption spectroscopy (TDLAS) [28-30], or an optical fiber system (OFS) [31] have been introduced and studied. Within the introduction of Chapter V, some of the named PAT tools are discussed in more detail.

In the context of QbD and the request for new PAT tools, two new technologies for freeze-drying gained interest in the last years: controlled ice nucleation (CN) and heat flux measurements. These two technologies raised great expectations for freeze-drying cycle optimization and control and their potential benefits have been discussed.

CONTROLLED NUCLEATION (CN)

CN enables the control of the ice nucleation temperature (T_N) (otherwise a random event), which gives more control over the freeze-drying process. Additionally, T_N significantly impacts process performance: High T_N results in larger ice crystals, which leave behind larger pores during sublimation and thus lower product resistance. This leads to reduced primary drying times. However, larger pores reciprocally result in a lower specific surface area (SSA), which hinders

desorption during secondary drying and can cause a higher residual moisture of the product. Vice versa, low T_N causes small ice crystals, resulting in small pores and longer primary drying times, but faster desorption during secondary drying [32, 33].

Furthermore, CN could help to ensure product quality during scale-up. As T_N is typically higher in a development environment where more particles can be introduced into the product that function as nucleation sites, T_p can be lower due to larger pores causing less resistance. For successful process transfer, it needs to be considered that the product in an almost particle free production environment tends to nucleate at lower T_N and thus T_p will be higher, which poses the risk for collapse. With CN, T_N could be defined and kept the same in development and production scale.

Another benefit of CN that has been discussed is its impact on homogeneity within a batch and between batches. The stochastic nature of ice nucleation could introduce e.g. vial-to-vial heterogeneities and as mentioned above cause variability between batches. With the control of T_N, all vials of a batch nucleate at the same time, at the same temperature; consequently, the drying behavior and product homogeneity should be improved. Up to now, two approaches to assess batch homogeneity, in this context, have been reported: (i) analysis of individual vials and (ii) batch representative methods. Rambhatla et al. [32] and Fang et al. [34], for example, compared the standard deviation of BET measurements (n=3) and LDH activity (n=6), respectively, of CN processed lyophilizates with randomly nucleated (RN) products to assess batch homogeneity. Given the small number of replicates, although taken from critical positions within the freeze-dryer (edge vials and center vials), extrapolation to a full batch could be challenging. In contrast, Passot et al. [35] or Oddone et al. [36] determined the average drying behavior of a complete batch by comparing the absolute value of the slope of the Pirani gauge profile (n=100) or by comparing the onset-offset time of the pressure ratio curve (n=70), respectively. One drawback of this method is that it only allows for determination of the homogeneity at the end of primary drying but not of the final product.

Besides the already mentioned reduction of primary drying time, facilitation of process transfer and improvement of intra-and inter-batch homogeneity, it was also suggested that the change in SSA could impact product quality. One the one hand, as pointed out above, a low SSA hinders desorption during secondary drying and could result in higher residual moisture of the product if the process is not adjusted. On the other hand, a reduced SSA exposes the protein to a smaller interface, which could theoretically be beneficial for interface sensitive proteins. This was confirmed by Schersch et al. [37-39], who found that a low SSA generated by collapse can be beneficial for the stability of pharmaceutically relevant proteins (e.g. monoclonal antibody type IgG1, Actilyse®, LDH). Another interesting aspect of a lyophilized product with a low SSA is the impact on reconstitution behavior. Geidobler et al. [40] applied controlled nucleation to highly concentrated protein formulations, as those often result in very long reconstitution times, and showed that besides reducing primary drying time, the resulting large pores could also improve wetting of the cake and thus shorten reconstitution times of a highly concentrated monoclonal antibody (mAb) formulation.

Today, various methods to induce CN are commercially available. The two key techniques are ice fog methods, e.g. FreezeBooster® (Millrock Technology), LyoCoN (Martin Christ), and VERISEQ® nucleation system (IMA life/Linde) and methods based on pressure changes, such as ControLyo™ (SP Scientific), SynchroFreeze (Hof) and a recently published method from OPTIMA pharma [41]. In a review, Geidobler et al. [42] summarized and discussed the different approaches to induce ice nucleation considering e.g. scalability, need of retrofitting, application to aseptic environments and efficiency.

HEAT FLUX MEASUREMENTS

Heat flux sensors have been used by e.g. plastics-, automotive-, or solar energy industry [43], and are now introduced to pharmaceutical freeze-drying, by Millrock Technology Inc., as a new approach to monitor T_p and process end points by measuring the heat flux between the freeze-dryer shelf and vial(s) [44]. Generally, these sensors are able to measure heat flux

resulting from different heat transfer, e.g. conductive, convective, and radiation heat transfer [43]. As, for the application in freeze-drying, the sensor is placed between the vials and the shelf, it mainly measures heat transferred by conduction and convection [44].

Theoretically, with heat flux measurements all steps of a freeze-drying process could be monitored, as throughout the freeze-drying cycle heat transfer always takes place. However, the heat flux direction changes. During freezing, the heat is transferred from the warmer vial to the colder shelf surface, which results in a negative heat flux. While, during primary and secondary drying, heat flux is positive as heat flows from the shelf to the vials.

As heat flux can only be determined as long as there is a temperature difference between heat source and heat sink, heat flux measurements could also be used to determine the end of primary drying, as heat flux approaches zero when the vials reach T_s. Additionally, heat flux measurements could indicate the end of ice crystallization during freezing by a change in heat flux direction, because the generated exothermic heat warms the vial during ice formation, whereas the vial temperature approaches the T_s after the crystallization event [45].

Moreover, when heat flux data are combined with thermocouple data, important parameters for process development and control such as the vial heat transfer coefficient (K_v) can be assessed. Currently, time consuming gravimetrical approaches are used for K_v determination. Heat flux measurements could provide a fast, simple and non-invasive alternative. However, it should be noted that the vial heat transfer coefficient determined by heat flux measurement (K_v(heat flux)) is based mainly on conduction and convection heat and thus differs from the K_v determined by gravimetrical measurements (K_v(gravimetrically)) and calculated as described by Pikal et al. [10], which takes, in addition to conduction and convection, also radiation into account. Additionally, mass flow per vial, mass flow of the entire batch, fraction of removed mass and the product resistance (R_p) could be calculated based on determined heat flux data. Ultimately, from R_p, T_p at the sublimation interface could be calculated.

Besides process monitoring, it was also suggested, that the heat flux can be used to control freeze-drying processes by adjusting the shelf temperature set point based on the measured heat flux in order to achieve maximum heat transfer while T_p is kept below the critical product temperature.

I.2 OBJECTIVES AND OUTLINE OF THE THESIS

The claimed potential of CN to improve product quality (by a low SSA) and facilitate process transfer raised great expectations for the application of CN for QbD. However, in practice, we face some challenges when we want to reach these goals by CN, e.g. how to non-destructively monitor successful performed CN and validate CN processes. As not every method can easily be implemented in development and production scale freeze-dryers, the question arises if different CN methods result in comparable product quality attributes. Furthermore, it is of high interest if besides the reduction in reconstitution time, CN could improve other product quality attributes.

The first part of this thesis, Chapter II to IV, comprises the critically and systematically assessment of the open challenges and questions regarding CN by using different ice fog techniques. In **Chapter II**, the objective was to combine CN with aggressive primary drying and investigate the impact of this combination on certain product properties, e.g. cake appearance, morphology, specific surface area, residual moisture, and reconstitution time of highly concentrated protein formulations.

In **Chapter III**, the question was assessed, if besides the reduction in reconstitution time, CN could be beneficial for other product quality attributes related to a low SSA, such as physico-chemical stability of a mAb. The performed study comprises the long-term storage of two mAbs formulated at a high and low concentration in a sucrose-based formulation. The current state of the art to protect proteins from interfaces is the use of polysorbate [46-48], thus, the effect of CN in formulations with and without polysorbate was investigated additionally.

In **Chapter IV**, challenges related to the practical application of CN were addressed. First, to solve the question how to non-destructively monitor successfully performed controlled nucleation and thus, be able to validate a CN process, frequency modulated spectroscopy was evaluated as PAT tool for CN success and as a method to study batch homogeneity. Second, the question if different ice fog methods result in comparable product quality attributes was

evaluated by comparing the optical appearance, microscopic structure, SSA and RM of lyophilizates generated by three different ice fog methods. Moreover, based on findings of the study presented in Chapter III, we investigated factors that, besides T_N, impact the SSA of a lyophilizate, when CN is applied.

In the second part of this thesis, **Chapter V**, heat flux measurements were evaluated regarding their usage as a new PAT tool for freeze-drying. Therefore, the performance and suitability of heat flux measurements for freeze-drying process monitoring under pharmaceutically relevant conditions was assessed. Heat flux measurements were compared to current state of the art techniques to monitor freeze-drying processes, such as comparative pressure measurement thermocouple readings or Karl Fischer titration. Furthermore, the accuracy of the determined K_v(heat flux) was investigated by calculating the product temperature out of K_v(heat flux) and comparing the calculated product temperature with actual thermocouple readings.

I.3 REFERENCES

[1] *Pharmaceutical cGMPs for the 21st century - a risk-based approach, Final Report*. US Food and Drug Administration, 2004. Available from: https://www.fda.gov/downloads/Drugs/DevelopmentApprovalProcess/Manufacturing/QuestionsandAnswersonCurrentGoodManufacturingPracticescGMPforDrugs/UCM176374.pdf. Acceessed: 26 August 2018.

[2] *Guidance for Industry: PAT — A Framework for Innovative Pharmaceutical Development, Manufacturing, and Quality Assurance* US Food and Drug Administration, 2004. Available from: https://www.fda.gov/downloads/Drugs/GuidanceComplianceRegulatoryInformation/Guidances/UCM070305.pdf. Acceessed: 26 August 2018.

[3] *Guidance for Industry: Quality Systems Approach to Pharmaceutical cGMP Regulations*. US Food and Drug Administration, 2006. Available from: https://www.fda.gov/downloads/Drugs/GuidanceComplianceRegulatoryInformation/Guidances/UCM070337.pdf. Acceessed: 26 August 2018.

[4] *Pharmaceutical Development Q8 (R2)*. (ICH), I.C.o.H., 2009. Available from: http://www.ich.org/fileadmin/Public_Web_Site/ICH_Products/Guidelines/Quality/Q8_R1/Step4/Q8_R2_Guideline.pdf. Acceessed: 28 August 2018.

[5] Agarabi, C., Mansoor, A.K., and Rakhi, B.S., *Challenges and Opportunities for Biotech Quality by Design* in *Quality by Design for Biopharmaceutical Drug Product Development*, Jameel, F., et al., Editors. 2015, Springer Science+Business Media.DOI 10.1007/987-1-4939-2316-8_1.

[6] Martin-Moe, S. and Nast, C., *An Overview of Quality by Design for Drug Product*, in *Quality by Design for Biopharmaceutical Drug Product Development*, Jameel, F., et al., Editors. 2015, Springer Science+Business Media.DOI 10.1007/987-1-4939-2316-8_4.

[7] Patel, S.M., Doen, T., and Pikal, M.J., *Determination of End Point of Primary Drying in Freeze-Drying Process Control.* AAPS PharmSciTech, 2010. 11(1): p. 73-84.

[8] Jameel, F. and Searles, J., *Development and Optimization of the Freeze-Drying Processes*, in *Formulation and Process Development Strategies for Manufacturing Biopharmaceuticals*. 2010, John Wiley & Sons, Inc. p. 763-796.10.1002/9780470595886.ch30.

[9] Patel, S.M. and Pikal, M.J., *Lyophilization process design space.* J. Pharm. Sci., 2013. 102(11): p. 3883--7.

[10] Pikal, M.J., Roy, M.L., and Shah, S., *Mass and heat transfer in vial freeze-drying of pharmaceuticals: Role of the vial.* J. Pharm. Sci., 1984. 73(9): p. 1224--1237.

[11] Pikal, M.J., *Use of laboratory data in freeze drying process design: heat and mass transfer coefficients and the computer simulation of freeze drying.* J. Parenter. Sci. Technol., 1985. 39(3): p. 115--39.

[12] Fissore, D., Pisano, R., and Barresi, A.A., *A Model-Based Framework to Optimize Pharmaceuticals Freeze Drying.* Drying Technology, 2012. 30(9): p. 946-958.

[13] Fissore, D., Pisano, R., and Barresi, A.A., *On the Methods Based on the Pressure Rise Test for Monitoring a Freeze-Drying Process.* Drying Technology, 2010. 29(1): p. 73-90.

[14] Pisano, R., Fissore, D., and Barresi, A.a., *A new method based on the regression of step response data for monitoring a freeze-drying cycle.* J. Pharm. Sci., 2014. 103(6): p. 1756--65.

[15] Pisano, R., Fissore, D., and Barresi, A.A., *In-Line and Off-Line Optimization of Freeze-Drying Cycles for Pharmaceutical Products.* Drying Technology, 2013. 31(8): p. 905-919.

[16] Wiggenhorn, M., Presser, I., and Winter, G., *The current state of PAT in freeze-drying.* American Pharmaceutical Review, 2005. 8: p. 38-44.

[17] Presser, I., *Innovative online Messverfahren zur Optimierung von Gefriertrocknungsprozessen*. 2003, LMU Munich.

[18] Milton, N., et al., *Evaluation of manometric temperature measurement as a method of monitoring product temperature during lyophilization.* PDA J. Pharm. Sci. Technol., 1997. 51(1): p. 7-16.
[19] Tang, X., Nail, S.L., and Pikal, M.J., *Evaluation of manometric temperature measurement, a process analytical technology tool for freeze-drying: part I, product temperature measurement.* AAPS PharmSciTech, 2006. 7(1): p. E14.
[20] Tang, X.C., Nail, S.L., and Pikal, M.J., *Evaluation of manometric temperature measurement (MTM), a process analytical technology tool in freeze drying, part III: heat and mass transfer measurement.* AAPS PharmSciTech, 2006. 7(4): p. 97.
[21] Tang, X.C., Nail, S.L., and Pikal, M.J., *Evaluation of manometric temperature measurement, a process analytical technology tool for freeze-drying: part II measurement of dry-layer resistance.* AAPS PharmSciTech, 2006. 7(4): p. 93.
[22] De Beer, T.R., et al., *In-line and real-time process monitoring of a freeze drying process using Raman and NIR spectroscopy as complementary process analytical technology (PAT) tools.* J. Pharm. Sci., 2009. 98(9): p. 3430-46.
[23] Pieters, S., et al., *Raman spectroscopy and multivariate analysis for the rapid discrimination between native-like and non-native states in freeze-dried protein formulations.* Eur. J. Pharm. Biopharm., 2013. 85(2): p. 263--271.
[24] Emteborg, H., et al., *Infrared thermography for monitoring of freeze-drying processes: instrumental developments and preliminary results.* J. Pharm. Sci., 2014. 103(7): p. 2088-97.
[25] Last, I.R. and Prebble, K.A., *Suitability of near-infrared methods for the determination of moisture in a freeze-dried injection product containing different amounts of the active ingredient.* J. Pharm. Biomed. Anal., 1993. 11(11-12): p. 1071--1076.
[26] Mensink, M.A.a., *In-line near infrared spectroscopy during freeze-drying as a tool to measure efficiency of hydrogen bond formation between protein and sugar, predictive of protein storage stability.* Int. J. Pharm., 2015.
[27] De Beer, T.R., et al., *Implementation of a process analytical technology system in a freeze-drying process using Raman spectroscopy for in-line process monitoring.* Anal. Chem., 2007. 79(21): p. 7992-8003.
[28] Gieseler, H., et al., *Evaluation of tunable diode laser absorption spectroscopy for in-process water vapor mass flux measurements during freeze drying.* J. Pharm. Sci., 2007. 96(7): p. 1776-93.
[29] Kuu, W.Y., Nail, S.L., and Sacha, G., *Rapid Determination of Vial Heat Transfer Parameters Using Tunable Diode Laser Absorption Spectroscopy (TDLAS) in Response to Step-Changes in Pressure Set-Point During Freeze-Drying.* J. Pharm. Sci., 2009. 98(3): p. 1136-1154.
[30] Kuu, W.Y., et al., *Product mass transfer resistance directly determined during freeze-drying cycle runs using tunable diode laser absorption spectroscopy (TDLAS) and pore diffusion model.* Pharm. Dev. Technol., 2010. 16(4): p. 343-357.
[31] Kasper, J.C., et al., *Implementation and evaluation of an optical fiber system as novel process monitoring tool during lyophilization*, in *Eur. J. Pharm. Biopharm.* 2013. p. 449-459.
[32] Rambhatla, S., et al., *Heat and mass transfer scale-up issues during freeze drying: II. Control and characterization of the degree of supercooling.* AAPS PharmSciTech, 2004. 5(4): p. 54-62.
[33] Konstantinidis, A.K., et al., *Controlled Nucleation in Freeze-drying: Effects on Pore Size in the Dried Product Layer, Mass Transfer Resistance, and Primary Drying Rate.* J. Pharm. Sci., 2011: p. 1-18.
[34] Fang, R., et al., *Effect of Controlled Ice Nucleation on Stability of Lactate Dehydrogenase During Freeze-Drying.* J. Pharm. Sci., 2018. 107(3): p. 824-830.
[35] Passot, S., et al., *Effect of controlled ice nucleation on primary drying stage and protein recovery in vials cooled in a modified freeze-dryer.* J. Biomech. Eng., 2009. 131(7): p. 74511-5.

[36] Oddone, I., et al., *Impact of vacuum-induced surface freezing on inter- and intra-vial heterogeneity.* Eur. J. Pharm. Biopharm., 2016. 103: p. 167-178.
[37] Schersch, K., et al., *Systematic investigation of the effect of lyophilizate collapse on pharmaceutically relevant proteins I: stability after freeze-drying.* J. Pharm. Sci., 2010. 99(5): p. 2256-78.
[38] Schersch, K., et al., *Systematic investigation of the effect of lyophilizate collapse on pharmaceutically relevant proteins, part 2: stability during storage at elevated temperatures.* J. Pharm. Sci., 2012. 101(7): p. 2288-306.
[39] Schersch, K., et al., *Systematic investigation of the effect of lyophilizate collapse on pharmaceutically relevant proteins III: collapse during storage at elevated temperatures.* Eur. J. Pharm. Biopharm., 2013. 85(2): p. 240-52.
[40] Geidobler, R., Konrad, I., and Winter, G., *Can controlled ice nucleation improve freeze-drying of highly-concentrated protein formulations?* J. Pharm. Sci., 2013. 102(11): p. 3915-9.
[41] Reuter, S., Philipp, J., and Dobner, J., *Gesteuertes Einfrieren in der Gefriertrocknung* TechnoPharm, 2018. 8(3): p. 140-149.
[42] Geidobler, R. and Winter, G., *Controlled ice nucleation in the field of freeze-drying: fundamentals and technology review.* Eur. J. Pharm. Biopharm., 2013. 85(2): p. 214-22.
[43] RdF Corporation. *Simplified Heat Flow Measurement*. 2003 [cited October 8th, 2014]; Available from: http://www.rdfcorp.com/anotes/pa-hfs/pa-hfs_pf.html.
[44] Ling, W., *Using surface heat flux measurement to monitor and control a freeze driyng process*, Millrock Technology Inc., K., NY, USA, Editor. 2013, Millrock Technology Inc., Kingston, NY, USA.
[45] Thompson, T.N. and Millrock Technology Inc., *LyoPAT(TM): real-time monitoring and control of the freezing and primary drying stages during freeze-drying for improved product quality and reduced cycle times.* American Pharmaceutical Review, 2013. 2013.
[46] Mahler, H.C., et al., *Induction and analysis of aggregates in a liquid IgG1-antibody formulation.* Eur. J. Pharm. Biopharm., 2005. 59(3): p. 407-17.
[47] Wang, S., et al., *Stabilizing two IgG1 monoclonal antibodies by surfactants: Balance between aggregation prevention and structure perturbation.* Eur. J. Pharm. Biopharm., 2017. 114(Supplement C): p. 263-277.
[48] Martos, A., et al., *Trends on Analytical Characterization of Polysorbates and Their Degradation Products in Biopharmaceutical Formulations.* J. Pharm. Sci., 2017. 106(7): p. 1722-1735.

CHAPTER II

II. CONTROLLED ICE NUCLEATION FOLLOWED BY AGGRESSIVE PRIMARY DRYING DURING LYOPHILIZATION OF HIGHLY CONCENTRATED PROTEIN FORMULATIONS

This chapter was partly presented orally at the *PBP World Meeting, Lisbon, 2014:*

Ilona Konrad[1,2], Raimund Geidobler[2], Angelika Freitag[1], Wolfgang Friess[2], Andrea Hawe[1], Gerhard Winter[2], (2014). "*Controlled ice nucleation followed by aggressive primary drying during lyophilization of highly concentrated protein formulations?*", 9th PBP World Meeting on Pharmaceutics, Biopharmaceutics and Pharmaceutical Technology, 2014.

This chapter was written by Ilona Vollrath. Experiments were partly performed by Martin Schubert within the scope of his bachelor thesis and partly by Ilona Vollrath. Raimund Geidobler, Angelika Freitag, Wolfgang Frieß, Andrea Hawe and Gerhard Winter provided scientific guidance during the experimental phase. In addition, Wolfgang Frieß, Andrea Hawe and Gerhard Winter reviewed the chapter and provided input throughout the writing process.

II.1 INTRODUCTION

Since Searles et al. [1] identified the ice nucleation temperature (T_N) as a relevant factor for the primary drying (PD) rate during lyophilization, the freezing step gained more attention in freeze-drying cycle optimization. A higher T_N causes formation of larger ice crystals, which result in larger pores. These larger pores facilitate sublimation due to reduced product resistance and thus, speed-up PD [1-3]. But larger pores come with reduced specific surface area (SSA), which induces slower water desorption during secondary drying (SD) and thus, could cause higher residual moisture (RM) levels of the final product [2, 4].

Consequently, methods emerged to control T_N by controlled nucleation of ice (CN). Rowe et al. [5] first proposed the use of ice crystals as seeds to induce ice nucleation purging cold nitrogen gas into the high humidity environment of the drying chamber to form an ice fog after the vials have achieved the temperature at which nucleation is desired. Rambhatla et al. [4] developed this ice fog technique further and achieved complete nucleation of all vials within 5 min. In a follow-up study, Patel et al. [6], could reduce the time needed for complete nucleation to 1 min. Geidobler et al. [7] presented an easy approach to induce ice nucleation by a modified ice fog method. Their technique does not require liquid nitrogen or any modification of the freeze-dryer. After equilibration of the vials at the desired T_N, the freeze-dryer is depressurized to e.g. 3.7 mbar and subsequently vented through the cold condenser back to atmospheric pressure. Thus, ice crystals are formed *in-situ* in the chamber, which results in a very fast ice fog distribution. The supercooled vials all nucleated within about 5 s. Millrock Technology Inc. introduced a similar ice fog method, the FreezeBooster® [8]. After equilibration of the product vials, the freeze-dryer is depressurized to approximately 66 mbar. In contrast to Geidobler et al., before venting, the isolation valve between the chamber and the condenser is closed, the condenser is backfilled to atmospheric pressure and water steam is sprayed into the cold condenser chamber to generate ice crystals. By opening the isolation valve, the ice fog is generated and transferred into the chamber. Geidobler and Winter [9] reviewed the different

approaches to induce ice nucleation in detail. Additionally, they provide an overview of the differences in product characteristics, such as SSA and RM, between samples nucleated in a controlled way or randomly.

Various studies investigated the impact of T_N on PD rate, product resistance, and SSA [2, 4, 6, 10-12]. Previously, we applied CN for the first time to highly concentrated protein formulations by using the method described by Geidobler et al. [7, 13]. The time for PD was reduced and the resulting large pores facilitated cake wetting and faster reconstitution. A rather conservative freeze-drying cycle with product temperatures (T_p) well below the glass transition temperature ($T_g`$) was used to avoid any change of the ice crystal structure generated by CN due to potential micro collapse. However, for highly concentrated protein formulations, the actual collapse temperature ($T_c$) can be significantly higher than $T_g`$, which enables PD above $T_g`$ without collapse [14-16]. Such an aggressive PD remarkably reduces PD times.

In this study, we combined CN, using the FreezeBooster® method, with aggressive PD to further reduce PD time of a highly concentrated protein formulation without changing product characteristics such as SSA and RM. We developed a freeze-drying cycle with T_p above $T_g`$ but below T_c using bovine serum albumin (BSA) and compared the product characteristics of those lyophilizates with the lyophilizates obtained from the conservative PD process of our previous study [13]. The developed aggressive PD protocols were than applied to a highly concentrated mAb formulation. The product characteristics of the mAb lyophilizates processed by the aggressive PD protocols were compared to the ones generated by the conservative PD protocol.

II.2 MATERIALS AND METHODS

II.2.1 MATERIALS

An IgG1 mAb, formulated at 161.2 mg/ml in a 10 mM histidine buffer (pH 5.4) was used in this study. BSA was purchased from Sigma-Aldrich (Munich, Germany). Sucrose was kindly provided by Suedzucker (Plattling, Germany). Di-sodium hydrogen phosphate, sodium dihydrogen phosphate, and trehalose were purchased from VWR (Ismaning, Germany). All chemicals were of analytical grade.

Low protein binding polyvinylidenfluorid (PVDF) 0.22 µm filters were purchased from Merck Millipore (Schwalbach, Germany). 2R glass type I tubing vials were kindly provided by MGlas AG (Münnerstadt, Germany). Rubber stoppers, 13 mm (Westar® RS, 4023/50, bromobutyl, grey, FluoroTec B2-40 coating) were kindly supplied by West Pharmaceutical Services (Eschweiler, Germany). Standard aluminum crimp caps, compatible with 13 mm stoppers, were used. All vials and stoppers were washed manually three times with highly purified water (Milli-Q, Merck Millipore, Hertfordshire, United Kingdom), autoclaved at 121 °C for 20 min and dried at 80 °C.

II.2.2 SAMPLE PREPARATION

BSA was formulated at 193 mg/ml in a 10 mM phosphate buffer (pH 7.4) with 5% sucrose. The mAb formulation was completed by adding 5% sucrose. The concentration of all formulations was determined at 280 nm using a Nanodrop 2000 UV photometer (Thermo Scientific, Wilmington, DE, USA). Sample aliquots of 1.0 ml of the BSA formulation and 0.37 ml of the mAb formulation were manually filled and the vials were semi-stoppered manually.

II.2.3 LYOPHILIZATION

Lyophilization was performed using a Millrock Magnum pilot scale freeze-dryer (Millrock Technology, Kingston, NY, USA). During freeze-drying the vacuum was controlled by a capacitance gauge. For T_p monitoring, thermocouples were used. End of PD was detected by comparative pressure measurement. The freeze-dryer automatically proceeded into SD when the detected pressure difference was less than 1 mTorr (0.0013 mbar). By default, the vials were stored at 5 °C after completion of the freeze-drying cycle. Stoppering was initiated manually after the chamber pressure (p_c) was backfilled to 600 Torr (800 mbar). After unloading the vials were crimp capped.

Freezing was performed either by CN using the Millrock FreezeBooster® [8] in manual mode (Millrock Technology, Inc, Kingston, NY; USA) or a ramp freezing protocol (RN). For CN, the vials were equilibrated for 2 h at the aimed nucleation temperature of -5 °C. Immediately after controlled nucleation, the shelf temperature (T_s) was ramped to -60 °C at 1 °C/min. RN samples were equilibrated at 2 °C for at least 1 h before the shelf temperature was lowered to -60 °C at 1 °C/min. A hold time of 120 min at -60 °C was applied to all freezing protocols prior to initiating primary drying.

Different PD and SD parameters (T_s and p_c) for aggressive drying were evaluated to achieve a T_p between T_g` and T_c and to meet the same target RM and SSA values as in the previous study [13] (Table II-1).

Table II-1: Overview of evaluated PD and SD parameters to optimize the aggressive PD protocol.

Lyo Cycle (LC)	Primary drying		Secondary drying		
	Temperature profile	Chamber pressure	Temperature profile	Chamber pressure	Duration [h]
CN1	20 °C (0.5 °C/min)	750 mTorr (1 mbar)	25 °C (0.1 °C/min)*	50 mTorr (0.06 mbar)	6
CN2	20 °C (0.5 °C/min); hold time: 30 min; 0°C (1 °C/min)		30 °C (0.1 °C/min)		6
CN3	20 °C (0.5 °C/min); hold time: 30 min; 0 °C (1 °C/min)		30 °C (0.05 °C/min)		6
CN4	0 °C (0.5 °C/min)		30 °C (0.1 °C/min)		6
RN1	20 °C (0.5 °C/min)		30 °C (0.1 °C/min)		6
RN2	0 °C (0.5 °C/min)		30 °C (0.1 °C/min)		6
RN3	20 °C (0.5 °C/min); hold time: 30 min; 0 °C (1 °C/min)		30 °C (0.1 °C/min)		6
RN4	20 °C (0.5 °C/min); no hold time; 0 °C (1 °C/min)		30 °C (0.1 °C/min)		6
RN5	20 °C (0.5 °C/min); hold time: 120 min; 0 °C (0.1 °C/min)	562 mTorr (0.75 mbar)	40 °C (0.1 °C/min)*		6
RN6	20 °C (0.5 °C/min); hold time: 90 min; -10 °C (0.2 °C/min)	375 mTorr (0. 5 mbar)	40 °C (0.1 °C/min)		3
RN7	20 °C (0.5 °C/min); hold time: 30 min; -10 °C (0.2 °C/min)	75 mTorr (0.1 mbar)	40 °C (0.1 °C/min)		1
Conservative PD CN [13]	-22 °C (0.5 °C/min)	50 mTorr (0.066 mbar)	25 °C (0.1 °C/min)		6

* For mAb formulation secondary drying temperature was set to 30 °C (0.1 °C/min) for 6 h.

II.2.4 SCANNING ELECTRON MICROSCOPY (SEM)

SEM was used to study the morphology of the lyophilizates (JSM-6500F Field Emission Electron Microscope, Jeol, Eching, Germany). The freeze-dried cake was broken with a spatula and the

generated pieces were fixed with carbon conductive cement on a sample holder such that the breakage border could be analyzed.

II.2.5 KARL FISCHER TITRATION (KF)

KF was used to determine the RM of the freeze-dried products. BSA samples were analyzed by the direct injection method using a 737 KF Coulometer (Metrohm, Filderstadt, Germany). Approximately 2.5 ml of anhydrous methanol was added to the sample. To extract the water, the sample was placed in an ultrasonic bath for 10 min. An aliquot of 1 ml was injected into the titrator. Results were calculated as relative water content (m/m). For the mAb samples, an Aqua 40.00 coulometric titrator combined with a headspace module (Analytik Jena GmbH, Jena, Germany) was used for the analysis. About 20 mg of sample was weighed into a 2R glass vial under a glovebox (r.h. ≤ 5%). The sample was analyzed at 150 °C. Prior to the measurements, a system suitability test was performed daily by measuring a pure water standard (Apura 1 water standard oven 1.0, Merck KGaA).

II.2.6 FREEZE-DRYING MICROSCOPY (FDM)

FDM was used to determine T_c (FDSC 196, Resultec, Illerkirchberg, Germany). A sample aliquot of 2 µl was pipetted in a quartz crucible. By a horseshoe-shaped spacer ring a defined distance between quartz crucible and cover slip was granted. The sample was frozen with a rate of 1 K/min to -50 °C. After exhausting to a vacuum of 0.1 mbar, the sample was heated at 1 K/min to 5 °C. During the heating step, images were taken every second. The temperature when the first translucent dots appeared was considered as collapse onset temperature (T_c,onset). The full collapse temperature (T_c) was determined at the temperature where a full loss of structure occurred.

II.2.7 DIFFERENTIAL SCANNING CALORIMETRY (DSC)

The glass transition temperatures T_g' of the frozen product was determined by DSC (Mettler Toledo DSC821e, Mettler Toledo, Giessen, Germany). Approximately 30 µl of the product were pipetted into an aluminum crucible (Mettler Toledo, Giessen, Germany). The samples were cooled to -40 °C with 5 K/min and further to -50 °C with 2 K/min. After an isothermal hold of 2 min, samples were re-heated to 20 °C with a heating rate of 20 K/min. The midpoint of the endothermic shift of the baseline during the heating scan was taken as $T_g`$.

II.2.8 BET ANALYSIS

The SSA of the lyohilizates was analyzed by the BET method using an Autosorb-1 (Quantachrome Instruments, Germany). Approximately 100 mg sample was crushed with a spatula and weighed into a glass sample tube. Degassing was performed for at least 2 h at 25 °C. Subsequently, Krypton sorption measurement was performed at 77.3 K. An 11-data point adsorption curve covering a p/p_0 region from 0.05 to 0.3 was recorded. The data points were evaluated according to the multipoint BET-method.

II.2.9 RECONSTITUTION PROCEDURE AND DETERMINATION OF RECONSTITUTION TIME

To reconstitute the lyophilizates, the vials were placed on an orbital shaker (VWR, Ismaning, Germany) and the desired amount of highly purified water was pipetted into the middle of the lyophilized cake and the samples were shaken at 400 rpm. The time until a clear solution resulted was recorded as reconstitution time. BSA samples were reconstituted with 1.6 ml and mAb lyophilizates with 0.32 ml. The reconstitution volume for the BSA samples was increased to avoid that dissolution effects impact the reconstitution time (as found in our previous work) [13]. The required volume for reconstitution of the mAb lyophilizates was calculated based on the density of the liquid formulation and the total solid content.

II.2.10 DATA ANALYSIS AND ILLUSTRATION

Throughout the manuscript error bars represent the standard deviation based on triplicates. If no error bars are shown, only one sample was analyzed due to material constraints.

II.3 RESULTS

II.3.1 DSC AND FDM

At first, $T_g`$ and $T_c$ of all samples were characterized. With increasing BSA concentration higher $T_g`$ and T_c values were determined except for BSA 100 mg/ml. As the $T_g`$ was followed directly by the onset of the melting, it was not possible to determine $T_g`$ at BSA concentrations higher than 100 mg/ml (Figure II-1) and for the mAb formulation at 161.2 mg/ml. Consequently, $T_g`$ values for 150 mg/ml and 193 mg/ml BSA were extrapolated by linear regression (Table II-2 and APPENDIX Figure VIII-1).

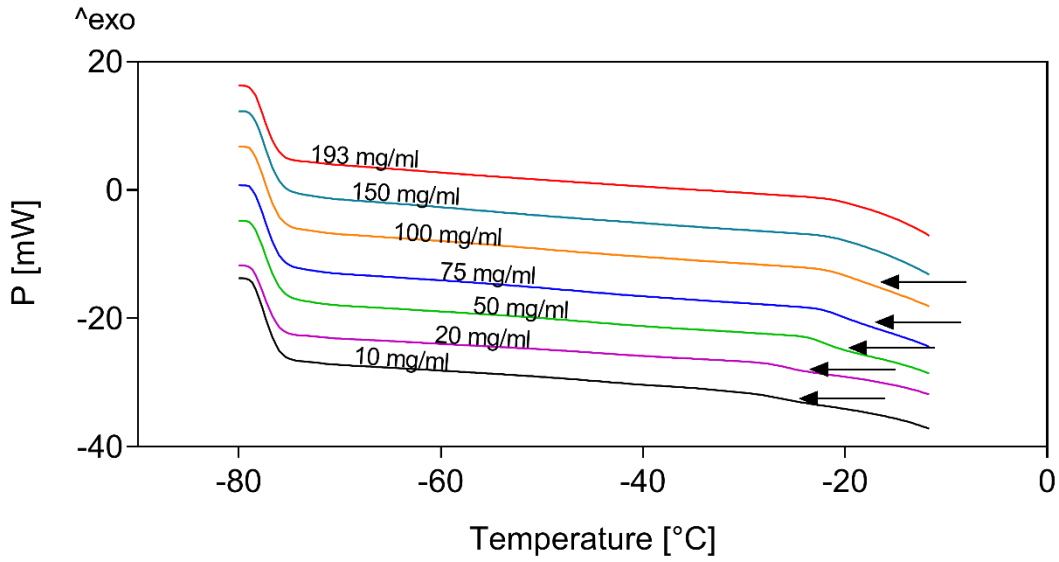

Figure II-1: Thermograms of BSA formulations ranging from 10 mg/ml to 200 mg/ml. The arrows point towards the baseline shift, which indicates $T_g`$.

Table II-2: T_g` and T_c values for formulations with different BSA concentrations and the mAb formulation.

Formulation	T_g` [°C]	T_c [°C]
BSA 10 mg/ml	-30.5	-24.5
BSA 20 mg/ml	-27.5	-18.7
BSA 50 mg/ml	-26.8	-14.2
BSA 75 mg/ml	-23.2	-13.4
BSA 100 mg/ml	-22.9	-15.1
BSA 150 mg/ml	-18.2*	-11.9
BSA 200 mg/ml	-14.7*	-10.1
mAb 161 mg/ml	------	-8.1

* extrapolated by linear regression (R^2=0.9776)

II.3.2 PRODUCT TEMPERATURES AND PRIMARY DRYING TIMES

Table II-3 provides the time required to complete PD for the tested lyo cycles. All lyo cycles with aggressive PD showed a remarkable reduction in PD time compared to the conservative drying method of Geidobler et al. [13].

For BSA formulations, the shortest primary drying time of about 4 h could be achieved by the most aggressive lyo cycles, CN1 and RN1, independent from the nucleation protocol. The least aggressive protocols, CN4 and RN2, revealed the longest primary drying times but PD was still faster compared to the conservative PD of Geidobler et al. [13]. Duration of PD was only slightly affected by the nucleation protocol. Compared to RN product, the T_p of the CN product is about 2-3 °C lower e.g. CN1 vs. RN1, CN4 vs. RN2, and CN2 vs. RN3.

Table II-3: T_p after 1 h of PD and PD durations of the lyo cycles.

Formulation	Lyo cycle	Product temperature [°C] after 1 h of PD	PD duration [h]*
BSA	CN1	-9.3	4.0
	CN2	-14.5	6.1
	CN3	-14.1	6.8
	CN4	-16.5	9.3
	RN1	-6.5	3.7
	RN2	-14.2	7.4
	RN3	-12.8	5.4
	RN4	-10.6	6.3
	RN5	-9.9	5.0
	RN6	-11.3	4.7
	RN7	-20.8	10.0
	Conservative CN	-39.9	18.0
mAb	CN1	+3.1	3.4
	RN2	-15.5	6.4
	RN5	-3.4	3.1
Geidobler et al [13]	CN (BSA 193.9 mg/ml)	-38.7 (7 h PD)	24.2[+]
	CN (mAb 161.2 mg/ml)	-33.2 (7 h PD)	20.0[+]
	RN (mAb 161.2 mg/ml)	-30.5 (7 h PD)	25.0[+]

* the time span between the time point when T_S reached the set point for PD until comparative pressure measurement indicated the end of PD.
[+] end of PD was determined by thermocouple readings.

Independent of the nucleation protocol, both more aggressive lyo cycles, CN1 and RN5, resulted in a PD time of about 4 h for the mAb formulation. For the less aggressive RN2 cycle a longer PD time was detected compared to CN1 and RN5. A markedly higher T_p was measured for much more aggressive CN1 conditions compared to RN5.

II.3.3 CAKE APPEARANCE AND SEM

The cakes of CN and RN lyophilizates markedly differed in appearance. CN lyophilizates exhibited a more porous, loose and shiny structure with substantial crack formation (Figure II-2A

and APPENDIX Figure VIII-2). In contrast, RN lyophilizates showed a compact cake with minor shrinkage in height and diameter, a shiny surface and only tiny cracks (Figure II-2B). The BSA CN cakes were light-yellow in color, whereas the BSA RN cakes were slightly beige. Both types of mAb lyophilizates appeared white (Figure II-2 and APPENDIX Figure VIII-2). The BSA and mAb cake appearance was independent of the PD protocols (APPENDIX Figure VIII-2).

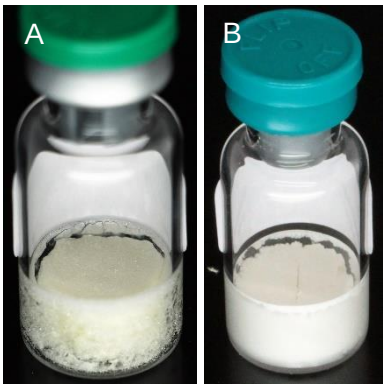

Figure II-2: Photographs of a CN1 lyophilizate (A) and a RN1 lyophilizate (B) of the BSA formulation.

After macroscopic characterization, microscopic analysis of selected lyophilizates was performed by SEM. All lyophilizates had a sponge like morphology in common (Figure II-3). The CN lyophilizates showed larger pores compared to the RN products. RN2 cake pores appeared slightly larger than the pores of RN5 lyophilizates. No effect of protein or PD protocol could be detected.

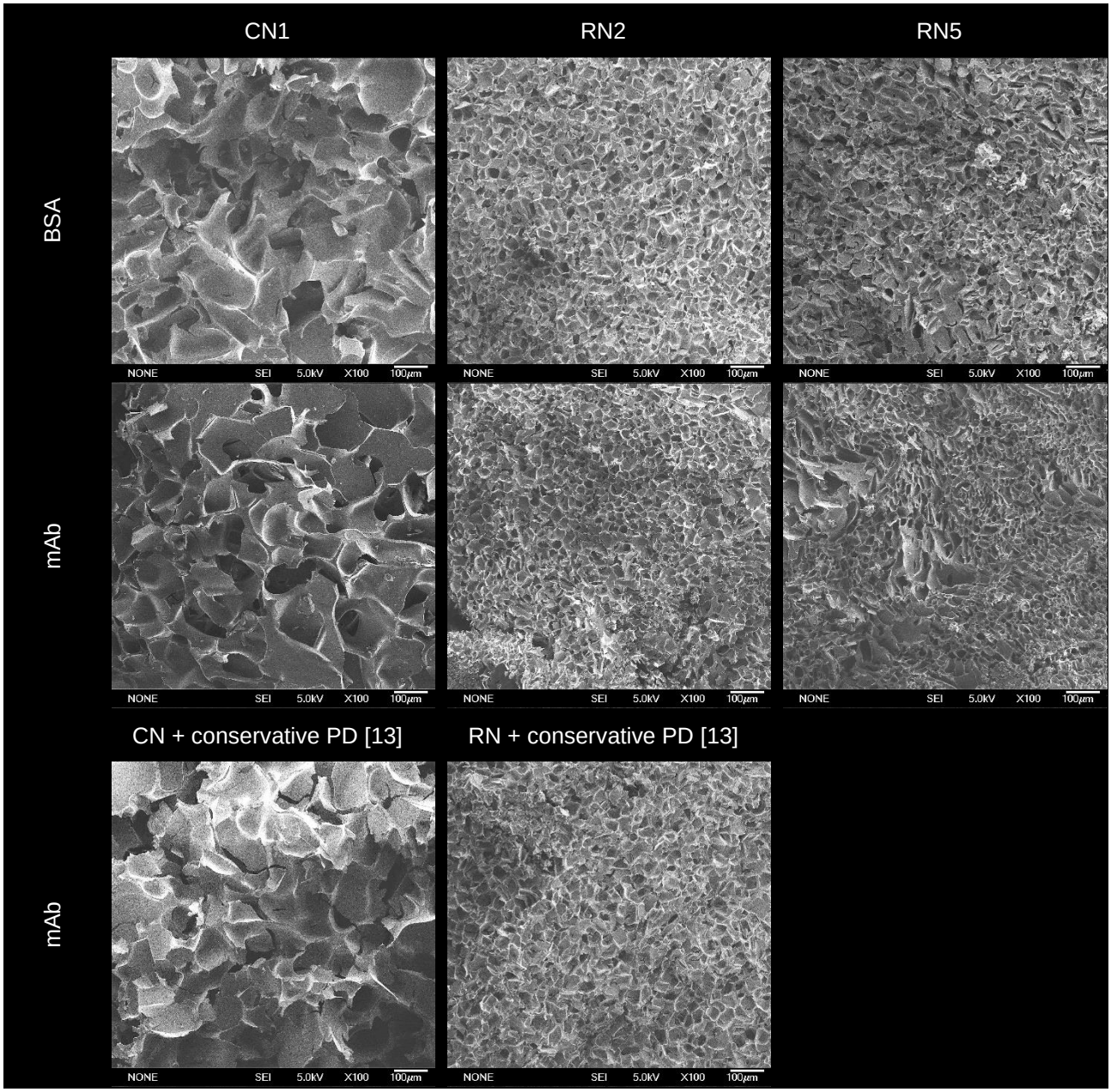

Figure II-3: SEM images of CN1, RN2, and RN5 of the BSA and mAb formulation and SEM images of CN and RN runs followed by conservative PD of the mAb formulation.

II.3.4 BET AND KARL FISCHER

The lyophilizates were analyzed by Krypton gas adsorption to determine the SSA and Karl Fischer to assess RM (Figure II-4 and Figure II-5). Corresponding to the larger pores seen in SEM, CN lyophilizates showed a lower SSA and higher RM compared to RN products (Figure II-4 and Figure II-5).

The SSA of the BSA formulations dried with conservative PD after CN, using the Millrock freeze-dryer, was comparable to one of the lyophilizates described by Geidobler et al. [13] (Figure II-4A). All aggressive PD CN protocols (CN1-4) resulted in a slightly lower SSA compared to conservative PD without a difference in SSA between CN1, 2, 3, and 4. SSA of RN2 and RN4 samples met the SSA of lyophilizates processed by the conservative PD of Geidobler et al. [13]. RN1 and RN3 led to slightly lower and RN5, 6, and 7 to markedly lower SSA values. The RM of CN cakes produced by Geidobler et al. [13] was lower compared to the conservative PD CN protocol as the secondary drying temperature differed (Geidobler et al.[13] =30 °C for 6 h; Conservative PD CN= 25 °C for 6 h) (Figure II-4B). This also explains the higher RM for CN1 compared to CN2, 3, and 4. RN1 to RN4 processed lyophilizates resulted in similar RM values as RN samples described by Geidobler et al. [13]. In RN5, 6, and 7 secondary drying was performed at 40 °C, which resulted in lower RM values.

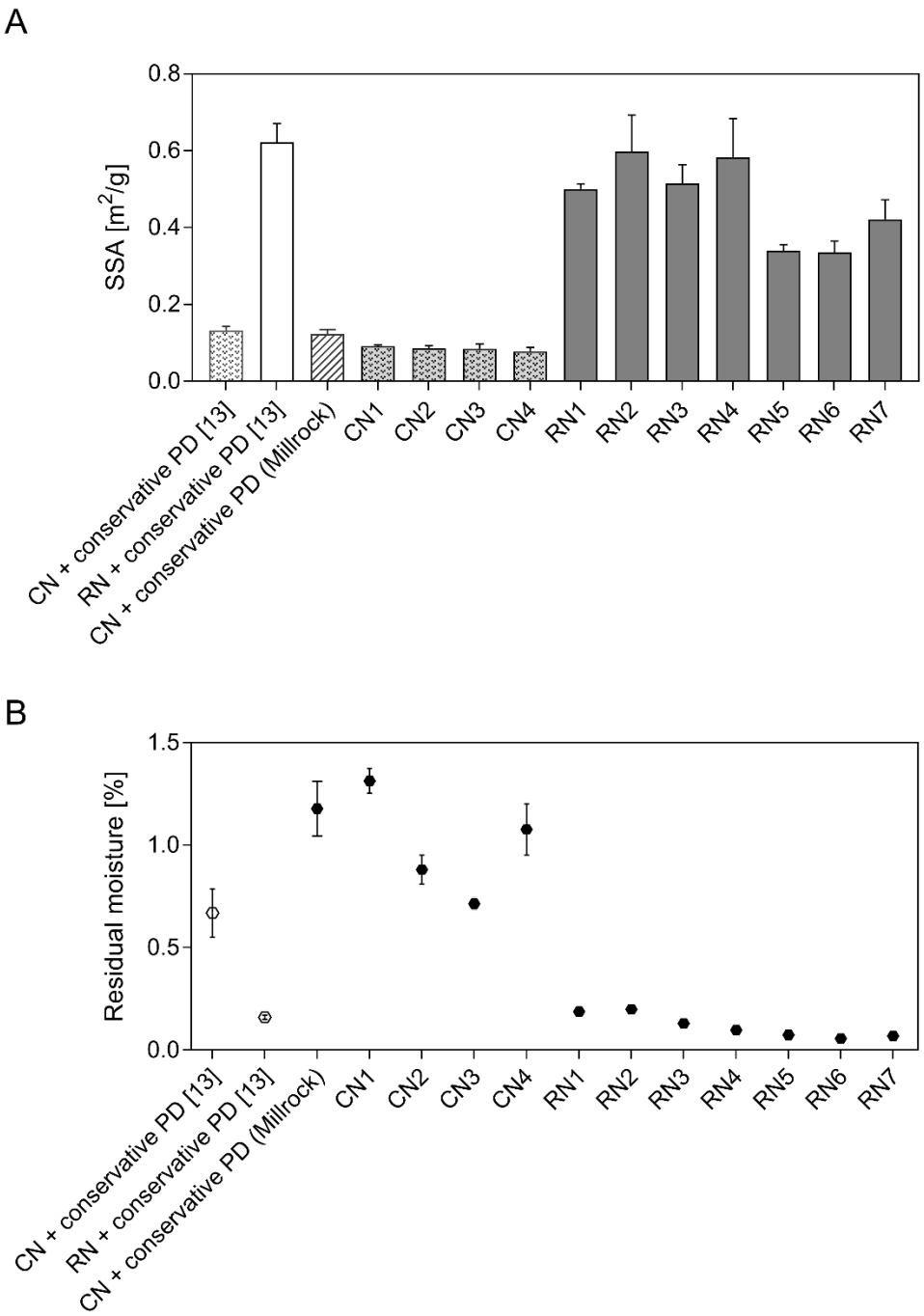

Figure II-4: Results of BET (A) and KF (B) measurements of all lyo cycles using the BSA formulation and results by Geidobler et al. [13].

The SSA of both CN1 and RN2 and 5 mAb lyophilizates was lower as compared to the results for products dried with the less aggressive approach by Geidobler et al. [13] (Figure II-5A). Whereas the RM content of CN1 lyophilizates was slightly higher than the RM detected by

Geidobler et al. [13] for CN (Figure II-5B), RN2 and RN5 rendered products with lower RM compared to Geidobler et al. [13] for RN.

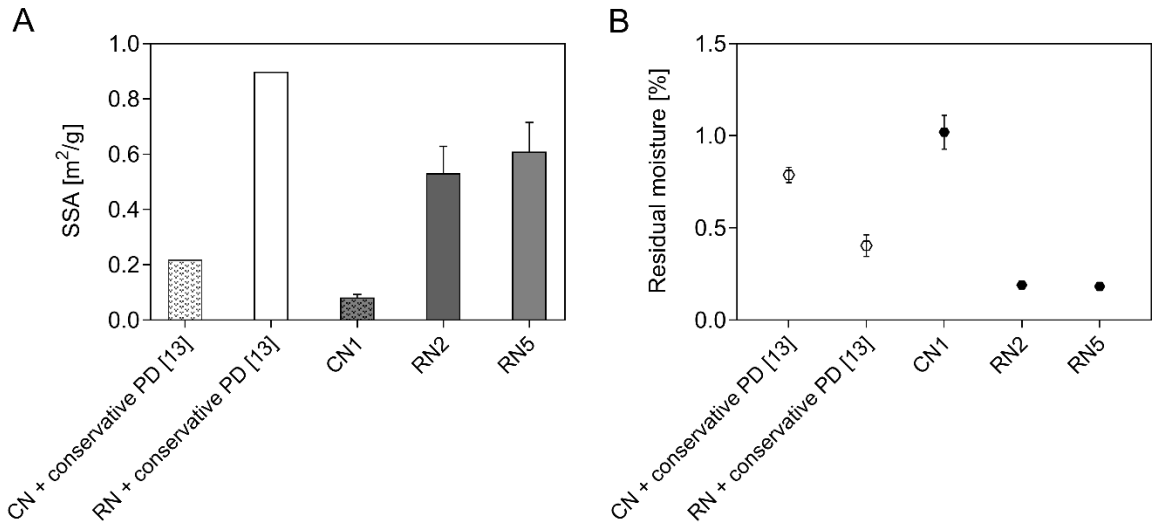

Figure II-5: Results of BET (A) and KF (B) measurements of all lyo cycles using the mAb formulation. Geidobler et al [13] mAb results were included for comparability.

II.3.5 RECONSTITUTION TIMES

For the mAb formulation also reconstitution times were determined (Figure II-6). Comparable to Geidobler et al. [13], CN resulted in a three-times faster cake dissolution compared to RN. The aggressive PD protocols showed shorter reconstitution times compared to the conservative PD.

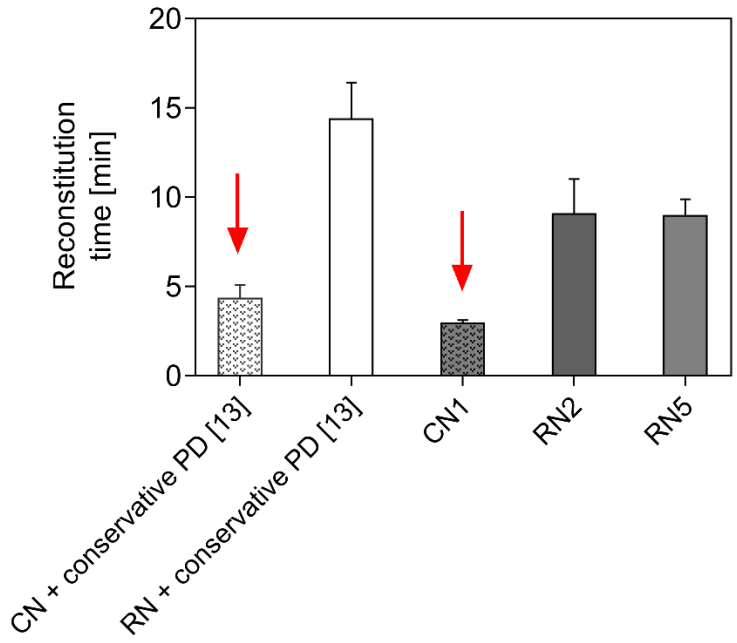

Figure II-6: Results of reconstitution times determination of the mAb lyophilizates. Geidobler et al. [13] mAb results were included for comparability.

II.4 DISCUSSION

In the first part of this study freeze-drying cycles with aggressive primary drying were developed for a CN process using the FreezeBooster® method, as well as for a RN process. The aggressive primary drying should not change the product properties compared to the lyophilizates prepared by conservative primary drying in our previous study [13]. We subsequently applied the developed aggressive freeze-drying to a highly concentrated mAb formulation and again compared the product properties to our previous results.

II.4.1 DEVELOPMENT OF A FREEZE-DRYING CYCLE WITH AGGRESSIVE PRIMARY DRYING

As we used the FreezeBooster® method instead of the method described by Geidobler et al. [7], which was used in our previous study, we first evaluated the impact of the change in CN method on product properties. Therefore, we performed CN with the FreezeBooster® and used the conservative drying protocol of our previous study [13]. However, by accident, the secondary drying temperature was set to 25 °C instead of 30 °C. Whereas the SSA of conservative PD CN (Millrock) was comparable to the SSA determined by Geidobler et al. [13] (Figure II-4A), RM was higher (Figure II-4B) due to the lower secondary drying temperature. We concluded that the two CN methods, performed on two freeze-dryers, resulted in comparable product properties.

For aggressive primary drying, the target T_p was to be between $T_g`$ and $T_c$. Thus, $T_p$ during PD should be below -10.1 °C but above -14.2 °C for the BSA formulation and slightly below -8.1 °C for the mAb formulation. For the mAb formulation $T_g`$ was not determined. For the BSA formulations, the $T_g`$ of the high concentration formulation had to be extrapolated from the results of a concentration series. Overall, $T_g`$ was several degrees below T_c, according to Patel et al. [15].

As the vapor pressure over ice at -12 °C is 1630 mTorr (2.17 mbar) and the freeze-dryer allows adequate pressure control below 1000 mTorr, 750 mTorr (1 mbar) were defined as the most aggressive p_c to be used. To achieve a T_p of approximately -11 °C the T_s was set to 20 °C for CN1 and RN1 (Table II-1). In the case of CN1, T_p marginally exceeded T_c by 0.8 °C, which is within the accuracy of the used thermocouples (Table II-3). Neither cake appearance nor cake morphology indicated collapse and were comparable to the CN lyophilizates processed by the conservative PD. However, SSA of CN1 lyophilizates was slightly lower than that of conservative PD CN lyophilizates, which could indicate micro-collapse (Figure II-4A). As T_p increases with ongoing PD due to the increasing dry layer resistance [17], T_s of CN2 was lowered after 30 min PD to 0 °C. Although T_p was well below T_c and even below the extrapolated T_g`, the determined SSA for CN2 products was comparable to CN1 lyophilizates. As the change in PD protocol did not result in an increase in SSA, we supposed that SD might be causing the slight differences in SSA and evaluated a slower ramp into SD with CN3 and a lower T_s (0 °C) in CN4. However, also these parameters resulted in the same SSA. Based on CN1-4, which all showed similar cake appearance and morphology as conservative PD products, we concluded that CN defines the ice crystal size during freezing and with this the resulting SSA, thus the slightly lower SSA of the aggressive PD lyophilizates was not caused by micro-collapse. Additionally, RM values of CN2 and CN3 lyophilizates were comparable to the CN lyophilizates of Geidobler et al. [13]. CN4 samples showed slightly higher RM values, which might be caused by a higher RM content after primary drying due to the lower T_s. As CN1 led to the shortest PD time and the T_p closest to -10.1 °C, CN1 PD settings were chosen as aggressive PD protocol for the CN process.

For the development of an aggressive PD protocol for the RN process, the same starting point as for the CN process was chosen with a p_c of 750 mTorr and a T_s of 20 °C. However, in case of RN1, T_p exceeded T_c by 3.6 °C compared to the 0.8 °C of the CN process, because the higher product resistance due to the smaller pores causes higher T_p. Although, macroscopically, no

collapse of the freeze-dried cake could be detected, a reduced SSA compared to the conservative PD of Geidobler et al. [13] indicated micro-collapse. In RN2-4 different temperature profiles, comparable to the considerations of CN2-4, were tested. The least aggressive RN2 protocol resulted in a T_p of -14.2 °C, which was just the determined $T_g`$ and a cake appearance, morphology, SSA and RM that was comparable to the lyophilizates processed by conservative PD. With RN3 and RN4 a $T_p$ above $T_g`$ (-14.7 °C) and below T_c (-10.1 °C), considering the measurement uncertainty of thermocouples, was reached (RN3: T_p=-12.8 °C; RN4: T_p=-10.6 °C). However, the SSA of RN3 lyophilizates was slightly lower compared to RN4 lyophilizates. In RN5-7, besides the hold time of T_s, also p_c and the end point of T_s was changed. Although p_c was reduced, the longer hold time at 20 °C led to a reduced SSA of RN5, 6, and 7 products compared to the conservative PD lyophilizates of Geidobler et al. [13]. The aggressive PD RN lyo cycles resulted in RM values comparable or slightly lower to the conservative PD cycles. In contrast to the CN processes, it was possible to impact the resulting SSA of RN processes by the PD protocol. RN2 led to product specifications that completely met the target values defined by Geidobler et al. [13] and was therefore chosen as aggressive PD protocol for the RN process. Additionally, RN5 that resulted in an SSA between CN1 and RN2 was included into the mAb study to investigate the impact of this SSA reduction on reconstitution times.

II.4.2 APPLICATION TO A MAB FORMULATION

The mAb formulation was processed by the aggressive PD protocols of CN1, RN2, and RN5. Secondary drying was performed at 30 °C (0.1 °C/min) for 6 h. Comparable to the BSA formulation, PD time of all aggressive lyo cycles was remarkably shorter compared to the conservative PD protocol of Geidobler et al. [13]. Additionally, this reduction in PD time was independent of the nucleation protocol.

Although T_p of CN1 and RN5 markedly exceeded T_c, no cake collapse was found. Microscopic analysis did not indicate micro collapse, a changed morphology or pore size, but in all three

cases a lower SSA compared to conservative lyophilizates of Geidobler et al. [13] was determined pointing to micro-collapse.

Also, faster dissolution of the cakes was observed after aggressive PD. Furthermore, the positive effect of CN on reconstitution time, reported by Geidobler et al. [13], was noted. The lower SSA determined for RN5 BSA samples was not observed for the mAb formulation. Consequently, no impact on reconstitution behavior could be evaluated.

The aggressive PD processes developed with a BSA formulation could successfully be applied to the mAb formulation without changing cake appearance, morphology or pore size, however, the processes were not optimized for the mAb formulation which resulted in different SSA.

II.5 CONCLUSION

In this study, we showed that it is possible to combine controlled nucleation with aggressive primary drying for highly concentrated protein formulation without changing the product characteristics, cake appearance, morphology, pore size, SSA and RM. In case that CN is combined with an aggressive lyo cycle, PD time is remarkably reduced independent of the nucleation protocol. The positive effect of CN on reconstitution time was detected after both conservative and aggressive PD. Consequently, the potential of CN to improve other product quality attributes, e.g. mAb stability, should be evaluated next.

II.6 REFERENCES

[1] Searles, J.A., Carpenter, J.F., and Randolph, T.W., *The ice nucleation temperature determines the primary drying rate of lyophilization for samples frozen on a temperature-controlled shelf.* J. Pharm. Sci., 2001. 90(7): p. 860-871.

[2] Konstantinidis, A.K., et al., *Controlled Nucleation in Freeze-drying: Effects on Pore Size in the Dried Product Layer, Mass Transfer Resistance, and Primary Drying Rate.* J. Pharm. Sci., 2011: p. 1-18.

[3] Kasper, J.C. and Friess, W., *The freezing step in lyophilization: physico-chemical fundamentals, freezing methods and consequences on process performance and quality attributes of biopharmaceuticals.* Eur. J. Pharm. Biopharm., 2011. 78(2): p. 248-63.

[4] Rambhatla, S., et al., *Heat and mass transfer scale-up issues during freeze drying: II. Control and characterization of the degree of supercooling.* AAPS PharmSciTech, 2004. 5(4): p. 54-62.

[5] Rowe, T.W., *A technique for the nucleation of ice.* International Symposium on Biological Product Freeze-Drying and Formulation. Geneva, Switzerland, 1990.

[6] Patel, S., Bhugra, C., and Pikal, M., *Reduced Pressure Ice Fog Technique for Controlled Ice Nucleation during Freeze-Drying.* AAPS PharmSciTech, 2009. 10(4): p. 1406-1411.

[7] Geidobler, R., Mannschedel, S., and Winter, G., *A new approach to achieve controlled ice nucleation of supercooled solutions during the freezing step in freeze-drying.* J. Pharm. Sci., 2012. 101(12): p. 4409-13.

[8] Weijia, L., *Controlled nucleation during freezing step of a freeze drying cycle using pressure differential ice crystals distribution from condensed frost*. 2016, Millrock Technology, Inc., Kingston, NY (US)

[9] Geidobler, R. and Winter, G., *Controlled ice nucleation in the field of freeze-drying: fundamentals and technology review.* Eur. J. Pharm. Biopharm., 2013. 85(2): p. 214-22.

[10] Hottot, A., Vessot, S., and Andrieu, J., *Freeze drying of pharmaceuticals in vials: Influence of freezing protocol and sample configuration on ice morphology and freeze-dried cake texture.* Chemical Engineering and Processing: Process Intensification, 2007. 46(7): p. 666-674.

[11] Passot, S., et al., *Effect of controlled ice nucleation on primary drying stage and protein recovery in vials cooled in a modified freeze-dryer.* J. Biomech. Eng., 2009. 131(7): p. 74511-5.

[12] Bursac, R., Sever, R., and Hunek, B., *A practical method for resolving the nucleation problem in lyophilization.* BioProcess International, 2009. 7(9): p. 66-72.

[13] Geidobler, R., Konrad, I., and Winter, G., *Can controlled ice nucleation improve freeze-drying of highly-concentrated protein formulations?* J. Pharm. Sci., 2013. 102(11): p. 3915-9.

[14] Colandene, J.D., et al., *Lyophilization Cycle Development for a High-Concentration Monoclonal Antibody Formulation Lacking a Crystalline Bulking Agent.* J. Pharm. Sci., 2007. 96(6): p. 1598-1608.

[15] Patel, S.M. and Pansare, S., *Can We Dry Above Tg ' for A High Concentration Antibody Formulation ?* 2012.

[16] Depaz, R.A., Pansare, S., and Patel, S.M., *Freeze-Drying Above the Glass Transition Temperature in Amorphous Protein Formulations While Maintaining Product Quality and Improving Process Efficiency.* 2016.

[17] Tang, X.C., Nail, S.L., and Pikal, M.J., *Freeze-drying process design by manometric temperature measurement: design of a smart freeze-dryer.* Pharm. Res., 2005. 22(4): p. 685-700.

CHAPTER III

III. DOES CONTROLLED NUCLEATION IMPACT THE PROPERTIES AND STABILITY OF LYOPHILIZED MONOCLONAL ANTIBODY FORMULATIONS?

This chapter was published in the *European Journal of Pharmaceutics and Biopharmaceutics* and appears in this thesis with the journal`s permission*:*

Ilona Vollrath[1,2], Wolfgang Friess[2], Angelika Freitag[1], Andrea Hawe[1], Gerhard Winter[2], (2018). "*Does controlled nucleation impact the properties and stability of lyophilized monoclonal antibody formulations?*" European Journal of Pharmaceutics and Biopharmaceutics, 129: 134-144.

Ilona Vollrath executed the experiments and wrote the manuscript for the paper. Wolfgang Frieß, Angelika Freitag, Andrea Hawe and Gerhard Winter provided scientific guidance and input during the experimental phase and the complete writing process. In addition, Wolfgang Frieß, Gerhard Winter and Andrea Hawe, who also serves as corresponding author, reviewed the final manuscript.

[1] Coriolis Pharma Research GmbH, D-82152 Martinsried, Germany

[2] Department of Pharmacy, Pharmaceutical Technology and Biopharmaceutics, Ludwig-Maximilians-University, D-81377 Munich, Germany.

III.1 ABSTRACT

This study provides the first systematic investigation of the impact of the nucleation protocol during freeze-drying on physico-chemical properties and long-term stability of two IgG1 antibodies in sugar formulations. We hypothesized that the lower specific surface area (SSA) generated by controlled nucleation could be beneficial for the stability of interface sensitive proteins. The study compares controlled nucleated (CN) and randomly nucleated (RN) lyophilizates with high and low antibody concentrations stored at different temperatures. Formulations with and without polysorbate (PS) were included.

In the “high concentration” study the formulation without PS showed reduced particle formation for CN samples compared to RN samples. PS containing formulations had an overall lower particle level with no further advantage of CN on stability. Besides the intended comparison of CN and RN samples, we observed that PS promoted sucrose crystallization in both low concentration antibody studies during storage. Additionally, our results indicate that the nucleation temperature (T_N) was not the only determining factor for the resulting ice crystal size and consequently the product`s SSA.

Overall, the application of CN had neither a positive nor a negative impact on the product`s physico-chemical stability. The surfactant had a much higher stabilizing effect than the reduction of the SSA by CN.

III.2 INTRODUCTION

Freeze-drying is the method of choice for proteins that cannot be stabilized sufficiently in a liquid formulation. Freeze-drying comprises the freezing step, primary drying, and secondary drying and is a time consuming and expensive process. Therefore, researchers aim to reduce especially the long primary drying phase by increasing the sublimation rates [1-3]. Searle et al. [4] found that the ice nucleation temperature (T_N) affects the primary drying rate and used T_N as an indicator for ice crystal size. Higher T_N resulted in higher primary drying rates and consequently shorter primary drying times [4]. An impact of T_N on primary drying rate had been reported before by Roy and Pikal, who observed that vials containing thermocouples nucleated at higher temperatures and completed primary drying earlier [5].

Recently, control over T_N gained high interest in the field of freeze-drying. Various studies have been conducted to investigate the impact of T_N on primary drying rate, specific surface area (SSA), and product resistance [6-11]. In a review, Geidobler and Winter [12] discuss the different technologies to induce ice nucleation and provide an overview of the difference in product characteristics, such as SSA and residual moisture (RM), between samples nucleated in a controlled way or randomly. Konstantinidis et al. [10] reported that higher T_N causes a small number of large ice crystals, resulting in a lyophilized product with large pores and corresponding low SSA [6]. In contrast, at low T_N a high number of small ice crystals is observed leading to a high SSA. On the one hand, the large pores of the controlled nucleated products reduce the product resistance and lead to a faster primary drying [4, 10]. On the other hand, during secondary drying, the low SSA hinders desorption leading to higher residual moisture levels [10], when secondary drying had not been adapted.

The above-mentioned studies focused mainly on process parameters e.g. primary drying rate and product resistance; however, the change in SSA and the eventually higher residual moisture could also impact product quality. Geidobler et al. [13] applied controlled nucleation to highly

concentrated protein formulations and showed that besides reducing primary drying time, the resulting large pores could also improve reconstitution times of a highly concentrated monoclonal antibody (mAb) formulation. A further aspect of a reduced SSA is the smaller interface the protein is exposed to. As proteins are known to be sensitive to interfaces [14-18], theoretically, a lower SSA could be beneficial as the product is less exposed to degradation reactions. Previously, Schersch et al. [19-21] found that a low SSA generated by collapse can be beneficial for the stability of pharmaceutically relevant proteins (e.g. monoclonal antibody type IgG1, Actilyse®, lactate dehydrogenase).

Although CN is getting more popular, there are only two published studies available on the influence of CN on protein stability. Awotwe-Otoo et al. [22] observed a lower degree of IgG1-glycation for lyophilizates with CN compared to RN. Recently, Fang et al. [23] correlated enzymatic activity and tetramer recovery of lactate dehydrogenase (LDH) with ice nucleation temperature. They found that at higher T_N reduced LDH degradation after freeze-thaw and freeze-drying. However, the study did not consider storage of the formulations.

Our study provides the first systematic investigation to evaluate the impact of the nucleation protocol, including T_N, on the physico-chemical properties and importantly the long-term stability of lyophilizates of two IgG1 antibodies. We compared formulations processed by CN at high and low T_N to samples processed by RN. Formulations at high and low concentration (76 or 100 mg/ml vs 1 mg/ml) were compared to study the effect of a different ratio of protein to stabilizer on stability after lyophilization with different nucleation protocols. Non-ionic surfactants, e.g. PS 80 or 20 are commonly used to stabilize proteins against interface related stress by covering the interface at concentrations above the critical micelle concentration (CMC) [15, 24, 25]. Although a polysorbate-free formulation is likely not stable, the beneficial effect of CN may be more pronounced. Therefore, formulations with and without PS were tested in this study to evaluate the impact of a reduced SSA by CN in the presence and absence of a surfactant.

III.3 MATERIALS AND METHODS

III.3.1 STUDY DESIGN

Two studies, one with high protein concentration (76 or 100 mg/ml) and one with low protein concentration (1 mg/ml), both with 2 different antibodies, were designed (Figure III-1). A model IgG1 mAb without PS (mAb1) and a model IgG1 mAb with PS (mAb2) were investigated. Within the high concentration study, both antibodies were subjected to (i) CN at -5 °C and (ii) a RN freezing protocol. The primary and secondary drying protocol was the same in all cases. Within the low concentration study, an additional CN temperature at -10 °C, which is in the range of T_N of the random nucleation process and the lowest achievable supercooling temperature allowing for CN before RN occurs, was included for mAb1. Thus, mAb1 was processed via (i) CN at -5 °C, (ii) CN at -10 °C, and (iii) RN. Furthermore, mAb1 was formulated with (+PS) or without polysorbate (-PS) to evaluate the influence of PS. MAb2 bulk drug substance solution already contained 0.04% polysorbate. Therefore, it was not possible to formulate mAb2 completely free of polysorbate. Instead, mAb2 was formulated with a nominal PS concentration of (i) 0.04% (+PS) and (ii) 0.0004% (dilution1:100), named as “without PS” (-PS). Based on the results of the at first performed mAb1 study, CN at -10 °C was not included in the mAb2 studies.

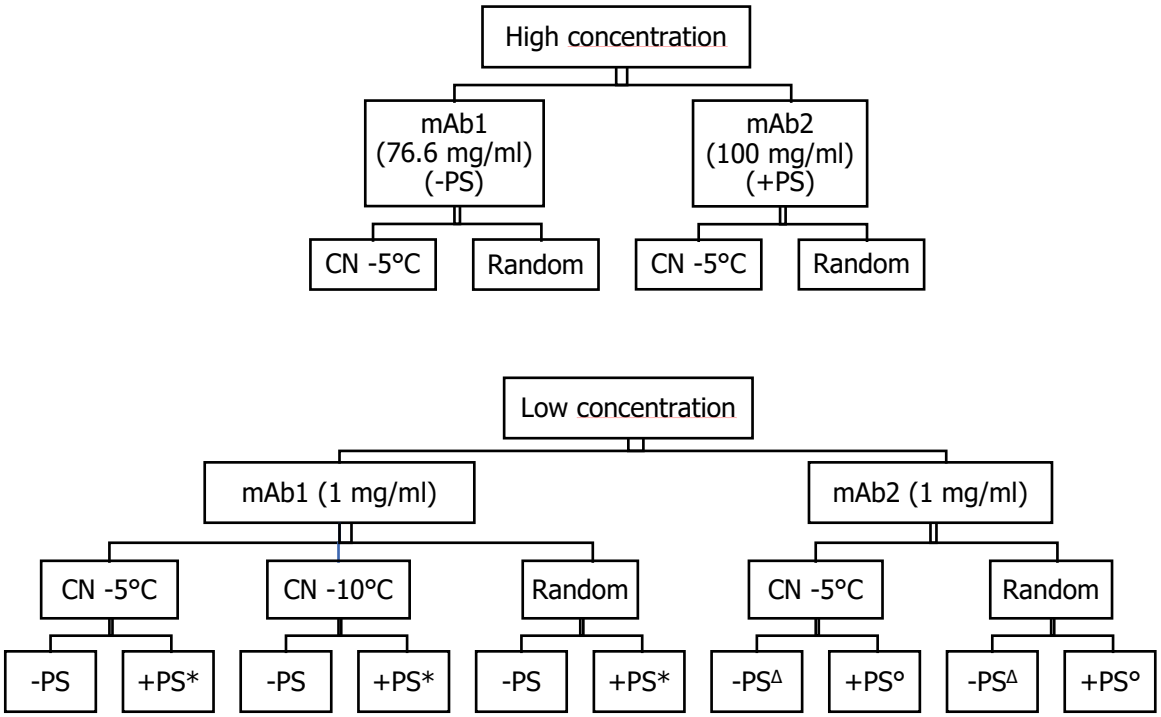

Figure III-1: Scheme of study designs for the high and low concentration study. * 0.04% PS 20. ° 0.04% PS 80. Δ 0.0004% PS 80; considered as "without polysorbate" (-PS).

III.3.2 MATERIALS

Two model monoclonal antibodies mAb1 and mAb2 (both IgG1) were used in this study. Di-sodium hydrogen phosphate (AppliChem), sodium dihydrogen phosphate (AppliChem), and Ph.Eur. grade sucrose were purchased from VWR. PS 20 and PS 80 Ph.Eur. grade were purchased from Sigma-Aldrich. Low protein binding polyvinylidenfluorid (PVDF) and polyethersulfone (PES) 0.22 µm filters were purchased from Merck Millipore (Millipore, Schwalbach, Germany). 2R glass type I tubing vials were kindly provided by MGlas AG (Münnerstadt, Germany). Rubber stoppers, 13 mm (Westar® RS, 4023/50, bromobutyl, grey, FluoroTec B2-40 coating) were kindly supplied by West Pharmaceutical Services (Eschweiler, Germany). Further, standard aluminum crimp caps compatible with 13 mm stoppers were used. All vials and stoppers were washed manually three times with highly purified water (Milli-Q, Merck Millipore, Hertfordshire, United Kingdom). Vials were heat sterilized for at least 120 min

at 180 °C; stoppers were autoclaved at 121 °C for 20 min and dried at 80 °C not longer than 8 h after autoclaving. The stoppers were not re-dried prior to lyophilization.

III.3.3 SAMPLE PREPARATION

For the mAb1 high concentration study, mAb1 stock solution was first concentrated using a Minimate II Tangential Flow Filtration (TFF) system (Pall, Crailsheim, Germany) equipped with a 30 kDa TFF capsule (Omega™ PES membrane). For the mAb1 low concentration study, the mAb1 stock solution was diluted with a 10 mM phosphate buffer (pH 6.4). The mAb2 stock solution was dialyzed against a 10 mM phosphate buffer (pH 6.4) containing 0.04% PS 20. Slide-A-Lyzer™ Dialysis Cassettes (10 kDa; 12-30 ml) (ThermoFisher Scientific, Ulm, Germany) were used and three buffer changes were performed (after 4 h, 6 h and overnight). The formulations were prepared according to the respective composition described in Table III-1.

Table III-1: Overview of the composition of the formulations used in this study.

Description	Buffer system	mAb concentration [mg/ml]	Sucrose [mg/ml]	Polysorbate 80 [%]	Polysorbate 20 [%]
mAb1 high concentration (-PS)	10.5 mM phosphate pH 6.4	76.6	50	0.00	----
mAb1 low concentration (+PS)		1.0		0.04	----
mAb1 low concentration (-PS)		1.0		0.00	----
mAb2 high concentration (+PS)		100.0		----	0.04
mAb2 low concentration (+PS)		1.0		----	0.04
mAb2 low concentration (-PS)		1.0		----	0.0004*

Compounding was performed as follows: For mAb1, the target sucrose amount was dissolved in buffer before the antibody was then added. Subsequently, the formulation was filtered through

a 0.22 µm PVDF filter before the PS was added to the corresponding formulations. For mAb2, the polysorbate was added to the buffer with sucrose and mAb2 before filtering the formulations through a 0.22 µm PES membrane filter. To mitigate PS adsorption, the filter was pre-rinsed with PS and sucrose containing buffer. As we aimed to allow certain degradation, a low stabilizer concentration (50 mg/ml sucrose) was used resulting in a high protein to sugar ratio whereby the protein is likely more prone to instabilities. Additionally, a placebo formulation of each formulation was prepared. Sample aliquots of 1.0 ml were manually filled under laminar flow conditions and the vials were semi-stoppered manually. The formulations were lyophilized on the same day or the day after.

III.3.4 LYOPHILIZATION

Lyophilization was performed using an Epsilon 2-12D pilot scale freeze-dryer (Martin Christ, Osterode, Germany). The vacuum during the freeze-drying process was controlled by a capacitance (MKS) gauge. For product temperature monitoring and end of primary drying determination, thermocouples were used.

By default, vials were backfilled to 600 mbar prior to stoppering. After completing backfill, the closed vials were stored at 5 °C until unloading. Subsequently, the vials were crimp capped with aluminum flip off caps. Deviation from this standard protocol will be stated in the affected sections.

CN was performed by following the protocol described by Geidobler et al. [26]. To increase the amount of water vapor in the chamber, a tray with 1000 ml high-purified water was placed into the freeze-dryer. The vials were equilibrated for 2 h at the aimed nucleation temperature of -5 °C or -10 °C. After nucleation, the water tray was removed, and the shelf temperature was ramped to -50 °C at 1 °C/min. RN samples were equilibrated to 2 °C for at least 1 h before the shelf temperature was lowered to -50 °C at 1 °C/min. A hold time of 120 min at -50 °C was applied to all freezing protocols prior to initiating primary drying.

III.3.4.1 HIGH CONCENTRATION STUDIES DRYING PARAMETERS

One CN and one RN freeze-drying cycle was performed. For both, primary drying was carried out at a shelf temperature of 0 °C (ramp rate: 0.5 °C/min) and a chamber pressure of 0.25 mbar. For secondary drying, the shelf temperature was raised to 30 °C for RN process and to 35 °C for CN process with a ramp of 0.1 °C/min and held for 6 h at unchanged pressure of 0.25 mbar.

III.3.4.2 LOW CONCENTRATION STUDIES DRYING PARAMETERS

One CN process and one combined process for RN and CN-10 was executed. For both, primary drying shelf temperature was set to -35 °C (ramp rate: 0.5 °C/min) and the chamber pressure to 0.02 mbar. Secondary drying was performed in two steps to allow adjustment of RM level between the different nucleation protocols. In a first step, the shelf temperature was raised to 30 °C (with 0.1 °C/min to 5 °C and 0.2 °C/min to 30 °C). After a holding time of 6 h, the shelf temperature was raised to 40 °C (0.2 °C/min) and held for another 6 h. The CN samples, which have slower desorption rates, were subjected semi stoppered to both secondary drying steps, whereas the CN-10 and RN samples (faster desorption rates) were completely stoppered after the first secondary drying step (under full vacuum) and subjected to the additional secondary drying step only to assure equal thermal history. For comparability, CN-5 samples were also stoppered under full vacuum after both secondary drying steps.

III.3.5 SAMPLING TIME POINTS AND STORAGE CONDITIONS

Samples of the mAb1 high concentration study and the mAb2 studies were incubated at 40 °C and 75% relative humidity. Due to material constraints and the high material requirements, the high concentration studies were performed only under accelerated conditions. MAb1 high concentration samples were investigated over 12 months and analyzed after freeze-drying, 1, 6, and 12 months upon storage. The mAb1 low concentration samples were stored at 40 °C/75% r. H. and at 2-8 °C and analyzed after freeze-drying and after 3, 6, and 12 months

of storage. MAb2 high and low concentration samples were stored at 40 °C/75% r. H. and studied over 7 months and analyzed after freeze-drying, 3, and 6 months. Selected analytical characterization was additionally performed after 7 months of storage.

III.3.6 DATA ANALYSIS AND ILLUSTRATION

Throughout the manuscript, error bars represent the standard deviation (based on n = 3). If no error bars are shown, only one sample was analyzed due to material constraints.

III.3.7 KARL FISCHER TITRATION (KF)

The residual moisture of the lyophilized cakes was determined using the coulometric Karl Fischer titrator Aqua 40.00 (Analytik Jena GmbH, Jena, Germany), which is equipped with a headspace module. About 20 mg of sample was weighed into a 2R glass vial under a glovebox (r.h. ≤ 5%). The sample was analyzed at 150 °C. Prior to the measurements, a system suitability test was performed daily by measuring a pure water standard (Apura 1 water standard oven 1.0, Merck KGaA).

III.3.8 DIFFERENTIAL SCANNING CALORIMETRY (DSC)

The glass transition temperatures T_g' (of the frozen product) and T_g (of the lyophilized product) were determined by DSC (Mettler Toledo DSC1_943, Mettler Toledo, Giessen, Germany). Approximately 30 µl or 10 mg, respectively, of the product were transferred into an aluminum crucible (Mettler Toledo, Giessen, Germany). For $T_g`$ determination, the samples were cooled to -80 °C with 10 K/min and re-heated to 20 °C with a heating rate of 10 K/min. For T_g determination, two heating cycles were performed. First, the samples were cooled to 0 °C with 10 K/min and re-heated to 130 °C with a heating rate of 10 K/min. Second, the samples were re-heated to 160 °C after cooling to 0 °C. The midpoint of the endothermic shift of the baseline during the heating scan was taken as $T_g`$ or T_g. For the high concentration studies, the 2nd

heating scan was considered, whereas for the low concentration studies the first heating scan was taken into account.

III.3.9 X-RAY POWDER DIFFRACTION (XRD)

The morphology of the lyophilized products was investigated by wide angle X-ray powder diffraction (XRD) (Empyrean; equipped with a copper anode (45 kV, 40 mA, $K_{\alpha 1}$ emission at a wavelength of 0.154 nm) and a PIXcel3D (Panalytical, Almelo, The Netherlands). Approximately 100 mg of the freeze-dried samples were analyzed in reflection mode in the angular range from 5-45° 2θ, with a step size of 0.05° 2θ and a counting time of 100 per step.

III.3.10 BET ANALYSIS

The SSA of the lyophilized material was analyzed by the BET method using an Autosorb-1 (Quantachrome Instruments, Germany). For sample preparation, approximately 100 mg lyophilized sample was carefully crushed with a spatula into small pieces and filled in a measurement tube. Degassing was performed for at least 2 h at 25 °C. Subsequently, Krypton sorption measurement was performed at 77.3 K. At least 5 data points were collected covering a p/p_0 region of 0.05 to 0.3. The data points were evaluated according to the multipoint BET-method with $r \geq 0.997$ for all samples.

III.3.11 RECONSTITUTION PROCEDURE AND DETERMINATION OF RECONSTITUTION TIME

The lyophilized products were reconstituted under laminar flow conditions. The required volume for reconstitution was calculated for each formulation based on the density of the liquid formulation and the total solid content. The desired amount of highly purified water was added to the center of the lyophilized product. The vial was carefully slewed. The time until complete reconstitution was recorded as reconstitution time.

III.3.12 MICRO-FLOW IMAGING (MFI)

MFI was chosen to determine micrometer-sized particles as it provides more information on particle`s morphology based on images, compared to the compendial required light obscuration method. Furthermore, MFI requires less sample volume, which was a limiting factor in our study. An MFI-5200 particle analyzer system (ProteinSimple, Santa Clara, CA, USA) equipped with a silane coated high-resolution 100 µm flow cell and controlled by MFI View software was used. The system was flushed with at least 3 ml highly purified water at maximum flow rate prior to each measurement. Corresponding placebo buffers were used to perform “optimize illumination” after the cell cleanliness was checked before each measurement. The samples of the high concentration studies were diluted to 1 mg/ml with the corresponding placebo buffer. For the mAb1 high concentration samples (0.75 ml), a purge volume of 0.3 ml was set, and 0.33 ml of the samples were analyzed. For all other samples (0.65 ml) a purge volume of 0.17 ml was used, and 0.28 ml were analyzed. All samples were pipetted using filter tips. MFI View System Software (MVSS) version 2-R2-6.1.20.1915 was used to perform the measurements and MFI View Analysis Suite (MVAS) software version 1.3.0.1007 was used to analyze the samples.

III.3.13 DYNAMIC LIGHT SCATTERING (DLS)

DLS was used to measure the size and size distribution of particles in the submicron region (1 nm-1 µm). Measurements were conducted using a Zetasizer APS 2000 plate reader (Malvern Instruments, Worcestershire, UK) instrument. Three wells (n=3, each with 150 µl of the sample) were analyzed using automatic measurement mode at 20°C at an angle of 90°. All samples were pipetted under laminar flow. MAb1 samples (high and low concentration study) were analyzed without dilution. Samples of the mAb2 high concentration study were diluted (w/w) to 1 mg/ml. The Malvern Zetasizer Software was used to fit the autocorrelation function using the

default settings for protein solutions and to calculate z-average diameter, polydispersity index (PDI), and particle size distribution by intensity.

III.3.14 HIGH PERFORMANCE SIZE EXCLUSION CHROMATOGRAPHY (HP-SEC)

Protein monomer, dimer, fragments, and high molecular weight soluble aggregates were determined by HP-SEC (HP 1100, Agilent Technology). All separations were performed using a TSKgel G3000 SWXL column (Tosoh Bioscience, Stuttgart, Germany) at a flow rate of 0.5 ml/min with a sample loading of 20 µg and UV detection at 280 nm. A 50 mM sodium phosphate buffer with 300 mM sodium chloride at pH 7.0 was used as mobile phase. Prior to analysis, the samples of the high concentration studies were diluted to 1 mg/ml with formulation buffer.

III.3.15 SODIUM DODECYL SULFATE-POLYACRYLAMIDE GEL ELECTROPHORESIS (SDS-PAGE)

Covalent aggregates and fragments of mAb2 low concentration study samples were assessed using reducing and non-reducing SDS-PAGE. Analysis was performed with a XCell SureLock™ Mini-Cell Electrophoresis System (Novex® by Life Technologies, Carlsbad, CA, USA). For reducing conditions, a NuPAGE® Novex® 4-12% Bis-Tris Protein Gel with NuPAGE® MES SDS Running Buffer (200 V for approximately 35 min) was used. Non-reducing conditions analysis was accomplished using a NuPAGE® Novex® 3-8% Tris-Acetate Protein Gel with NuPAGE® Tris-Acetate SDS Running Buffer (150 V for approximately 55 min). For reducing conditions, 80 µl sample at 100 µg/ml was admixed with 40 µl NuPAGE® LDS Sample Buffer, 16 µl of NuPAGE® Reducing Agent and 24 µl of the corresponding placebo buffer (final concentration of 50 µg/ml). For non-reducing conditions, the 16 µl of reducing agent were replaced by placebo buffer. All samples were denatured at 90 °C for 5 min. Each well was loaded with 12 µl sample which resulted in a total mass of 0.6 µg protein per well. Gels were stained with a SilverQuest™

Staining Kit (Invitrogen® by Life Technologies) according to supplier's instructions. To assess size of protein bands, Molecular weight markers were added on each gel. For reducing conditions, Mark12™ Unstained Standard and for non-reducing conditions HiMark™ Pre-stained Protein Standard (both from Invitrogen® by Life Technologies) was applied. SDS-PAGE gels were scanned with a GS-800 densitometer (BioRad Laboratories, Hercules, CA, USA).

III.4 RESULTS

III.4.1 HIGH CONCENTRATION STUDY

CHARACTERISTICS OF THE LYOPHILIZATES

First, product appearance was compared. After freeze-drying, mAb1 and mAb2 RN cakes showed a white to yellowish, compact, appearance with a shiny surface, minor shrinkage in height, and tiny cracks. The structure of CN cakes was more porous, loose, and shiny. Comparable shrinkage in height was observed for RN and CN samples, however crack formation was more pronounced in CN samples. During storage, minor loss in cake structure was observed for RN and CN samples similarly (Photographs provided in APPENDIX Figure VIII-3).

Next, the freeze-dried product´s RM content, morphology, and glass transition temperature was analyzed. Immediately after freeze-drying the RM were below 1% for all samples (APPENDIX Figure III-2). As expected, the CN samples had higher RM content as the RN samples after freeze-drying in mAb1 and mAb2 study. During storage, RM increased in parallel for CN and RN samples. DSC results were in line with the KF results. After freeze-drying, overall high T_g values, 75 °C for mAb1 CN and 79 °C for mAb1 RN samples, were determined (APPENDIX Figure VIII-4). The higher RM of the CN samples resulted in an initially lower T_g compared to RN. Upon storage, the T_g values decreased in all cases. XRD showed that the samples were fully amorphous without crystallization during storage (APPENDIX Figure VIII-5).

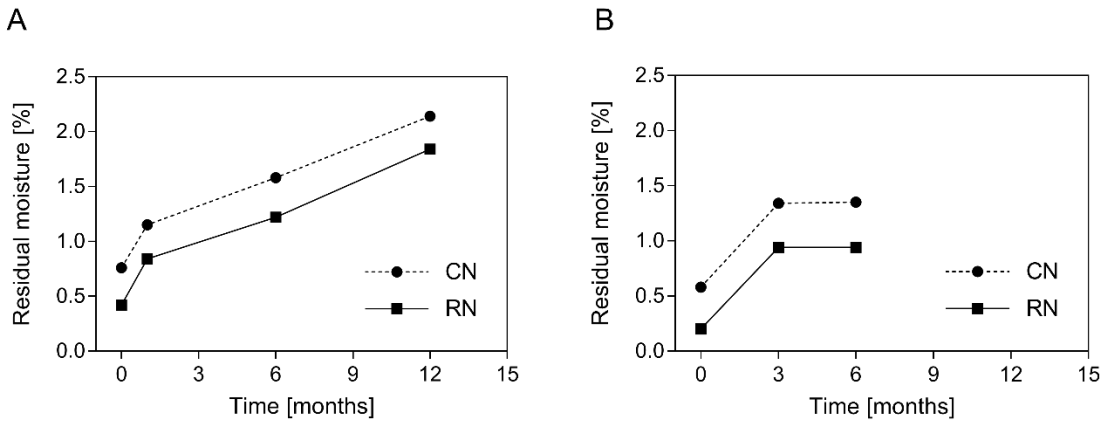

Figure III-2: RM content of CN and RN samples of (A) mAb1 and (B) mAb2 high concentration study over storage time at 40°C/75% r.h..

The results of the SSA measurements confirmed the successful performance of CN because after freeze-drying, a lower SSA was observed for CN samples compared to RN samples for both mAb studies (Figure III-3). Over 6 months storage time, a decrease in SSA by 16% for mAb1 CN samples and of 33% for mAb1 RN samples was noted. The same tendency was observed for mAb2 (CN samples decreased by 24%; RN samples by 38%).

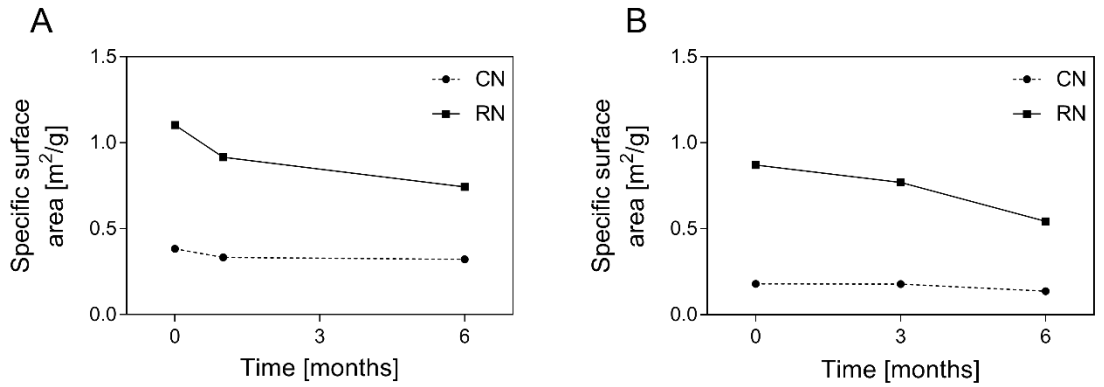

Figure III-3: SSA of CN and RN samples of (A) mAb1 and (B) mAb2 high concentration study over storage at 40°C/75% r.h..

MAB STABILITY

No difference in the relative content of monomer and higher molecular weight species (HMW) determined by HP-SEC was observed when comparing CN and RN within one study (Figure III-4). During the stability study, both antibodies showed an increase in HMW content and aggregate formation in mAb1 samples was more pronounced than in mAb2 samples.

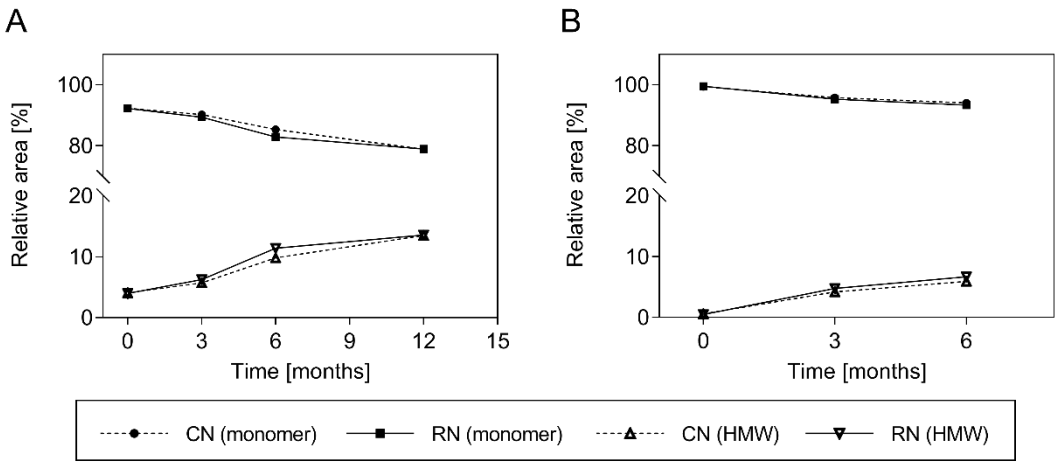

Figure III-4: Monomer and HMW relative content for mAb1 (A) and mAb2 (B) over storage at 40°C/75% r.h. (standard deviations below resolution; n=3).

MFI was used to quantify particles in the micrometer size range. After freeze-drying, comparable particle counts were measured for mAb1 CN and RN samples. During storage, mAb1 CN samples showed less particle formation in the micrometer size range compared to the RN samples (Figure III-5A). For mAb2, no difference between the samples generated by the different nucleation protocols could be detected after freeze-drying and upon storage (Figure III-5B).

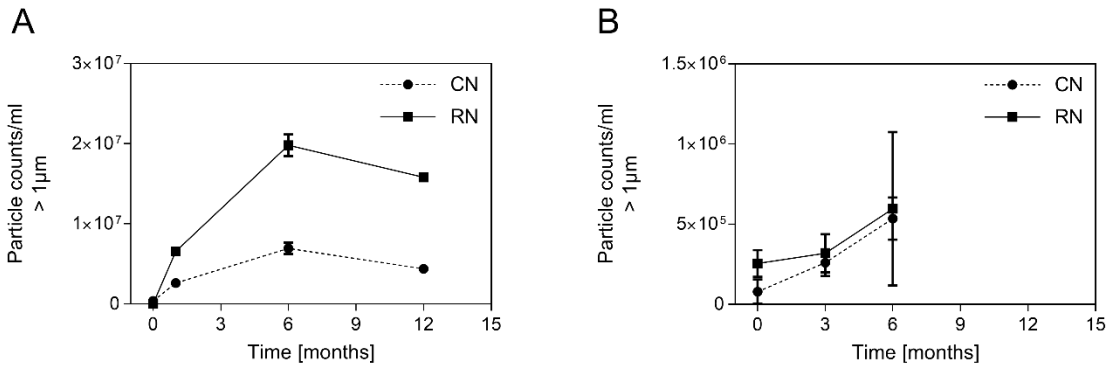

Figure III-5: Cumulative particle counts of particles ≥ 1 µm for (A) mAb1 and (B) mAb2 over storage at 40°C/75% r.h.. Please note that the y-axis is scaled differently in A and B to achieve better resolution.

Additionally, the particle size distribution in the nm-size range was measured by DLS. For mAb1, a difference in z-average between CN and RN samples was observed. After lyophilization (T0), a z-average of ~ 10 nm was measured for both formulations, which is expected for a mAb. MAb1 CN samples show less increase in z-average values over storage than corresponding RN samples (Figure III-6A). Further, the size distribution for mAb1 CN samples showed a lower level of aggregates with increasing storage time compared to the RN samples (APPENDIX Figure VIII-6A and B). For the mAb2 study, no difference between the CN and RN samples regarding z-average values and size distribution was identified (Figure III-6B, APPENDIX Figure VIII-6C and D).

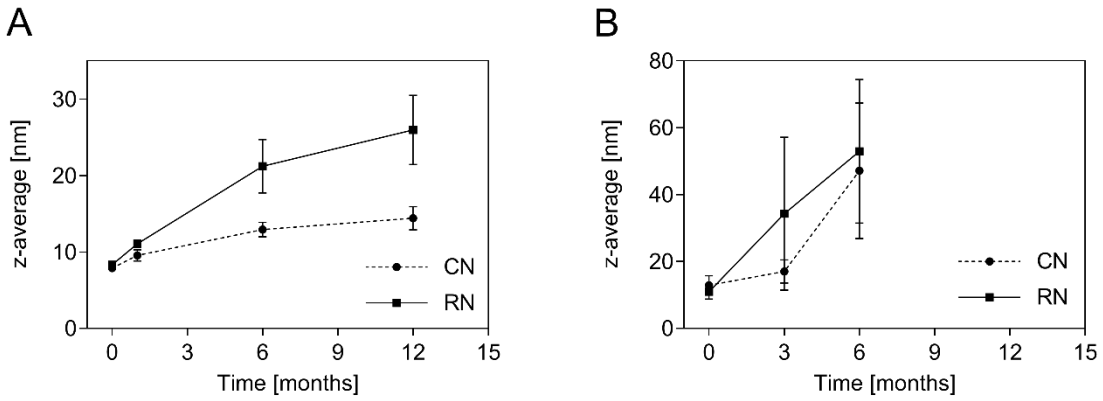

Figure III-6: z-average of CN and RN samples of (A) mAb1 and (B) mAb2 high concentration study over storage at 40°C/75% r.h..

III.4.2 LOW CONCENTRATION STUDY

STORAGE AT 5°C (MAB1)

The analysis of the freeze-dried products of the mAb1 samples stored at 5 °C did not show any change over a storage time of 12 months. T_g, RM and XRD refractograms of T12m were comparable to T0 for both nucleation protocols. No change in monomer content over 12 months of storage was recognized. However, a minor increase in micrometer sized particles in both nucleation protocols of formulations without PS was observed compared to T0. Formulations with PS were comparable to T0. As these results did not indicate any difference between CN and RN samples and the changes over time are minor, the 5°C data are not discussed further.

STORAGE AT 40°C/75% R.H. (MAB1 AND 2)

CHARACTERISTICS OF THE LYOPHILIZATES

MAb1 RN samples showed a white, compact, cylindrical cake with a shiny surface, minor shrinkage in height, and tiny cracks. The structure of mAb1 CN-5 cakes was more porous, loose and shiny. Shrinkage in height and crack formation was more pronounced in mAb1 CN-5 samples compared to RN samples. The cake structure of mAb1 CN-10 samples was more

comparable to CN-5 samples than to RN samples. However, the level of shrinkage in height and crack formation ranged between the CN-5 and RN samples of mAb1. After 3 months of storage at 40 °C/75% r.h., no change in optical appearance was determined for any of the mAb1 samples (all nucleation protocols). At 6 months' time point mAb1 CN-5 and CN-10 samples showed a loss in cake structure and began to collapse. The degree of collapse was higher in CN-10 samples, which had a higher residual moisture (see below). For mAb1 RN samples, no change was documented. After 12 months of storage at 40 °C/75% r.h., collapse was observed in all mAb1 samples (Photographs provided in APPENDIX Figure VIII-7).

For mAb2, the differences in cake structure between CN-5 and RN samples were less pronounced. The change in cake appearance over storage time (40 °C/75% r.h.) was comparable to mAb1 with no change up to 3 months and beginning collapse at 6 months. In contrast to mAb1, mAb2 RN samples collapsed to the same degree as CN-5 samples. As for mAb1, no difference between the formulation with and without PS was determined (Photographs provided in APPENDIX Figure VIII-7).

Next, the freeze-dried product was analyzed by KF titration, SSA measurement, XRD and DSC. At T0, immediately after freeze-drying, all formulations of mAb1 and mAb2 showed RM below 1% (Figure III-7). The alignment of the RM content to a similar level between the CN and RN samples by two secondary drying steps was successful for the CN-5 and RN samples. The samples of mAb1 nucleated at CN-10 were expected to show drying properties comparable to RN samples due to the comparable low T_N. Therefore, the mAb1 CN-10 samples had been subjected to the same secondary drying protocol as the RN samples. However, the drying behavior differed from the RN samples, thus, the CN-10 samples of mAb1 showed higher RM (Figure III-7A). An increase in RM over storage time was observed for all samples of both antibodies (Figure III-7A and B). After 6 months of storage, no differences between the nucleation protocols and the formulations with and without PS were observed.

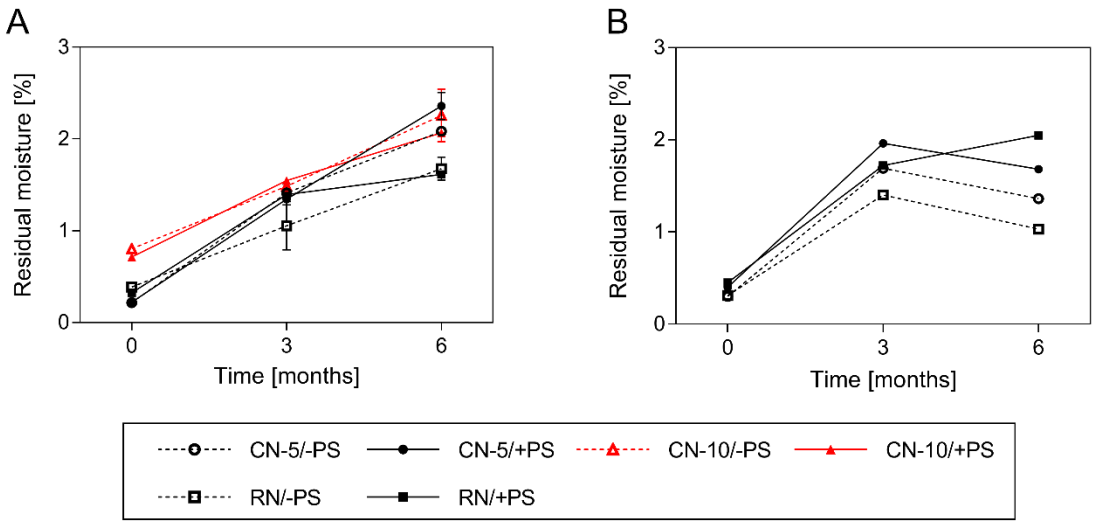

Figure III-7: Residual moisture content of CN and RN samples of low concentration study over storage time. (A) mAb1 and (B) mAb2. After 12 months, analysis via KF titration was not possible for the collapsed samples.

SSA measurements confirmed the explanation for the higher RM of mAb1 CN-10 samples. Although CN-10 samples were nucleated at a low T_N, their SSA and consequently their drying behavior was comparable to the samples controlled nucleated at -5 °C (Figure III-8A) and not to the randomly nucleated samples. In both mAb studies, for all CN samples a lower SSA was determined compared to the RN samples (Figure III-8). Thus, CN was successfully performed. With increasing storage time, a loss in cake structure based on both appearance and SSA was observed. For mAb1 RN samples a loss in SSA of about 15% was determined, whereas for mAb1 CN-5 and CN-10 samples a loss of about 40% was noted. For mAb2, SSA decreased comparably in CN and RN samples. Additionally, no difference between formulations with and without PS could be identified.

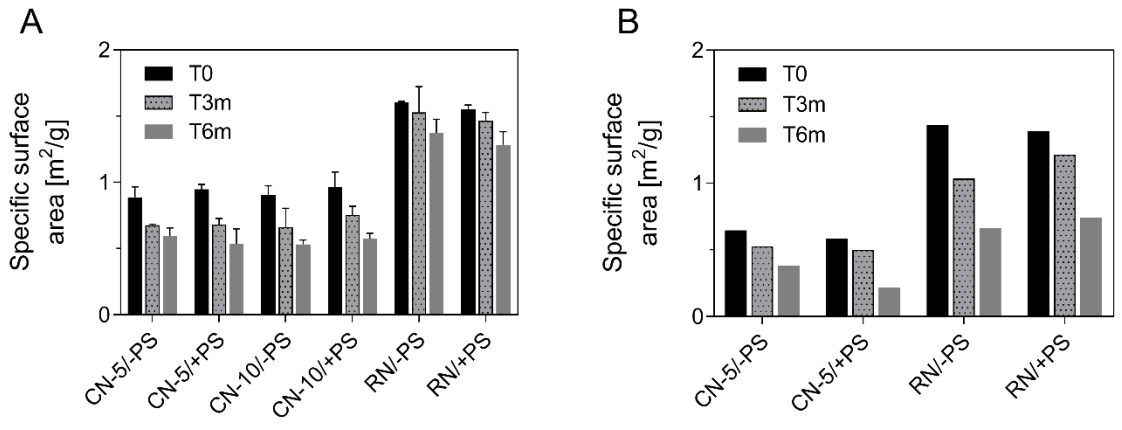

Figure III-8: Results of SSA measurements of CN and RN samples over storage time. (A) mAb1 and (B) mAb2 low concentration study. After 12 months, analysis via BET was not possible for the collapsed samples.

XRD measurements pointed towards an amorphous structure of all formulations after freeze-drying (Figure III-9). Formulations without PS did not change morphology during storage. Surprisingly, PS provoked sucrose crystallization within the lyophilized formulations during storage. After 12 months of mAb1 storage and after 7 months of mAb2 storage, respectively, sucrose crystallization was observed only in the PS containing formulations, independent of the nucleation protocols in both antibody studies.

The above observed increase in RM during storage resulted in a decrease of T_g measured by DSC (APPENDIX Figure VIII-8). Comparable to the RM results, no differences between the nucleation protocols could be detected. The DSC thermograms confirmed sucrose crystallization provoked by PS, which agrees with XRD. Figure III-10 displays examples of thermograms of CN-5 and RN (-PS/+PS) samples of mAb1 and mAb2. Sucrose crystallization during storage was only observed in PS containing formulations, when no T_g could be measured anymore (Figure III-10: right column).

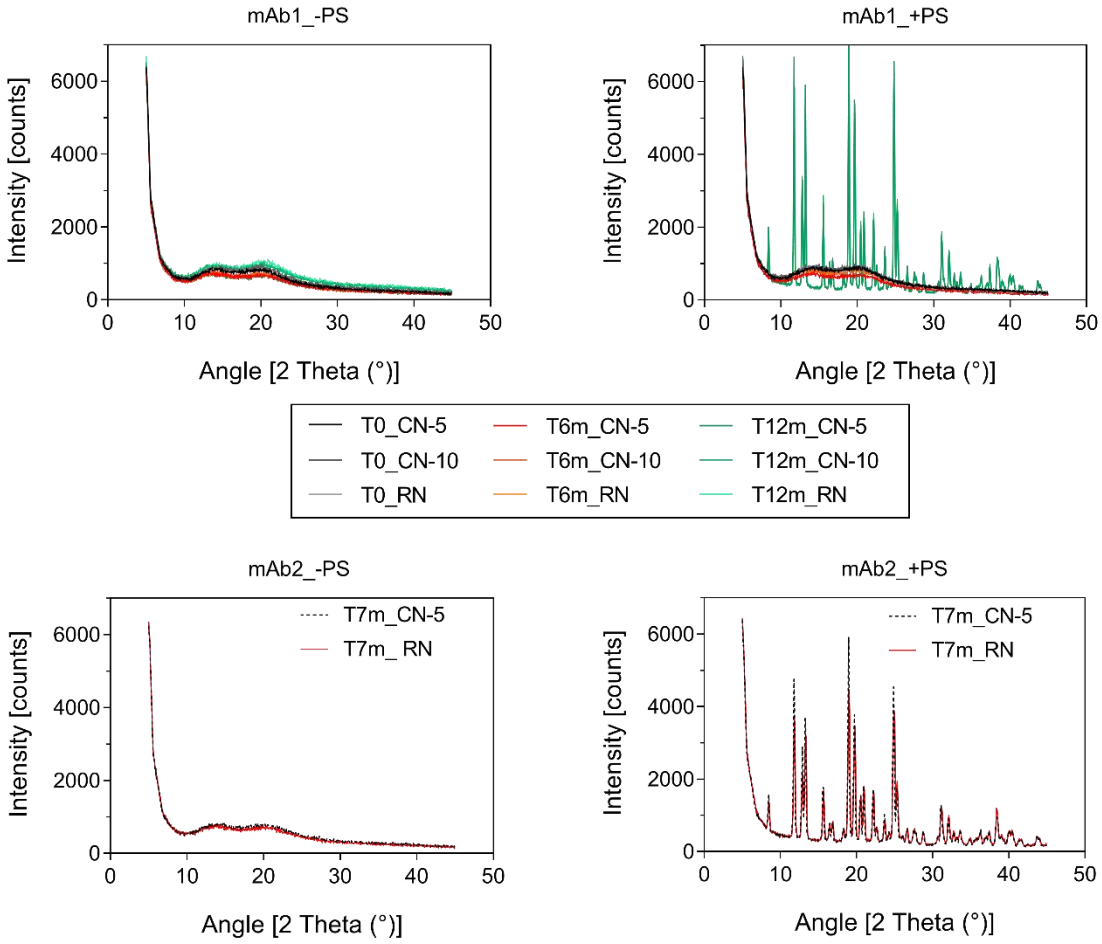

Figure III-9: XRD-refractograms of all nucleation protocols of mAb1 (top row) and mAb2 (bottom row) of the formulations without PS (left column) and the formulations containing PS (right column). For mAb1 the results at T0, T6m and T12m are exemplarily shown. For mAb2 XRD measurements were performed only at T7m to confirm DSC results.

The peak, observed at temperatures ≥ 70 °C, appears due to sucrose degradation at elevated temperatures and does not indicate the sample morphology (amorphous or crystalline) upon storage. (Figure III-10: top row, right column, CN-5 is provided as example). Sucrose crystallization in PS containing samples of mAb2 was first observed for the CN-5 samples after T6m, and slightly later for mAb2 RN samples (between 6 months and 7 months of storage). For the mAb2 RN samples, a T_g was determined at T6m, indicating an amorphous structure (Figure III-10: bottom row, right column), whereas at T7m no T_g could be detected anymore (pointing towards sucrose crystallization).

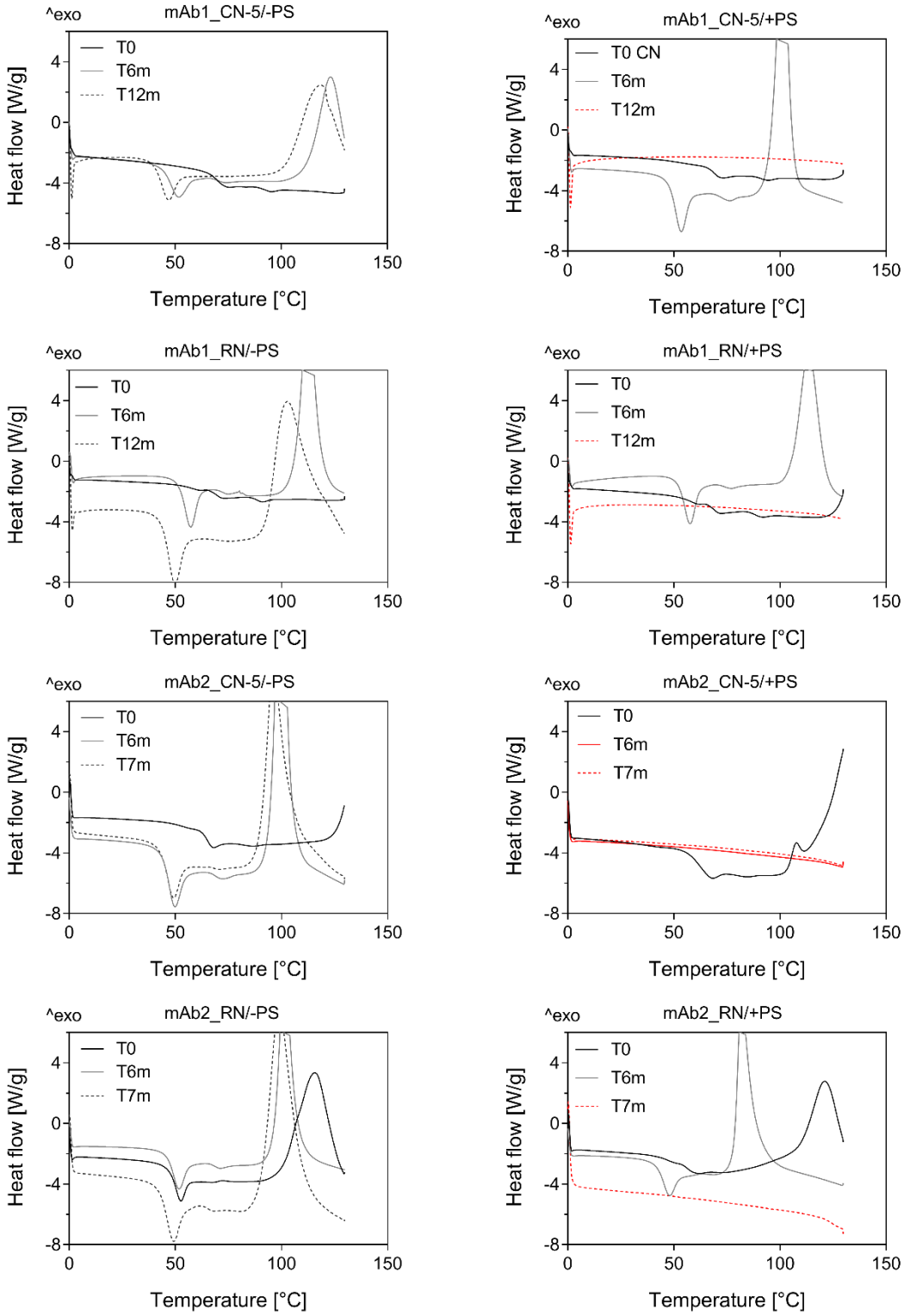

Figure III-10: Examples of DSC thermograms of controlled nucleated and random nucleated samples of mAb1 at T0, after 6 months (T6m) and 12 months (T12m) of storage and mAb2 at T0, after 6 months (T6m) and 7 months (T7m) of storage. The graphs of the left column display the formulations without PS, whereas the graphs in the right column show the corresponding formulations with PS.

MAB STABILITY

HP-SEC was used to study protein aggregation and fragmentation. Additionally, nanometer and micrometer range particles of all reconstituted samples were assessed by DLS or MFI, respectively. The HP-SEC results for mAb1 did neither show aggregation nor fragmentation of mAb1 independent of the nucleation protocol (Figure III-11A and B). For mAb2 CN-5/+PS samples, a decrease in monomer content and a corresponding increase in HMW species at T6m was detected (Figure III-11C and D). The mAb2 RN/+PS samples showed the same trend at T7m. A slight increase in fragments was determined for both nucleation protocols at T7m. The corresponding formulations without PS did not show any change in monomer content, HMW or fragments over a total storage time of 7 months. The increase in HMW was observed at the same time points as the sucrose crystallization.

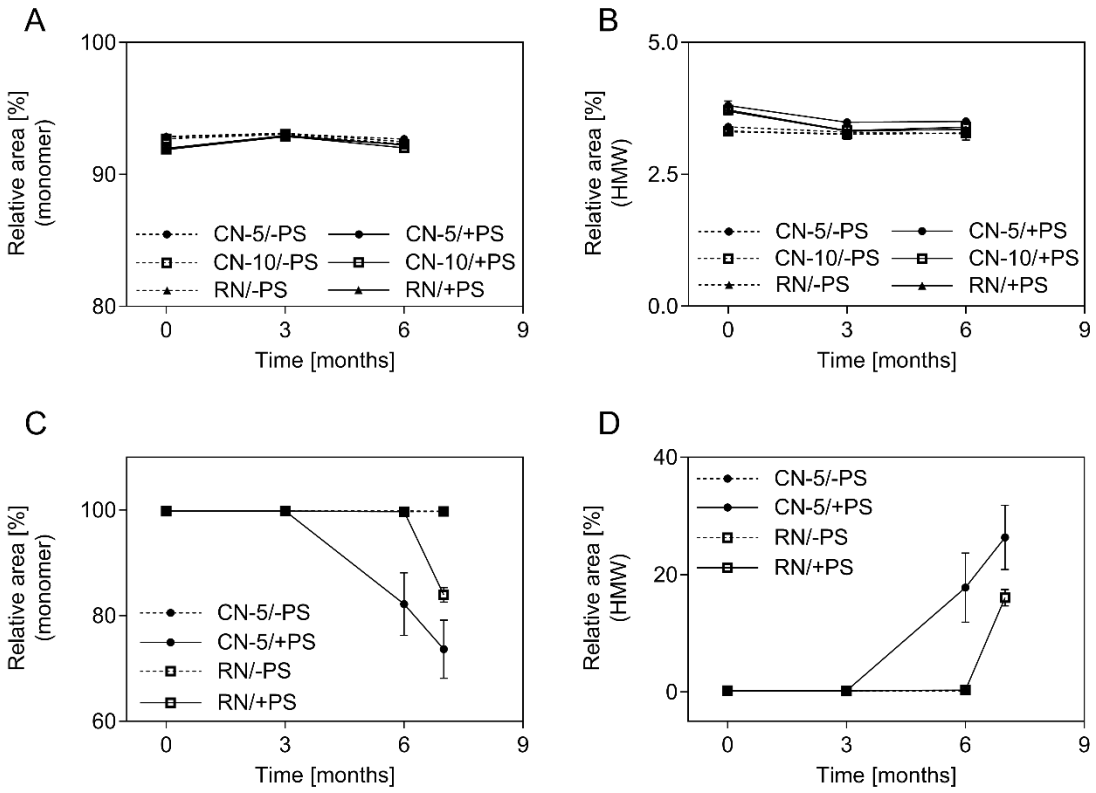

Figure III-11: (A) Monomer content of mAb1, (B) HMW species content of mAb1, (C) monomer content of mAb2 and (D) HMW species content of mAb2, measured by HP-SEC.

For mAb2 samples, reducing and non-reducing SDS-PAGE was performed to further characterize the HMW species observed in HP-SEC. The observed aggregation in SDS-PAGE was more pronounced in mAb2 CN-5/+PS than in the mAb2 RN/+PS samples at T7m. From SDS-PAGE under reducing conditions, it could be proven that the aggregates were S-S-linked (APPENDIX Figure VIII-9and Figure VIII-10).

Both, DLS and MFI data did not indicate a difference with respect to nanometer and micrometer range particle formation between the nucleation protocols after freeze-drying and upon storage in both antibody studies (APPENDIX Figure VIII-11 and Figure VIII-12). Independent from the nucleation protocol, lower particle numbers were observed for the PS containing formulations.

III.5 DISCUSSION

Our study provides a systematic investigation on the impact of CN protocols (including T_N) on long-term stability of pharmaceutically relevant IgG1 formulations over a storage time of at least 6 months. We hypothesized that the lower SSA generated by CN at higher T_N could be beneficial for the stability of proteins, which are sensitive to interfaces. We investigated this hypothesis by a high concentration and a low concentration mAb study. Furthermore, as the relevance of a potential surface exposure and other stresses could be diminished by the surfactant effect, formulations with and without PS were compared.

First, the results of the high concentration study will be discussed. Then, a discussion of the results of the low concentration study including a comparison of both studies will follow. Details of the freeze-drying processes and primary drying times are provided as supplementary material (APPENDIX Figure VIII-13, Figure VIII-14, Table VIII-1), as the optimization of the drying time was not focus of this study. As expected, CN processes resulted in either a faster primary drying or CN and RN processes did not differ [4, 6, 10].

We noted a difference in cake appearance between the CN and RN samples for both antibodies at both concentrations. Overall, cake appearance can be considered as pharmaceutically acceptable for both CN and RN, with the cakes from RN having a more elegant appearance. As such an optical difference has been reported before by Awotwe-Otoo et al. [27], our results confirm the literature and were not surprising. A recently published commentary by Patel et al. [28] on cake appearance suggests judging product quality mainly with respect to patient safety. Transferring this perspective to our study, the different appearance of CN samples can be accepted as we did not observe a negative effect of CN on protein stability.

III.5.1 HIGH CONCENTRATION STUDIES

We expected a higher RM for CN samples due to the lower SSA and the therefore slower desorption rate during secondary drying [6, 10] as, in contrast to the low concentration study, the secondary drying process was not adjusted. At T0, CN and RN samples have RMs of less than 1% and are therefore considered as well dried. However, based on the higher RM of CN samples, a higher level of SSA loss over storage time would have been expected for CN samples, while we observed a faster decrease of SSA in RN samples. Additionally, DSC and XRD data did not indicate any effect (e.g. excipient crystallization) due to the higher RM content of the CN samples. This observation holds true for both antibodies.

For mAb 1 without surfactant (-PS), less particle formation (nanometer and micrometer sized range) was found for CN samples compared to RN samples, which confirms our hypothesis that a reduced surface/interface prevents proteins from surface induced instabilities. For mAb2 with surfactant (+PS), no differences between CN and RN samples were determined. Thus, the surfactant concentration was sufficient to protect CN and RN processed proteins equally. The presence of PS outweighed the differences based on nucleation protocols. Consequently, CN nucleation and the resulting low SSA did not lead to additional benefits with respect to the stability of a highly concentrated IgG1 formulation if a surfactant is present in the formulation. Additionally, the relative monomer content decreased comparably in both nucleation protocols over storage time and did not indicate stability improvements by CN for both antibodies.

III.5.2 LOW CONCENTRATION STUDIES

A difference between the residual moisture of CN and RN samples could be eliminated without changing the thermal history of the samples by introducing a further secondary drying step at higher temperatures. CN-10 samples were treated comparably to RN samples, because for both a fast desorption was assumed (= low nucleation temperature). However, against our assumption, CN-10 samples resulted in physical properties comparable to CN-5 samples. Thus,

CN itself and not T_N was the determining factor. Further, we suppose that CN at different T_N results in rather similar product characteristics.

In contrast to the high concentration study, no difference with respect to particle formation between the CN and RN samples was detected; neither for the formulations without surfactant (-PS) nor for the formulations with surfactants (+PS) for both antibodies. However, as expected, +PS formulations showed clearly reduced particle numbers compared to the corresponding -PS formulations. From theory, the percentage of protein in contact with an interface/surface is higher in samples of a low protein concentration compared to samples with a high protein concentration. Thus, it was expected that the potential positive effect of CN on particle formation would be more pronounced in the low concentration study. However, this was not the case, as we did not detect any difference between CN and RN samples. HP-SEC data supported the comparability of both nucleation protocols. Even though, the decrease of monomer content of mAb2 RN samples occurred time-delayed, the decrease was determined in CN and RN samples by HP-SEC and confirmed by SDS-PAGE.

Additionally, we observed that PS20 and PS80 surprisingly promoted sucrose crystallization in both antibody studies during storage at 40°C/75% r.h.. The phenomenon of sucrose crystallization in lyophilizates stored at elevated temperatures is well-known in literature, but to our knowledge, the promotion of this crystallization by PS has not been reported before. Further, it is well-known that excipient crystallization can cause aggregation, structural loss, and loss of activity as the glassy matrix stabilizing the protein by forming hydrogen bonds is lost [29-31]. This was also observed in our study, as with the crystallization of sucrose, the monomer content of mAb2, measured by HP-SEC, decreased significantly.

III.6 CONCLUSION

This systematic study pointed out three remarkable findings. First, CN applied during the freezing step of a freeze-drying cycle did neither improve mAb stability nor negatively affect stability. These conclusions are based on a large dataset with two different antibodies, studied at two different concentrations (low and high) in typical formulations with and without surfactant. Second, in this study, the CN protocol and not T_N determined the SSA and cake appearance. This hypothesis will be investigated further in a separate study. Third, the notable impact of PS on the crystallization of sucrose in lyophilizates stored at elevated temperatures has been demonstrated for the first time.

III.7 REFERENCES

[1] Jameel, F. and Searles, J., *Development and Optimization of the Freeze-Drying Processes*, in *Formulation and Process Development Strategies for Manufacturing Biopharmaceuticals*. 2010, John Wiley & Sons, Inc. p. 763-796.10.1002/9780470595886.ch30.

[2] Patel, S.M., Doen, T., and Pikal, M.J., *Determination of End Point of Primary Drying in Freeze-Drying Process Control.* AAPS PharmSciTech, 2010. 11(1): p. 73-84.

[3] Tang, X.C., Nail, S.L., and Pikal, M.J., *Freeze-drying process design by manometric temperature measurement: design of a smart freeze-dryer.* Pharm. Res., 2005. 22(4): p. 685-700.

[4] Searles, J.A., Carpenter, J.F., and Randolph, T.W., *The ice nucleation temperature determines the primary drying rate of lyophilization for samples frozen on a temperature-controlled shelf.* J. Pharm. Sci., 2001. 90(7): p. 860-871.

[5] Roy, M.L. and Pikal, M.J., *Process Control in Freeze Drying: Determination of the End Point of Sublimation Drying by an Electronic Moisture Sensor.* PDA J. Pharm. Sci. Technol., 1989. 43(2): p. 60-66.

[6] Rambhatla, S., et al., *Heat and mass transfer scale-up issues during freeze drying: II. Control and characterization of the degree of supercooling.* AAPS PharmSciTech, 2004. 5(4): p. 54-62.

[7] Hottot, A., Vessot, S., and Andrieu, J., *Freeze drying of pharmaceuticals in vials: Influence of freezing protocol and sample configuration on ice morphology and freeze-dried cake texture.* Chemical Engineering and Processing: Process Intensification, 2007. 46(7): p. 666-674.

[8] Patel, S., Bhugra, C., and Pikal, M., *Reduced Pressure Ice Fog Technique for Controlled Ice Nucleation during Freeze-Drying.* AAPS PharmSciTech, 2009. 10(4): p. 1406-1411.

[9] Passot, S., et al., *Effect of controlled ice nucleation on primary drying stage and protein recovery in vials cooled in a modified freeze-dryer.* J. Biomech. Eng., 2009. 131(7): p. 74511-5.

[10] Konstantinidis, A.K., et al., *Controlled Nucleation in Freeze-drying: Effects on Pore Size in the Dried Product Layer, Mass Transfer Resistance, and Primary Drying Rate.* J. Pharm. Sci., 2011: p. 1-18.

[11] Bursac, R., Sever, R., and Hunek, B., *A practical method for resolving the nucleation problem in lyophilization.* BioProcess International, 2009. 7(9): p. 66-72.

[12] Geidobler, R. and Winter, G., *Controlled ice nucleation in the field of freeze-drying: fundamentals and technology review.* Eur. J. Pharm. Biopharm., 2013. 85(2): p. 214-22.

[13] Geidobler, R., Konrad, I., and Winter, G., *Can controlled ice nucleation improve freeze-drying of highly-concentrated protein formulations?* J. Pharm. Sci., 2013. 102(11): p. 3915-9.

[14] Wang, W., *Instability, stabilization, and formulation of liquid protein pharmaceuticals.* Int. J. Pharm., 1999. 185(2): p. 129-88.

[15] Mahler, H.C., et al., *Induction and analysis of aggregates in a liquid IgG1-antibody formulation.* Eur. J. Pharm. Biopharm., 2005. 59(3): p. 407-17.

[16] Mahler, H.-C., et al., *Protein aggregation: Pathways, induction factors and analysis.* J. Pharm. Sci., 2009. 98(9): p. 2909-2934.

[17] Bee, J.S., et al., *Effects of surfaces and leachables on the stability of biopharmaceuticals.* J. Pharm. Sci., 2011. 100(10): p. 4158-70.

[18] Xu, Y., et al., *Protein quantity on the air-solid interface determines degradation rates of human growth hormone in lyophilized samples.* J. Pharm. Sci., 2014. 103(5): p. 1356-66.

[19] Schersch, K., et al., *Systematic investigation of the effect of lyophilizate collapse on pharmaceutically relevant proteins I: stability after freeze-drying.* J. Pharm. Sci., 2010. 99(5): p. 2256-78.
[20] Schersch, K., et al., *Systematic investigation of the effect of lyophilizate collapse on pharmaceutically relevant proteins, part 2: stability during storage at elevated temperatures.* J. Pharm. Sci., 2012. 101(7): p. 2288-306.
[21] Schersch, K., et al., *Systematic investigation of the effect of lyophilizate collapse on pharmaceutically relevant proteins III: collapse during storage at elevated temperatures.* Eur. J. Pharm. Biopharm., 2013. 85(2): p. 240-52.
[22] Awotwe-Otoo, D., et al., *Product and process understanding to relate the effect of freezing method on glycation and aggregation of lyophilized monoclonal antibody formulations.* Int. J. Pharm., 2015. 490(1-2): p. 341-50.
[23] Fang, R., et al., *Effect of Controlled Ice Nucleation on Stability of Lactate Dehydrogenase During Freeze-Drying.* J. Pharm. Sci., 2018. 107(3): p. 824-830.
[24] Wang, S., et al., *Stabilizing two IgG1 monoclonal antibodies by surfactants: Balance between aggregation prevention and structure perturbation.* Eur. J. Pharm. Biopharm., 2017. 114(Supplement C): p. 263-277.
[25] Martos, A., et al., *Trends on Analytical Characterization of Polysorbates and Their Degradation Products in Biopharmaceutical Formulations.* J. Pharm. Sci., 2017. 106(7): p. 1722-1735.
[26] Geidobler, R., Mannschedel, S., and Winter, G., *A new approach to achieve controlled ice nucleation of supercooled solutions during the freezing step in freeze-drying.* J. Pharm. Sci., 2012. 101(12): p. 4409-13.
[27] Awotwe-Otoo, D., et al., *Impact of controlled ice nucleation on process performance and quality attributes of a lyophilized monoclonal antibody.* Int. J. Pharm., 2013. 450(1-2): p. 70-8.
[28] Patel, S.M., et al., *Lyophilized Drug Product Cake Appearance: What Is Acceptable?* J. Pharm. Sci., 2017. 106(7): p. 1706-1721.
[29] Costantino, H.R., et al., *Effect of excipients on the stability and structure of lyophilized recombinant human growth hormone.* J. Pharm. Sci., 1998. 87(11): p. 1412-20.
[30] Heljo, V.P., et al., *The effect of water plasticization on the molecular mobility and crystallization tendency of amorphous disaccharides.* Pharm. Res., 2012. 29(10): p. 2684-97.
[31] Singh, S.K., et al., *Frozen state storage instability of a monoclonal antibody: aggregation as a consequence of trehalose crystallization and protein unfolding.* Pharm. Res., 2011. 28(4): p. 873-85.

CHAPTER IV

IV. Comparison of ice fog methods and monitoring of controlled nucleation success after freeze-drying

This chapter was published in the *International Journal of Pharmaceutics* and appears in this thesis with the journal`s permission*:*

Ilona Vollrath[1,2], Wolfgang Friess[2], Angelika Freitag[1], Andrea Hawe[1], Gerhard Winter[2], (2019). "*Comparison of ice fog methods and monitoring of controlled nucleation success after freeze-drying*". International Journal of Pharmaceutics, 558: 18-28.

The experiments were performed by Ilona Vollrath, who also wrote the manuscript for the paper. Wolfgang Frieß, Angelika Freitag, Andrea Hawe and Gerhard Winter provided scientific guidance and input during the experimental phase and the complete writing process. In addition, Wolfgang Frieß, Gerhard Winter and Andrea Hawe, who also serves as corresponding author, reviewed the final manuscript.

[1] Coriolis Pharma Research GmbH, D-82152 Martinsried, Germany

[2] Department of Pharmacy, Pharmaceutical Technology and Biopharmaceutics, Ludwig-Maximilians-University, D-81377 Munich, Germany

IV.1 ABSTRACT

Improving freeze-drying processes regarding drying time and batch homogeneity is subject of ongoing research work. In this context, controlled nucleation raised great expectations. However, practically we face some challenges, e.g. how to non-destructively monitor successfully performed controlled nucleation. The question if different controlled nucleation methods lead to comparable products, as not every method can easily be implemented in lab and production scale equipment, is also of high interest. Additionally, the optimal nucleation temperature for controlled nucleation is an open question. In our study, we addressed these challenges. We successfully evaluated frequency modulated spectroscopy as a fast and non-destructive method to monitor controlled nucleation success and batch homogeneity. We found that the better homogeneity generated by controlled nucleation during the freezing step did not sustain in the dried product. Lyophilizates produced by three different ice fog methods for controlled nucleation were characterized by comparable specific surface areas but differed in residual moisture content. To investigate the impact of T_N on the resulting specific surface area, we performed CN at -3 °C and -10 °C. We concluded that T_N is not the only specific surface area determining factor and a high T_N does not necessarily lead to larger pores but poses a higher risk of not-nucleating vials.

IV.2 INTRODUCTION

One important aspect in lyophilization process development is the optimization of the primary drying time by adjusting shelf temperature and chamber pressure to increase sublimation rate [1-6]. Since Searles et al. [4] identified the ice nucleation temperature (T_N) as a relevant factor for the primary drying rate during lyophilization, the freezing step gained in importance for freeze-drying cycle optimization. A higher T_N generally results in larger ice crystals; and with these larger pores during sublimation, product resistance is reduced and thus, primary drying time shortened [4, 7, 8]. Moreover, larger pores (generated at higher T_N) reduce the specific surface area (SSA), which induces slower desorption rates during secondary drying and thus can cause higher residual moisture (RM) levels of the final product if secondary drying is not modified when compared to the step utilized in a process where ice nucleation was not controlled [7, 9].

Lyophilization cycle control, scale-up and transfer are important steps in product development and large-scale production. The stochastic nature of T_N and its dependency on process and formulation variables may induce heterogeneity from vial to vial within a batch. T_N is typically higher in a development environment where more particles can be introduced into the vials that function as nucleation sites. For successful process transfer, it needs to be considered that the vials tend to nucleate at lower T_N during production due to the almost particle free environment. This can result in longer primary drying times than expected based on the experience from process development. Therefore, it is of major interest to control T_N in order to control product resistance, drying times and (indirectly, as a result of cake resistance) T_p [7, 9, 10], and additionally, to reduce vial to vial heterogeneity [10-12]. However, it needs to be considered that differences in the heat transfer, e.g. edge vial effects or temperature inhomogeneity of the shelf, could also cause vial to vial heterogeneity within a batch [6, 13-17]. In our study, we did not focus on those heat transfer differences across a batch. They are well known and occur in different freeze-dryers to a different extent. We wanted to investigate if it is possible to improve

the vial to vial homogeneity of a batch although the heat transfer might be different across the shelf. If the heat transfer differences overcome the homogeneity generated by CN, the application of CN does not enhance product quality and uniformity.

Geidobler and Winter [18] summarized the different approaches to induce ice nucleation that lead to the development of today's commercial methods. Ice fog and pressure change methods are the two key techniques to induce ice nucleation and thus control T_N. Commercially available ice fog methods are, e.g. FreezeBooster® (Millrock Technology), LyoCoN (Martin Christ), and VERISEQ® nucleation system (IMA life/Linde). ControLyo™ (SP Scientific), SynchroFreeze (Hof) and a recently published method from OPTIMA pharma [19] represent three methods based on pressure change.

For the claimed benefits of controlled nucleation (CN), in particular improved batch homogeneity, it is crucial that the applied methods result in CN of 100% of all vials of a batch. Furthermore, as CN at higher T_N results in lower SSA and a higher RM compared to random nucleation (RN) [7, 9], a non-destructive method to distinguish between controlled nucleated and not-controlled nucleated vials is needed. Currently, non-destructive approaches to monitor successfully performed CN are lacking. It is furthermore an open question, if it is necessary to apply the same CN method in development and production scale to achieve comparable product properties. In a recently published study, Gitter et al. [20] compared two mechanistically different methods to induce controlled nucleation, ice fog and depressurization, regarding nucleation behavior, process length and properties of the resulting lyophilizates. They exhibited that both techniques led to comparable process performance and product quality attributes.

Additional effects of CN that have been reported are the reduction of reconstitution time for highly concentrated protein formulations [21], and the impact of CN on the degree of protein glycation [22] as well as enzyme activity (lactate dehydrogenase) [23]. In a previous work, we found that CN did neither have a positive nor a negative effect on the stability of an IgG1. Additionally, we observed that for the used mAb formulation, also the application of CN versus

RN and not primarily T_N determined the resulting SSA [24]. Thus, it needs to be investigated if the morphology of the seeding crystals or the formulation composition, besides T_N, defines the ice crystal morphology and thus product resistance, primary drying time and the product`s SSA.

In this study we evaluated frequency modulated spectroscopy (FMS) as a tool to non-destructively monitor successful performance of CN. FMS determines the water activity as a surrogate parameter for RM at high throughput. RM is considered as a key quality attribute for lyophilizates and is known to alter if CN is applied. Therefore, we generated a CN batch with a certain percentage (~10%) of randomly nucleated vials by using a non-optimized controlled nucleation protocol. The 100% control of the batch by FMS also enabled us to study batch homogeneity.

The product properties optical appearance, microscopic cake structure, SSA and RM, and the process times of lyophilizates generated by three different ice fog methods, namely FreezeBooster® (Millrock Technology), VERISEQ® nucleation system (IMA life/Linde), and the method described by Geidobler et al. [25], were compared to address the question if different nucleation methods result in comparable product properties. These three methods differ in ice fog generation temperature and induction pressure, which suggests a different morphology of nucleation seeds (e.g. hexagonal, dendritic, and dispersed spherulitic) and thus texture of the and texture of the ice fog.

The ice fog method described by Geidobler et al [25], generates an in-situ ice fog in the chamber by releasing the previously applied vacuum of ~ 3.7 mbar through the cold condenser (approximately -70 °C). During the FreezeBooster® method, the chamber was evacuated to 66 mbar (50 Torr) and prior to nucleation induction, the condenser was loaded with nucleation seeds by spraying water steam into the -80 °C cold condenser [26]. This generated a snow-flake like ice fog. As third method the VERISEQ® nucleation system was used. Here, liquid nitrogen is combined with water vapor to generate a very fine ice fog dispersion. For ice fog

injection, the chamber pressure is reduced to 275 mbar [27]. All methods could be optimized with respect to 100% CN success by modifying the vacuum used for injection.

IV.3 MATERIALS AND METHODS

IV.3.1 STUDY DESIGN

Three ice fog methods, the VERISEQ® nucleation system, the Millrock FreezeBooster® and the method published by Geidobler et al., were compared (Figure IV-1). Each method was applied at two different T_N, -3 °C and -10 °C, to investigate the impact of T_N on SSA when CN is applied. A T_N of -3 °C was the highest possible T_N that resulted in acceptable nucleation success. A T_N of -10 °C was chosen as it is within the range of RN nucleation temperatures where the risk of spontaneous random nucleation is low. As the VERISEQ® nucleation system was attached to a Christ Epsilon 2-12D freeze-dryer, whereas the Millrock FreezeBooster® and the method by Geidobler et al. were performed on a Millrock Magnum freeze-dryer, two random nucleation protocols, applied on both freeze-dryers, were used to account for freeze-dryer differences. In one random protocol, the vials were equilibrated to 2 °C, and in the other, the vials were equilibrated to -3 °C, comparable to the CN-3°C nucleation protocol. To investigate the impact of formulation composition, all experiments were performed with a sucrose-based (F1) and a trehalose-based (F2) formulation of a monoclonal antibody (mAb; final concentration 10 mg/ml (Table IV-1). Additionally, the impact of protein concentration on SSA was investigated. Therefore, three additional mAb concentrations, 1, 50, and 100 mg/ml (F3, F4, F5, respectively; all sucrose-based), were studied with the method published by Geidobler et al.

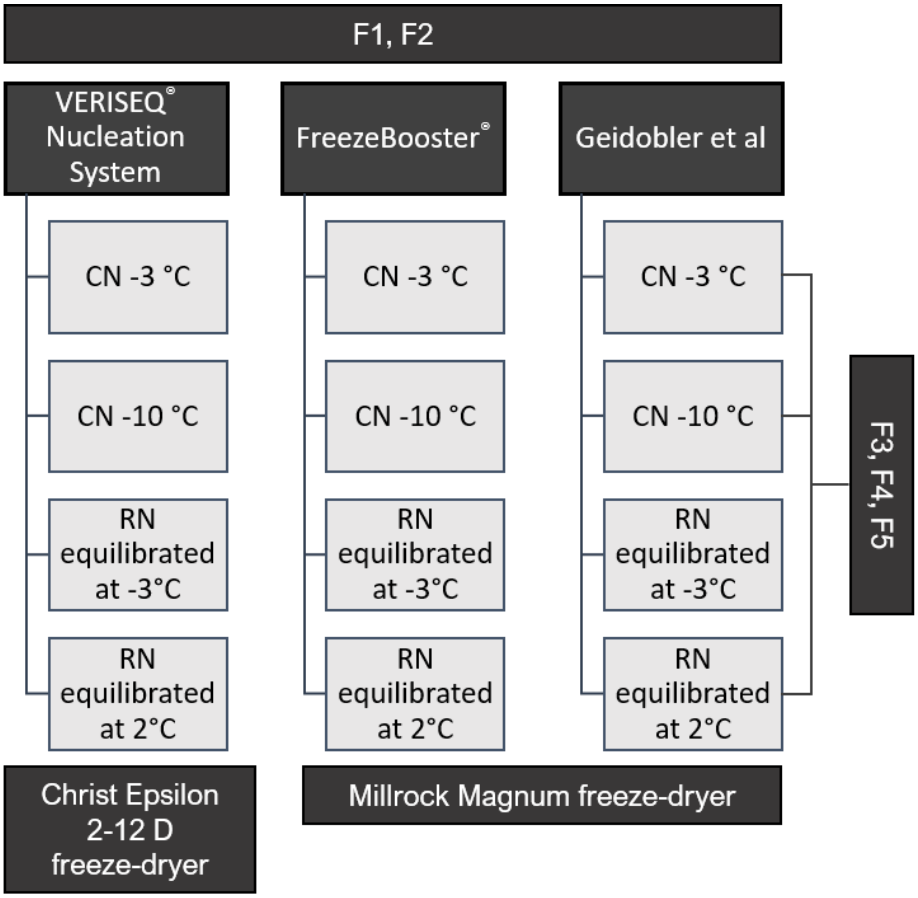

Figure IV-1: Study design

IV.3.2 MATERIALS

A monoclonal antibody (mAb), IgG1, was used in this study. Ph. Eur. grade sucrose, trehalose, and polysorbate 20 were purchased from Sigma-Aldrich; di-Sodium hydrogen phosphate (AppliChem), sodium dihydrogen phosphate (AppliChem) were purchased from VWR. Low protein binding polyvinylidene fluoride (PVDF) filters (0.22 µm) were purchased from Merck Millipore (Millipore, Schwalbach, Germany).

6R glass type I tubing vials were purchased from Schott AG (Mainz, Germany). Stoppers (Westar® RtS, 20 mm, Silicone A) and flip off caps were supplied by West Pharmaceutical Services (Eschweiler, Germany). All vials and stoppers were washed with highly purified water

(Milli-Q, Merck Millipore, Hertfordshire, United Kingdom) and heat sterilized or autoclaved and dried, respectively.

IV.3.3 FORMULATION PREPARATION

After complete thawing (2-8°C) and mixing of mAb bulk solution, each formulation was prepared and lyophilized latest 24 h after preparation. The formulations were prepared according to the respective composition described in Table IV-1. Prior to filling, all formulations were filtered through a 0.22 µm PVDF membrane filter.

Table IV-1: Overview of the composition of the formulations used in this study.

Description	Buffer system	mAb concentration [mg/ml]	Sucrose [mg/ml]	Trehalose [mg/ml]	Polysorbate 20 [%]
F1	10.5 mM phosphate pH 6.4	10.0	75	-----	0.04
F2		10.0	-----	75	0.04
F3		1.0	75		0.04
F4		50.0	75		0.04
F5		100.0	75		0.04

Aliquots of 2.5 ml were manually filled per vial under laminar flow and the vials were semi-stoppered. In total 20 vials of each formulation were prepared and placed in the center of the shelf.

IV.3.4 LYOPHILIZATION

Lyophilization was performed by using an Epsilon 2-12D pilot scale freeze-dryer (Martin Christ, Osterode, Germany) or a Millrock Magnum pilot scale freeze-dryer (Millrock Technology Inc., Kingston, NY, USA). The vacuum during the freeze-drying process was controlled by a Pirani

gauge or an MKS capacitance manometer depending on the technical capabilities of the freeze-dryers. T_p and end of primary drying was determined by thermocouples. Table IV-2 provides an overview over the performed freeze-drying cycles and presents the technical setup for each cycle.

Before CN, the vials were equilibrated for at least 3 h to the desired T_N prior to induction of nucleation. Immediately after CN, solidification was achieved by reducing the shelf temperature at 1 °C/min to -50 °C in all cases. For random nucleation, the vials were equilibrated (i) at 2 °C and (ii) at -3 °C for at least 3 h prior to decrease the shelf temperature at 1 °C/min to -50 °C. To ensure complete solidification, the shelf temperature was held at -50 °C for 1 h.

Primary drying was initiated by increasing the shelf temperature at 0.5 °C/min to -25 °C. Chamber pressure was set to 0.066 mbar.

Secondary drying was carried out at 20 °C for 6 h. The ramp for the shelf temperature from primary to secondary drying was 0.1 °C/min. After secondary drying was completed, the chamber was backfilled to 100 mbar with nitrogen gas and the vials were stoppered. After backfilling with nitrogen to atmosphere, the samples were unloaded, crimp capped and stored at 5 °C.

Table IV-2: Overview of performed freeze-drying cycles and technical setup.

Lyo Cycle (LC)	Formulation	Freezing protocol	Ice fog method	Freeze-dryer	Primary drying endpoint determination
LC 1	F1, F2	CN at -3 °C	VERISEQ® system	Christ 2-12D (pressure control by Pirani)	Thermocouples
LC 2	F1, F2	CN at -10 °C			
LC 3	F1, F2	RN equilibration at -3 °C			
LC 4	F1, F2	RN equilibration at 2 °C			
LC 5	F1, F2	CN at -3 °C	Millrock FreezeBooster®	Millrock Magnum (pressure control by MKS)	Thermocouples
LC 6	F1, F2	CN at -10 °C			
LC 7	F1, F2	RN equilibration at -3 °C			
LC 8	F1, F2	RN equilibration at 2 °C			
LC 9	F1, F2, F3, F4, F5	CN at -3 °C	Geidobler et al.	Millrock Magnum (pressure control by MKS)	Thermocouples
LC 10	F1, F2, F3, F4, F5	CN at -10 °C			
LC 11	F1, F2, F3, F4, F5	RN equilibration at -3 °C			
LC 12	F1, F2, F3, F4, F5	RN equilibration at 2 °C			
LC 13	F1, F2	CN at -3 °C performed twice (1 h secondary drying)	VERISEQ® system	Christ 2-12D (pressure control by Pirani)	Thermocouples
LC 14	F1, F2	RN equilibration at 2 °C (1 h secondary drying)			

IV.3.5 DATA ANALYSIS AND ILLUSTRATION

Throughout the manuscript, error bars represent the experimental mean (based on n=10 or n=4 (for different concentration investigation)) ± standard deviation.

IV.3.6 OPTICAL EVALUATION OF THE FREEZE-DRIED PRODUCT

The freeze-dried cakes were optically evaluated after drying. Parameters taken into consideration were compactness of the cake, contact to walls of vial, shape of the cake, color and overall appearance. Furthermore, photos were taken of the dried products.

IV.3.7 KARL FISCHER TITRATION (KF)

The residual moisture of the lyophilized cakes was determined by headspace Karl Fischer titration (Aqua 40.00, Analytik Jena GmbH, Jena, Germany). About 20 mg of sample was weighed into a 2R glass vial under a glovebox (r.h. ≤ 5%) and was analyzed at 150 °C. Prior to the measurements, a system suitability test was performed daily by measuring a pure water standard (Apura 1 water standard oven 1.0, Merck KGaA).

IV.3.8 HEADSPACE MOISTURE MEASUREMENT BY FMS

Headspace moisture analysis by frequency modulated spectroscopy (FMS) (LIGHTHOUSE FMS-1400, LIGHTHOUSE, Charlottesville, Virginia, USA) was performed to monitor water activity. Nitrogen was used as background gas. Prior to measurements, a calibration and a system suitability test with five standards was performed daily. The samples were equilibrated to room temperature for at least 2 h before analysis.

IV.3.9 NUCLEATION SUCCESS AND BATCH HOMOGENEITY

To evaluate FMS as a non-destructive method to monitor nucleation success, a not-optimized nucleation protocol (T_N=-3°C; injection pressure=275 mbar; VERISEQ® nucleation system) was used to intentionally produce ~10% not-controlled nucleated vials within the batch. Water activity of a full shelf (332 vials) after primary drying and incomplete (1 h) and complete (6 h) secondary drying was analyzed by FMS to assess batch homogeneity.

IV.3.10 BET ANALYSIS

The SSA of the lyophilizates was analyzed by the BET method (Autosorb-1, Quantachrome Instruments, Germany). Approximately 100 mg of a lyophilizate was carefully crushed with a spatula into small pieces and filled in a measurement tube. Prior to Krypton sorption measurement performed at 77.3 K, the samples were degassed for approximately 2 h at 25 °C. At least 5 data points were collected covering a p/p_0 region of 0.05 to 0.3. In this pressure range the linearized version of the BET equation, used for analysis, is most reliable. The data points were evaluated according to the multipoint BET-method. Correlation coefficient (R^2) was ≥ 0.997 for all samples.

IV.3.11 SCANNING ELECTRON MICROSCOPY (SEM)

Scanning electron microscopy (SEM) was used to study the morphology of the freeze-dried cake. A FEI Helios G3 UC equipped with a scanning-transmission-detector (Hillsboro, Oregon, USA) was used to generate the images. The freeze-dried cake was broken by using a spatula. The generated pieces were fixed with carbon conductive cement on a sample holder in the way that the breakage border could be analyzed. In that way it was assured that the structure was not changed due to the spatula.

IV.4 RESULTS

IV.4.1 PRIMARY DRYING TIMES

Table IV-3 provides the time required to finish primary drying for all performed freeze-drying runs. A primary drying time reduction could only be achieved after CN at -3 °C by using Geidobler et al. method (LC 9) or FreezeBooster® (LC 5). All other lyo cycles led to an about 15 h longer primary drying time of 53-60 h.

Table IV-3: Primary drying times* of all freeze-drying cycles. It was not distinguished between sucrose and trehalose formulations.

Nucleation method/ freeze-dryer	**CN-3 °C**	**CN-10 °C**	**RN equi -3 °C**	**RN equi 2 °C**
VERISEQ® system/ Christ 2-12D (Pirani gauge)	56 h	60 h	56 h	57 h
Millrock FreezeBooster®/ Millrock Magnum (MKS)	43 h	55 h	55 h	59 h
Geidobler et al./ Millrock Magnum (MKS)	41 h	53 h	---	57 h

* the time when the shelf temperature reached -25 °C until the thermocouples indicated the end of primary drying was considered as primary drying time.

IV.4.2 NUCLEATION SUCCESS AND BATCH HOMOGENEITY

For monitoring the success of CN, a non-destructive method was necessary to identify samples that have undergone CN and to make them available for further analysis. Within this study, we used the visible difference in cake appearance between controlled nucleated and not-controlled

nucleated lyophilizates, and the difference in water activity, determined by FMS, to assess the successful performance of CN.

RN lyophilizates showed a compact cake with minor shrinkage in height and isolated shrinkage in diameter, a shiny surface and tiny cracks. CN lyophilizates differed and had a more porous, loose and shiny structure. Additionally, crack formation was more pronounced in CN cakes (Figure IV-2).

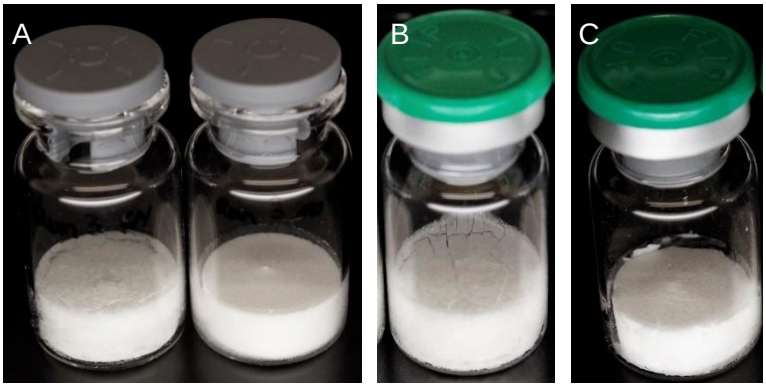

Figure IV-2: (A) Vial photos from LC 3 (Sucrose). Controlled nucleated vial (left): more porous and loose structure. Random-nucleated vial (right): less porous, more compact structure. (B) CN: Example of a vial of LC 7 (Sucrose). (C) RN: Example from LC 8 (Sucrose).

With FMS the partial pressure of water vapor (p_{H2O}), which corresponds to the water activity in the vial headspace, was determined in a fast and non-destructive way. CN samples had higher water activity (p_{H20}=0.6-0.8 mbar for LC 1 and 2) compared to RN vials (p_{H2O}=0.1-0.2 mbar for LC 3 and p_{H2O}=0.2-0.4 mbar for LC 4) (Figure IV-3). Based on this difference, it was possible to identify not-controlled nucleated vials also within a batch and thus monitor CN success by FMS measurements (Figure IV-3, LC 1; not-controlled nucleated vials are indicated in light grey). The not-optimized CN protocol of LC 1 (T_N=-3 °C; induction pressure=275 mbar; VERISEQ® nucleation system) resulted in 43 not-controlled nucleated vials (indicated in light grey) out of 332 vials of the shelf (=13%). In contrast, for the CN protocol in LC 2 at a lower T_N, only 1 vial out of 332 vials (< 1%) did not undergo controlled nucleation.

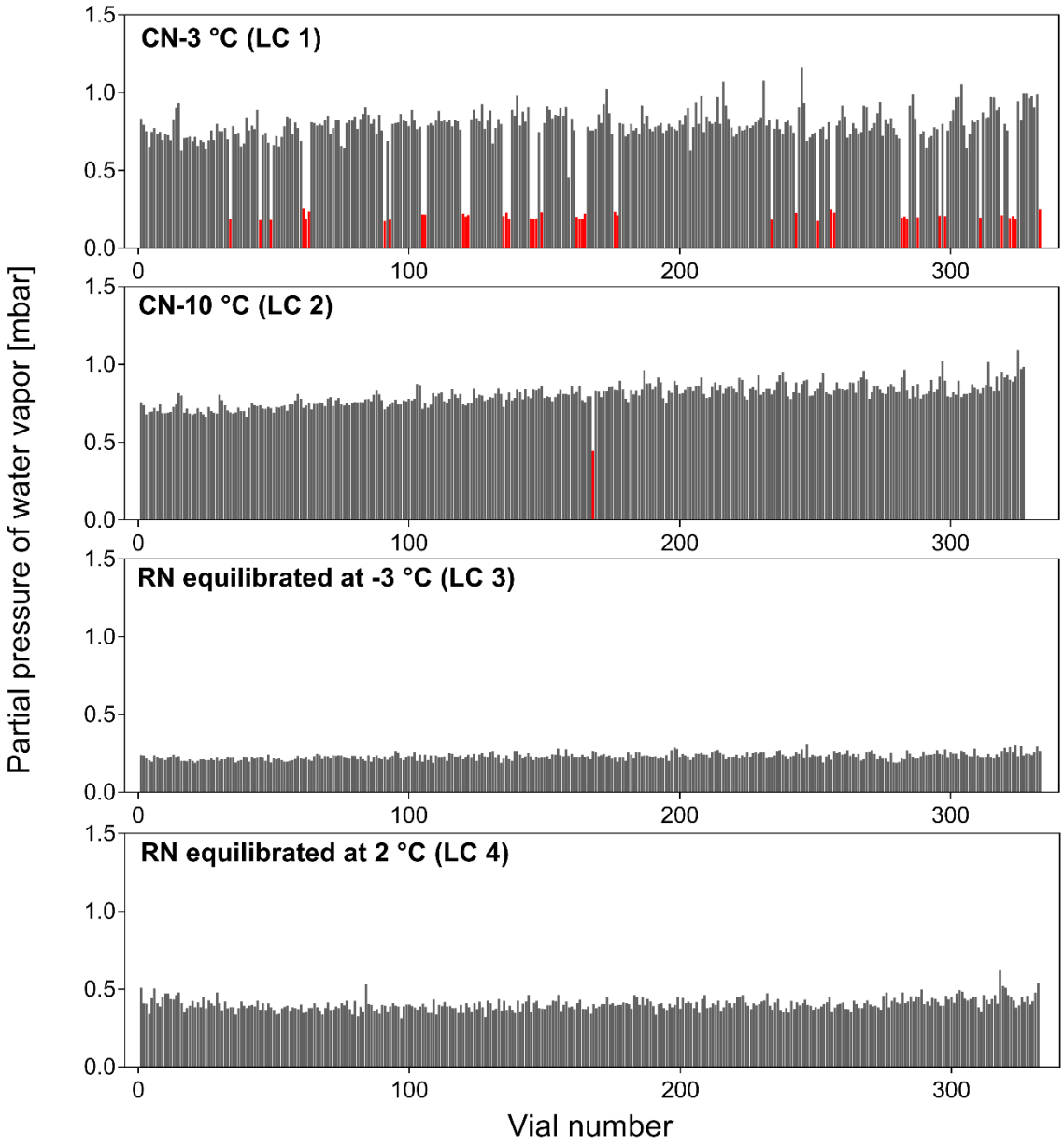

Figure IV-3: FMS data of complete freeze-dryer shelves à 332 vials of LC 1, LC 2, LC 3 and LC 4 (Sucrose-based formulation F1); not-controlled nucleated, defective vials within a CN lyophilization cycle are indicated in red.

We additionally investigated the FMS data shown in Figure IV-3 with respect to batch homogeneity only considering the vials that underwent controlled nucleation. A detailed evaluation of the relative and absolute standard deviations (rel STD and abs STD, respectively), provided in Table IV-4, illustrated that the determined rel STD for the CN-10 °C (LC 2), RN equi -3 °C (LC 3) and RN equi 2 °C (LC 4) runs were comparable with 9.0, 9.5, and 9.6%,

respectively. Although, the defect vials had been excluded, the shelf processed by LC 1 showed a slightly higher rel STD of 10.5% compared to the other cycles after 6 h of secondary drying.

Table IV-4: Determined absolute and relative standard deviations for all shelves and both secondary drying times.

Nucleation protocol	**Secondary drying duration**	**Mean: Partial pressure of water vapor [mbar]**	**Absolute STD [mbar]**	**Relative STD 5 [%]**	**Residual moisture [%] of 10 vials**
CN -3 °C*	6 h	0.80	0.08	10.5	**0.92**
CN -10 °C		0.80	0.07	9.0	1.51
RN equi -3 °C		0.23	0.02	9.5	**1.00**
RN equi 2 °C		0.40	0.04	9.6	0.97
CN-3 °C	1 h	4.84	0.4	7.6	
RN equi 2 °C		1.38	0.2	13.1	

*not-optimized protocol: defective, not-controlled nucleated vials (~13%) have been excluded from analysis.

To study how batch homogeneity after CN develops during the process, we performed LC 13 and LC 14 (Figure IV-4). Both cycles were terminated after 1 h of secondary drying. In fact, after incomplete secondary drying, vials from a CN process showed a lower rel STD (7,3%) than RN vials (13.1%), but after 6 h the difference vanished, and CN and RN revealed about the same rel STD (Table IV-4). Thus, CN did not improve homogeneity with respect to RM.

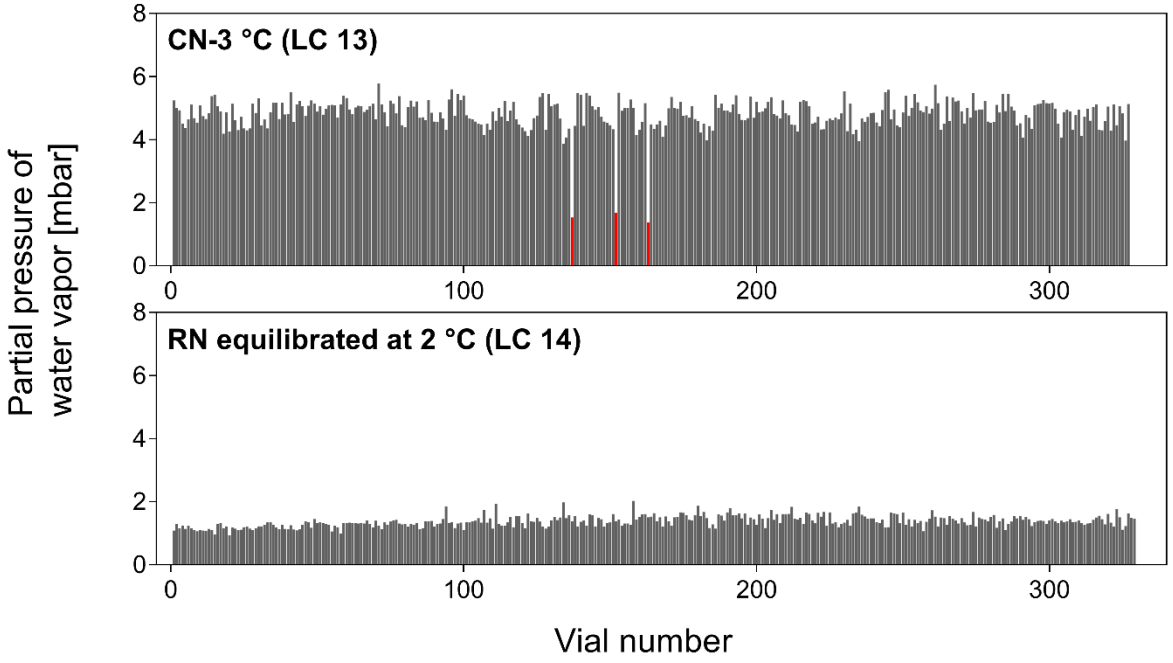

Figure IV-4: FMS analysis of complete freeze-dryer shelves à 332 vials of LC 13 and LC 14 (Sucrose-based formulation F1); not-controlled nucleated vials within a CN lyophilization cycle are indicated in red.

IV.4.3 ANALYSIS OF PRODUCT PROPERTIES

Three ice fog methods and the resulting product properties of the lyophilizates, such as optical appearance, microscopic structure and morphology, SSA, and RM were compared. Additionally, the impact of T_N and formulation composition on these product properties was assessed. All vials used for the analysis of product properties were tested visually and by FMS for successfully performed controlled nucleation.

As for LC 1, a non-optimized protocol was used to evaluate FMS as a monitoring tool for nucleation success, lyophilizates generated by LC 1 were not included in this section.

IV.4.3.1 CAKE APPEARANCE

As described above, CN lyophilizates differed in cake appearance from RN samples independent of the nucleation method and formulation. However, for sucrose-based

lyophilizates an impact of T_N was observed (Figure VIII-15): CN -3°C lyophilizates showed a porous and loose structure with minor shrinkage in height and substantial crack formation. CN-10 °C lyophilizates were more compact, less porous with reduced crack formation. Sucrose-based RN samples equilibrated at -3 °C or at 2 °C had a compact cake, with minor shrinkage in height, only isolated tiny crack formation and negligible shrinkage in diameter. No difference between the nucleation methods was detected.

For trehalose-based samples (Figure VIII-16), most of the samples revealed the same dependency on T_N as noted for the sucrose-based products. Exclusively the CN-10 °C Geidobler et al. vials (LC 10) did not differ from the CN-3 °C samples. Again, all RN samples appeared comparable with a compact cake and minor shrinkage in height. However, the RN equi-3 °C 2-12D products (LC 3) showed adhesion to the vial wall in contrast to all other RN samples.

IV.4.3.2 SEM

After macroscopic characterization, microscopic analysis of the lyophilizates was performed by SEM. All lyophilizates had a sponge like morphology in common.

Sucrose-based samples (Figure IV-5): The CN lyophilizates showed, as expected, larger pores than RN products. Again, a dependency of T_N was observed, as CN-3 °C resulted in larger pores compared to CN-10 °C. The smallest pores were noted for the RN protocols. All nucleation methods resulted in similar pore size and morphology. Additionally, no difference in RN lyophilizates was detected between the freeze-dryers.

Trehalose-based samples (Figure IV-6): Like for the sucrose-based formulation, a smaller pore size was observed for CN-10 °C as compared to CN-3 °C in all cases. All nucleation methods resulted in comparable microscopic appearance. RN equilibrated at 2 °C samples processed in the 2-12D freeze-dryer (LC 4) showed slightly larger pores than the other RN lyophilizates.

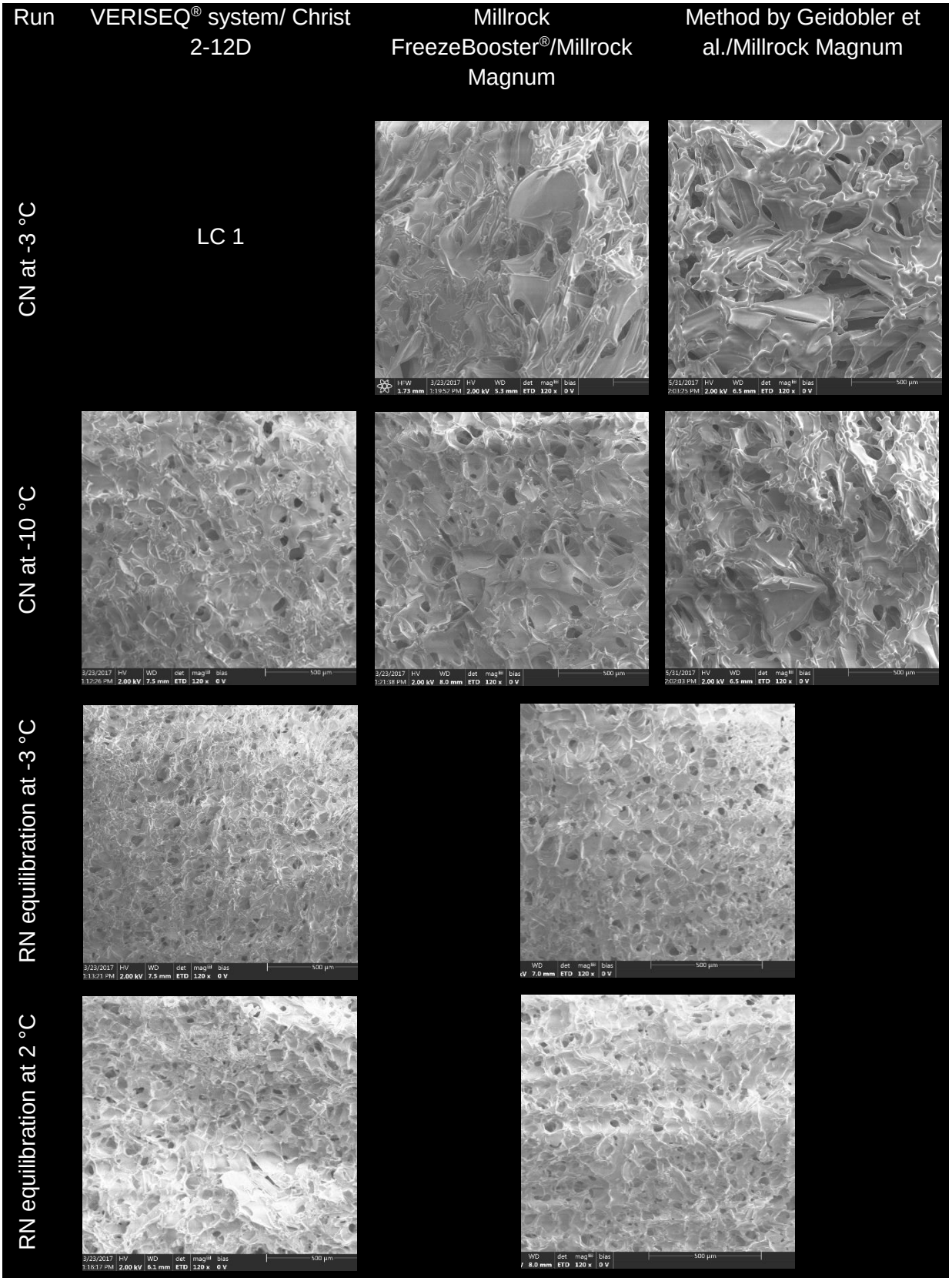

Figure IV-5: SEM images of all freeze-drying cycles of the sucrose-based samples.

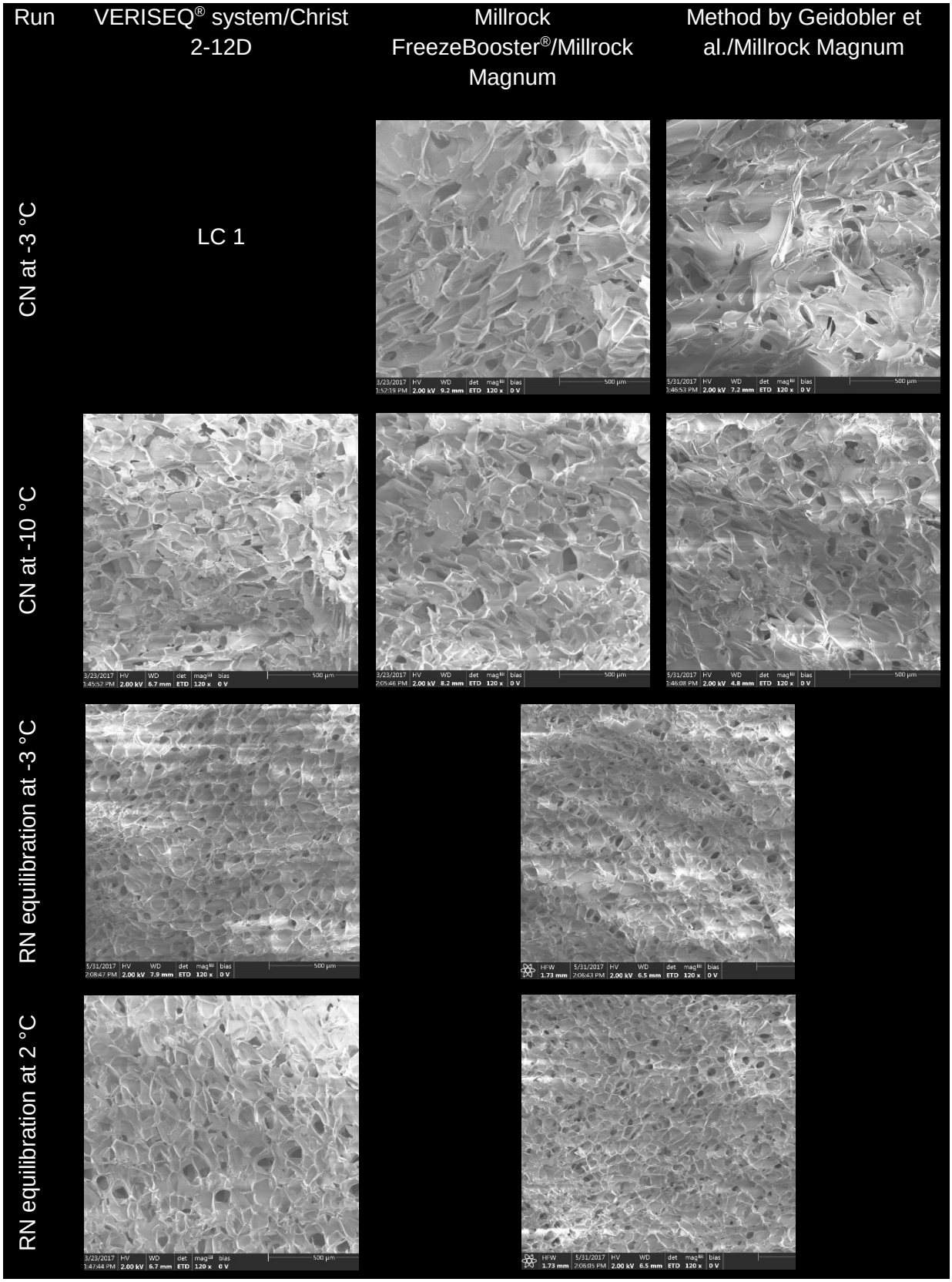

Figure IV-6: SEM images of all freeze-drying cycles of the trehalose-based samples.

IV.4.3.3 BET

The lyophilizates were analyzed by Krypton gas adsorption to determine the SSA (Figure IV-7). In accordance with the SEM images, CN lyophilizates of both formulations showed, reciprocally to pore size, lower SSA compared to the RN protocols. Sucrose-based lyophilizates generated by FreezeBooster® (LC 5 and 6) and according to Geidobler et al. (LC 9 and 10), showed an increase in SSA with decreasing T_N (Figure IV-7A). These two methods showed similarly low SSA values at a T_N of -3 °C and -10 °C, whereas for VERISEQ® CN-10 °C lyophilizates slightly higher SSA values were determined. RN samples generated in a Christ 2-12D and a Millrock Magnum freeze-dryer resulted in similar SSA values.

For trehalose-based products generated by FreezeBooster® (LC 5 and 6) and Geidobler et al. (LC 9 and 10), SSA was independent from T_N, as CN-3 °C and CN-10 °C resulted in comparable SSA (Figure IV-7B). All CN methods resulted in assimilable SSA values. SSA values of RN equi 2 °C lyophilizates were comparable between freeze-dryers. For trehalose-based samples, higher SSA values as for the corresponding sucrose-based samples were detected.

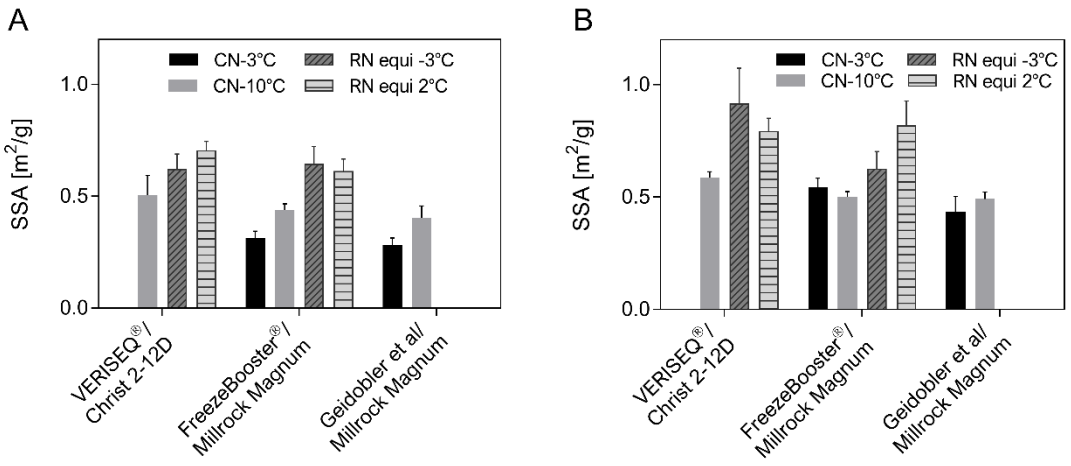

Figure IV-7: Results of BET measurements of all runs. (A) sucrose formulation. (B) Trehalose formulation.

To investigate the impact of formulation composition on SSA, besides CN and T_N, mAb concentration was varied. Formulations (sucrose-based) in the concentration range from 1-100 mg/ml mAb were subjected to three different nucleation protocols.

Independent of the mAb concentration, an increase of SSA was found with decreasing T_N (Figure IV-8). Furthermore, the characteristically lower SSA for CN sampes was determined throughout all mAb concentrations.

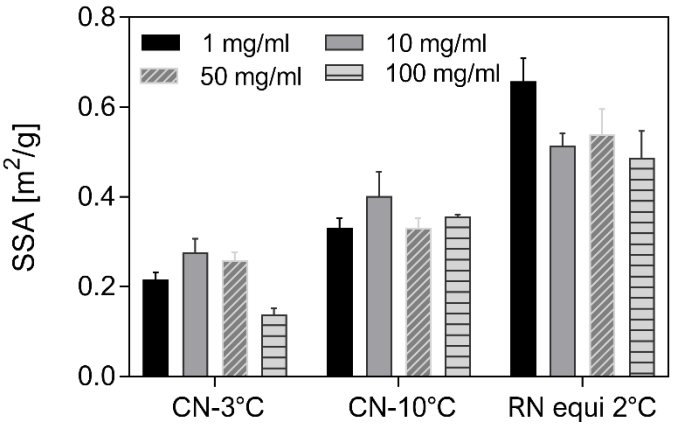

Figure IV-8: BET results of all mAb concentrations and T_N processed according to the Geidobler et al. method in the Millrock Magnum Freeze-Dryer.

IV.4.3.4 KF RESULTS

RM of the freeze-dried products was assessed by KF titration. In accordance with the SEM images and BET results, CN lyophilizates showed the expected higher RM compared to the RN samples.

Sucrose-based lyophilizates (Figure IV-9A): No dependency of RM on T_N was detected (similar RM values for CN-3 °C and CN-10 °C). Slightly higher RM values were determined for Geidobler et al. samples (LC 9 and 10) compared to FreezeBooster® lyophilizates (LC 5 and 6). At CN-10 °C, VERISEQ® lyophilizates (LC 2) exhibited higher RM values (1.5%) as the other

two methods (FreezeBooster®=1.2% (LC 6), Geidobler et al.=1.3% (LC 10). The two RN protocols resulted in assimilable RM values.

Trehalose-based products (Figure IV-9B): Like the sucrose-based samples, lyophilizates generated by VERISEQ® nucleation system had the highest RM values compared to the other two methods. The lowest RM values were detected for Millrock FreezeBooster® processed samples. Additionally, FreezeBooster® and Geidobler et al. processed samples revealed a decrease in RM content with decreasing T_N. No trend between the RN samples equilibrated at -3 °C and 2 °C could be noted.

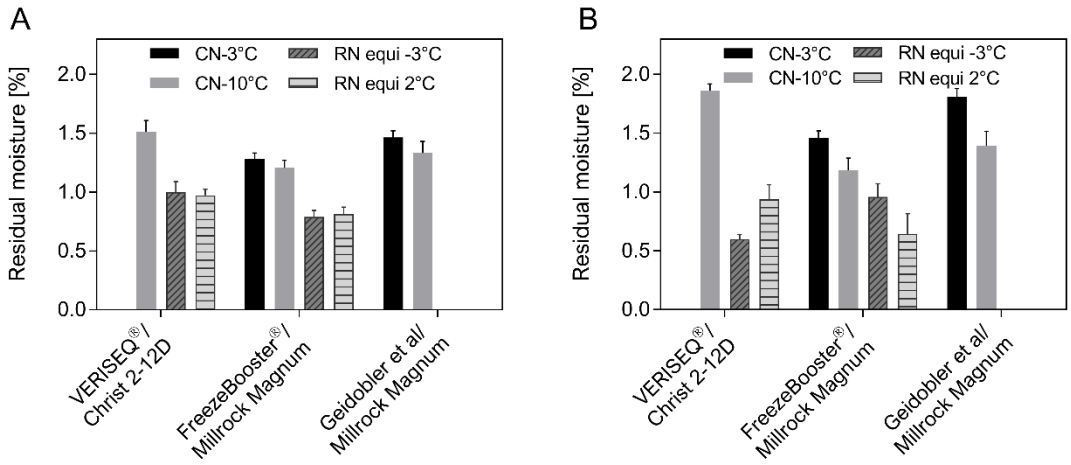

Figure IV-9: Results of Karl Fischer measurements of all runs. (A) sucrose formulation. (B) trehalose formulation.

Similar to BET sample set, formulations with different mAb concentrations (sucrose-based) were analyzed to assess the impact of formulation composition on RM. As expected and in accordance with SSA results, higher RM content was detected for CN lyophilizates compared to RN products independent of the protein concentration (Figure IV-10). A decrease in RM with a decrease of T_N was found independent of mAb concentration.

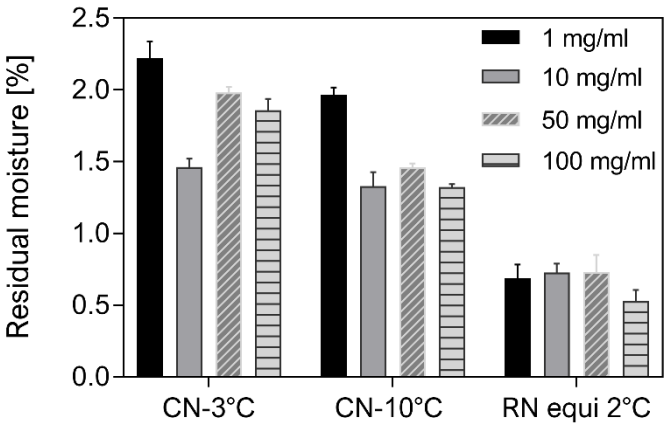

Figure IV-10: KF results of all mAb concentrations and T_N processed according to the Geidobler et al. method in the Millrock Magnum Freeze-Dryer.

IV.5 DISCUSSION

IV.5.1 MONITORING OF NUCLEATION SUCCESS AND BATCH HOMOGENEITY

As CN is known to change product properties [7, 9, 21, 28], a non-destructive, high-throughput method to monitor CN success as 100% control is required. In this study, we applied FMS as such a method (5 seconds per vial) to monitor nucleation success via analysis of water activity as surrogate for residual moisture. By using FMS, it was possible to distinguish between CN vials, showing high residual water activity, and RN samples, showing low residual water activity within one batch (Figure IV-3, LC 1). All samples detected as not-controlled nucleated by FMS within a batch could be identified and were excluded from further analysis by SEM, BET and KF, when we compared the effects of the nucleation process on the product properties. The ability to detect these defects within a batch could be used for optimization and validation of the CN process and even in commercial production for quality assurance.

Obviously, the target would be 100% successfully controlled nucleated vials within one batch. For the proof-of-concept, we applied a not-optimized CN protocol using the VERISEQ® nucleation system. This system generates a very fine ice fog dispersion from liquid nitrogen and water vapor, in contrast to the snow-flake like ice fog structures that we observed during condenser loading of the FreezeBooster®. Additionally, the CN by the VERISEQ® method was performed at a comparably high chamber pressure (VERISEQ®: 275 mbar; FreezeBooster®: 66 mbar; Geidobler et al: 3.7 mbar), thus, the resistance for the very fine ice fog within the chamber was approximately 4 or 74 times higher in the VERISEQ® method compared to FreezeBooster® or Geidobler et al., respectively. This resulted in a defect rate of 13% (Figure IV-3, LC 1). By lowering the nucleation temperature, the probability for controlled nucleation strongly increases. By this, we were able to reduce the number of defects from 43 (13%) to 1 vial (0.3%) (Figure IV-3, LC 2).

The generated FMS data was further analyzed to assess batch homogeneity. CN is expected to facilitate scale-up and process transfer by overcoming the stochastic nature of ice nucleation and a consequently more homogeneous drying behavior [10-12]. Mainly two different approaches to determine homogeneity have been used: (i) analysis of individual vials and (ii) batch-representative methods. Rambhatla et al. [9] for example, used the standard deviation of BET measurements of the final product (n=3) as surrogate for nucleation homogeneity. In a different approach, Fang et al. [23] chose the standard deviation of measured LDH activity and tetramer recovery (n=6) to assess homogeneity. Given the small number of replicates, it may be difficult to extrapolate the results to a full batch. In contrast, Passot et al. [12] evaluated the degree of homogeneous drying by comparing the absolute value of the slope of the Pirani gauge profile. With this method, they were able to consider the average drying behavior for a complete batch (n=100). However, the homogeneity of the residual water content at the end of primary drying was considered instead of the final product homogeneity. Similarly, Oddone et al. [11] studied the homogeneity of drying behavior of a whole batch (n=70) by determining the onset-offset time of the pressure ratio curve as a surrogate for vial batch behavior.

By comparing CN and RN processed shelves after complete and incomplete drying, we investigated if the homogeneity generated through the freezing step is maintained through the lyophilization cycle until the final product. We excluded the not-controlled nucleated vials from analysis. When determining the homogeneity after 1 h of secondary drying, we found a remarkably improved homogeneity for CN samples compared to RN samples (rel STD of 7.6% for CN-3 °C vs 13.1% for RN equi 2 °C). These results confirmed the findings of Passot et al. and Oddone et al. and indicate that CN could be beneficial to transfer primary drying protocols from development to production scale freeze-dryers [11, 12]. However, after completing the cycle, after 6 h of secondary drying, inter-vial batch homogeneity between CN and RN protocols was practically identical, which confirms the results of Arsiccio et al.[29]. Based on that data, we suggest that the initially higher heterogeneity after RN did not result in a reduced inter-batch

homogeneity of the final product. Presumably, desorption during secondary drying overrules small differences in RM content of individual vials.

IV.5.2 COMPARABILITY OF NUCLEATION METHODS WITH RESPECT TO PRODUCT PROPERTIES

As mentioned above, CN is expected to facilitate scale-up because T_N can be kept from lab to production scale [7, 9, 10]. Different technologies are available to control T_N and to induce ice nucleation. However, not every method can easily be implemented in lab and production scale equipment [18]. Thus, it is of high interest to investigate the comparability of CN methods with respect to product properties. If different CN methods result in comparable product properties, the most convenient and suitable CN method for the freeze-dryer could be chosen and thus expensive retrofits and investments could be avoided. Therefore, we investigated the comparability of three ice fog methods, the VERISEQ® nucleation system, the FreezeBooster® and the method described be Geidobler et al [25], which differ in ice fog generation temperature and induction pressure. The three ice fog methods were compared with respect to primary drying time and product properties such as SSA and RM for two different sugar-based formulations. These product parameters correlate as T_N defines the pore size; a high T_N =-3 °C results in larger pores and by this reduced product resistance and faster primary drying. The larger pores can be detected by SEM and a reciprocally low SSA can be measured, which in turn hinders desorption during secondary drying and leads to a higher RM content [7, 9].

Comparable to the results of Gitter et al. [20], all applied nucleation methods resulted in similar cake appearance for the different nucleation protocols (T_N) and both sugar formulations. Minor differences in terms of contact with the vial wall were not considered as critical, because all methods and protocols resulted in an elegant cake. SEM micrographs confirmed the results of primary drying time evaluation. The larger pores generated by FreezeBooster® and Geidobler et al. method at CN-3 °C led to reduced product resistance and consequently reduced primary

drying times. All nucleation methods showed PD times at CN-10 °C, close to or even comparable to the RN cycles. It can be assumed that the smaller pore size generated at CN-10 °C (Figure 5 and 6) resulted in higher product resistance and thus longer primary drying times, compared to CN-3 °C samples. The three methods resulted in comparable product properties, such as pore size and structure (Figure IV-5 and Figure IV-6) as well as SSA values with only minor differences in RM content between the methods (Figure IV-10).

IV.5.3 SSA DETERMINING FACTORS: CN, T_N AND FORMULATION COMPOSITION

Already in 1925, Tammann reported that the ice crystal morphology is a unique function of T_N [30]. Luyet and Rapatz [31] found a variety of ice crystal morphologies, including hexagonal, dendritic and dispersed spherulitic morphologies. The morphologies were dependent on T_N, solute and concentration. In the more recent studies [4, 7, 9], T_N was also identified to be the determining factor for the ice morphology and consequently, the ice crystal size and thus the SSA of the freeze-dried product. Another factor, which can impact the SSA and should be accounted for is the roughness of the pore surface. The roughness can vary for a given formulation, if the formulation contains e.g. crystallizing excipients [32]. We observed in a previous study, that CN-3 °C and CN-10 °C CN samples resulted in comparable SSA and therefore suggested that T_N is not the only SSA determining factor when an ice fog method is used [24]. Bhatnagar et al. [33] investigated the effect of a change in formulation composition at a controlled ice nucleation temperature on the SSA. To further investigate this observation, we applied two different ice fog methods, which differed in ice fog generation and injection pressure at two different T_N. CN-3 °C and CN-10 °C were chosen as desired T_N to test the presumed limits of feasible controlled nucleation temperatures with -3 °C being the highest applicable T_N with satisfying nucleation success and -10 C being the lowest applicable T_N without risking spontaneous random nucleation. By including two sugar formulations, sucrose

and trehalose-based, and four mAb concentrations, we examined the formulation effect on the resulting SSA.

For the sucrose-based formulation, we determined a correlation between SSA and T_N for the FreezeBooster® and Geidobler et al method (Figure 7A and B). Trehalose-based lyophilizates did not show a difference between the CN-3 °C and the CN-10 °C samples, which confirmed our suggestion that if CN is applied T_N is not the only SSA determining factor. Additionally, the fact that CN-10 C samples revealed lower SSA compared to RN samples, although T_N was in the same range, supported the theory that the application of an ice fog CN method itself impacts the ice crystal structure and thus primary drying behavior. Furthermore, the resulting SSA was shown to be dependent on the formulation as sucrose-based and trehalose-based samples did not exhibit the same SSA, which confirmed the results of Luyet and Rapatz [31] and Bhatnagar et al. [33]. However, the mAb concentration did not notably impact the resulting SSA (Figure 8). Throughout the mAb concentrations tested (1-100 mg/ml), the observed correlation between T_N and resulting SSA for sucrose-based lyophilizates was detected. Thus, pore size and SSA were dependent on the application of an ice fog CN, the formulation and not only T_N. Thus, for CN process development it should be considered that a high T_N (e.g. -3 °C) does not necessarily result in a relevant reduction of primary drying time; especially when considering the prolonged equilibration time but poses a higher risk for not-controlled nucleated vials within a batch. On the other hand, a low T_N (e.g. -10 °C) constitutes a risk of spontaneous nucleation of isolated vials. Therefore, it is recommended to choose a robust T_N (e.g. -5°C to -8°C) focusing on 100% successful CN of the batch.

IV.6 CONCLUSION

Recently, great expectations were raised on CN, such as primary drying time reduction, improved batch homogeneity or facilitated scale-up and process transfer. However, the achievement of these goals by CN practically faces some challenges.

Within this study, we could show that FMS is a promising tool that enables non-destructive high throughput measurements of nucleation success and with this could support the validation of a CN process.

We detected an improved inter-vial batch homogeneity after primary drying for CN samples compared to RN samples. Although this suggests that CN could facilitate scale-up of freeze-drying processes, we observed that after complete secondary drying initial advantages in homogeneity for CN processes are no longer present.

Furthermore, we exhibited that three ice fog methods, VERISEQ® system, FreezeBooster® and Geidobler et al., resulted in similar product quality attributes with only slight differences in RM of the product cakes. Thus, we assume that different ice fog CN methods can be applied in development and production scale with a low risk of changing the product properties.

Finally, we conclude that T_N is not the only determining factor for ice morphology and consequently SSA. Aside from T_N, the fact whether nucleation was induced by an ice fog method or occurred randomly and the used formulation (sugar) impacted the SSA. Consequently, a higher T_N does not necessarily lead to additional primary drying time reduction compared to a T_N that safely assures 100% controlled nucleation of the product vials.

IV.7 REFERENCES

[1] Jameel, F. and Searles, J., *Development and Optimization of the Freeze-Drying Processes*, in *Formulation and Process Development Strategies for Manufacturing Biopharmaceuticals*. 2010, John Wiley & Sons, Inc. p. 763-796.10.1002/9780470595886.ch30.

[2] Tang, X. and Pikal, M., *Design of Freeze-Drying Processes for Pharmaceuticals: Practical Advice.* Pharm. Res., 2004. 21(2): p. 191-200.

[3] Franks, F., *Freeze-drying of bioproducts: putting principles into practice.* Eur. J. Pharm. Biopharm., 1998. 45(3): p. 221-9.

[4] Searles, J.A., Carpenter, J.F., and Randolph, T.W., *The ice nucleation temperature determines the primary drying rate of lyophilization for samples frozen on a temperature-controlled shelf.* J. Pharm. Sci., 2001. 90(7): p. 860-871.

[5] Bosca, S., Barresi, A.A., and Fissore, D., *Fast freeze-drying cycle design and optimization using a PAT based on the measurement of product temperature.* Eur. J. Pharm. Biopharm., 2013. 85(2): p. 253--262.

[6] Pisano, R., Fissore, D., and Barresi, A.A., *In-Line and Off-Line Optimization of Freeze-Drying Cycles for Pharmaceutical Products.* Drying Technology, 2013. 31(8): p. 905-919.

[7] Konstantinidis, A.K., et al., *Controlled Nucleation in Freeze-drying: Effects on Pore Size in the Dried Product Layer, Mass Transfer Resistance, and Primary Drying Rate.* J. Pharm. Sci., 2011: p. 1-18.

[8] Kasper, J.C. and Friess, W., *The freezing step in lyophilization: physico-chemical fundamentals, freezing methods and consequences on process performance and quality attributes of biopharmaceuticals.* Eur. J. Pharm. Biopharm., 2011. 78(2): p. 248-63.

[9] Rambhatla, S., et al., *Heat and mass transfer scale-up issues during freeze drying: II. Control and characterization of the degree of supercooling.* AAPS PharmSciTech, 2004. 5(4): p. 54-62.

[10] Pikal, M., Rambhatla, S., and Ramot, R., *The impact of the freezing stage in lyophilization: effects of the ice nucleation temperature on process design and product quality.* American Pharmaceutical Review, 2002. 5: p. 48-53.

[11] Oddone, I., et al., *Impact of vacuum-induced surface freezing on inter- and intra-vial heterogeneity.* Eur. J. Pharm. Biopharm., 2016. 103: p. 167-178.

[12] Passot, S., et al., *Effect of controlled ice nucleation on primary drying stage and protein recovery in vials cooled in a modified freeze-dryer.* J. Biomech. Eng., 2009. 131(7): p. 74511-5.

[13] Pikal, M.J., Roy, M.L., and Shah, S., *Mass and heat transfer in vial freeze-drying of pharmaceuticals: Role of the vial.* J. Pharm. Sci., 1984. 73(9): p. 1224--1237.

[14] Rambhatla, S. and Pikal, M.J., *Heat and mass transfer scale-up issues during freeze-drying, I: atypical radiation and the edge vial effect.* AAPS PharmSciTech, 2003. 4(2): p. E14.

[15] Sane, P., et al., *Spatial Variation of Pressure in the Lyophilization Product Chamber Part 2: Experimental Measurements and Implications for Scale-up and Batch Uniformity.* AAPS PharmSciTech, 2016.

[16] Pikal, M.J., et al., *Freeze-Drying Process Development and Scale-Up: Scale-Up of Edge Vial Versus Center Vial Heat Transfer Coefficients, Kv.* J. Pharm. Sci., 2016. 105(11): p. 3333-3343.

[17] Wegiel, L.A., Ferris, S.J., and Nail, S.L., *Experimental Aspects of Measuring the Vial Heat Transfer Coefficient in Pharmaceutical Freeze-Drying.* AAPS PharmSciTech, 2018. 19(4): p. 1810-1817.

[18] Geidobler, R. and Winter, G., *Controlled ice nucleation in the field of freeze-drying: fundamentals and technology review.* Eur. J. Pharm. Biopharm., 2013. 85(2): p. 214-22.

[19] Reuter, S., Philipp, J., and Dobner, J., *Gesteuertes Einfrieren in der Gefriertrocknung* TechnoPharm, 2018. 8(3): p. 140-149.
[20] Gitter, J.H., et al., *A Comparison of Controlled Ice Nucleation Techniques for Freeze-Drying of a Therapeutic Antibody.* J. Pharm. Sci., 2018.
[21] Geidobler, R., Konrad, I., and Winter, G., *Can controlled ice nucleation improve freeze-drying of highly-concentrated protein formulations?* J. Pharm. Sci., 2013. 102(11): p. 3915-9.
[22] Awotwe-Otoo, D., et al., *Product and process understanding to relate the effect of freezing method on glycation and aggregation of lyophilized monoclonal antibody formulations.* Int. J. Pharm., 2015. 490(1-2): p. 341-50.
[23] Fang, R., et al., *Effect of Controlled Ice Nucleation on Stability of Lactate Dehydrogenase During Freeze-Drying.* J. Pharm. Sci., 2018. 107(3): p. 824-830.
[24] Vollrath, I., et al., *Does controlled nucleation impact the properties and stability of lyophilized monoclonal antibody formulations?* Eur. J. Pharm. Biopharm., 2018. 129: p. 134-144.
[25] Geidobler, R., Mannschedel, S., and Winter, G., *A new approach to achieve controlled ice nucleation of supercooled solutions during the freezing step in freeze-drying.* J. Pharm. Sci., 2012. 101(12): p. 4409-13.
[26] Weijia, L., *Controlled nucleation during freezing step of a freeze drying cycle using pressure differential ice crystals distribution from condensed frost*. 2016, Millrock Technology, Inc., Kingston, NY (US)
[27] Kaltenegger, J., et al., *Neuartiges Verfahren zur Steuerung der Eiskeimbildung.* ThechnoPharm, 2012. 2(6): p. 420-427.
[28] Awotwe-Otoo, D., et al., *Impact of controlled ice nucleation on process performance and quality attributes of a lyophilized monoclonal antibody.* Int. J. Pharm., 2013. 450(1-2): p. 70-8.
[29] Arsiccio, A., et al., *Vacuum Induced Surface Freezing as an effective method for improved inter- and intra-vial product homogeneity.* Eur. J. Pharm. Biopharm., 2018. 128: p. 210-219.
[30] Knight, C.A., *The Freezing of Supercooled Liquids*. 1967: D. Van Nostrand Company.
[31] Luyet, B. and Rapatz, G., *Patterns of ice formation in some aqueous solutions.* Biodynamica, 1958. 8(156): p. 1--68.
[32] Oddone, I., Barresi, A.A., and Pisano, R., *Influence of controlled ice nucleation on the freeze-drying of pharmaceutical products: the secondary drying step.* Int. J. Pharm., 2017. 524(1-2): p. 134-140.
[33] Bhatnagar, B.S., Pikal, M.J., and Bogner, R.H., *Study of the individual contributions of ice formation and freeze-concentration on isothermal stability of lactate dehydrogenase during freezing.* J. Pharm. Sci., 2008. 97(2): p. 798-814.

CHAPTER V

V. EVALUATION OF HEAT FLUX MEASUREMENT AS A NEW PAT MONITORING TOOL IN FREEZE-DRYING

This chapter was published in the *Journal of Pharmaceutical Sciences and* appears in this thesis with the journal`s permission*:*

Ilona Vollrath[1,2], Victoria Pauli[1,2], Wolfgang Friess[2], Angelika Freitag[1], Andrea Hawe[1], Gerhard Winter[2], (2017). „*Evaluation of Heat Flux Measurement as a New Process Analytical Technology Monitoring Tool in Freeze-Drying.”* Journal of Pharmaceutical Sciences, 106(5): 1249-1257.

The manuscript was written by Ilona Vollrath. Experiments were performed by Victoria Pauli, within the scope of her master thesis, and Ilona Vollrath. Wolfgang Frieß, Angelika Freitag, Andrea Hawe and Gerhard Winter provided scientific guidance and input during the experimental phase and the complete writing process. In addition, Wolfgang Frieß, Andrea Hawe, and Gerhard Winter, who also serves as corresponding author, reviewed the final manuscript.

[1] Coriolis Pharma Research GmbH, D-82152 Martinsried, Germany

[2] Department of Pharmacy, Pharmaceutical Technology and Biopharmaceutics, Ludwig-Maximilians-University, D-81377 Munich, Germany

V.1 ABSTRACT

This study investigates the suitability of heat flux measurement as a new technique for monitoring product temperature and critical endpoints during freeze-drying. The heat flux sensor is tightly mounted on the shelf and measures non-invasively (no contact with the product) the heat transferred from shelf to vial. Heat flux data were compared to comparative pressure measurement, thermocouple readings and Karl Fischer titration as current state of the art monitoring techniques. The whole freeze-drying process including freezing (both by ramp freezing and controlled nucleation), primary and secondary drying was considered. We found that direct measurement of the transferred heat enables more insights into thermodynamics of the freezing process. Furthermore, a vial heat transfer coefficient can be calculated from heat flux data, which ultimately provides a non-invasive method to monitor product temperature throughout primary drying. The endpoint of primary drying determined by heat flux measurements was in accordance with the one defined by thermocouples. During secondary drying, heat flux measurements could not indicate the progress of drying as monitoring the residual moisture content. In conclusion, heat flux measurements are a promising new non-invasive tool for lyophilization process monitoring and development using energy transfer as a control parameter.

V.2 INTRODUCTION

Freeze-drying is the method of choice to dry temperature sensitive products such as pharmaceutical proteins, peptides, and vaccines. However, freeze-drying cycles need product specific optimization to ensure, for example, that the product temperature (T_p) does not exceed the critical product temperature during primary drying and that primary drying is completed. Non-optimized processes can result in elevated residual moisture, cake shrinkage or even cake collapse, and can ultimately lead to the rejection of an entire production batch [1, 2]. Thus, the accurate monitoring of T_p and the determination of the end of primary and secondary drying are crucial to assure product quality and process economy [2]. Consequently, the need for rigorous product monitoring and process analytical technology (PAT) tools during cycle development is high.

Temperature sensors, such as thermocouples (TC), wireless temperature sensors, or resistance temperature detectors (RTD) [3, 4], are commonly used to monitor the product temperature and to assess the completion of primary drying (i.e. when T_p approaches the shelf temperature). However, inserting a temperature sensor into a vial can increase sublimation rates compared to unmonitored vials. Hence, monitored vials complete primary drying earlier and may not be batch representative [5]. Tang and Pikal recommended the inclusion of a safety margin or a “soak time” for the use of thermocouples to ensure that all vials have finished primary drying [6]. More recent studies performed by Bosca et al. [7] have shown that in non GMP conditions the cake structure and product temperature in monitored and unmonitored vials are comparable. Additionally, product dynamics are almost unaffected by the insertion of a thermocouple [7]. However, temperature sensors are usually handled manually, which poses a challenge with respect to sterility [5].

Other methods to determine the product temperature and the end of primary drying are based on pressure rise tests (PRT) and mathematical modeling. In early works, product temperature and completion of primary drying was estimated based on the saturating vapor pressure of ice

by the pressure response measured during a PRT [8, 9]. Another method to use PRT data for product temperature estimation is barometric temperature measurement (BRT), where the maximum value of the first derivative of the pressure rise curve is used to estimate the temperature at the sublimation interface [10, 11]. Further, several mathematical models based on PRT data, such as manometric temperature measurement (MTM) [12-15], pressure rise analysis (PRA) [16] and dynamic parameters estimation (DPE) [17] were proposed in literature to determine product temperature and assess various process parameters. These methods allow for a non-invasive estimation of the product temperature at the sublimation interface, reducing the impact on product sterility [1, 18]. They all provide an average product temperature, which does not account for heterogeneities across the batch (edge vials (higher temperatures) and centre vials (lower temperatures)) [19]. For MTM, for example, it has been described that the estimated product temperature is more representative for the lowest product temperature [13]. The named mathematical models differ by the used algorithm and the parameters estimated [18].

Comparative pressure measurement is yet another way of assessing the end of primary drying, where a Pirani pressure gauge and a capacitance manometer are employed. During primary drying, the measured pressure differs between the two instruments, while at the end of primary drying this difference approaches zero. The comparative pressure measurement is also a batch representative and non-invasive method that accounts for the very last vials to complete primary drying [1, 2, 4].

Additionally, electronic moisture sensors have been described as a technique for assessing the end of primary drying by Roy and Pikal [5]. The electronic moisture sensor detects a change in capacitance based on the adsorption of water on a thin aluminum oxide film. The capacitance measurement is translated into a voltage output. Roy and Pikal showed that the sensor is able to detect as few as approximately 0.3% of not completely dried vials and is therefore a batch representative method. However, it needs to be noted that the sensor is not able to withstand steam sterilization [5].

In the last years, substantial effort has been made to implement new technologies to monitor the end of primary drying and to facilitate process development and transfer. Examples are mass spectrometry (MS) [20, 21], optical fiber system (OFS) [22], and tunable diode laser absorption spectroscopy (TDLAS) [23, 24].

Mass spectrometry is used for residual gas analysis. Therefore, a mass spectrometer is connected directly to the freeze-dryer chamber or as an alternative to the duct between the chamber and the condenser. The gas composition during primary drying changes with ongoing drying time. At the beginning of the primary drying step water vapor is the most predominant gas species. When all ice is sublimed, the amount of water vapor steeply decreases, and nitrogen becomes the more dominant gas species. Residual gas analysis by mass spectrometry not only allows for assessing the end of primary drying but also for the detection of leaks of the drying equipment as up to 16 components can be monitored simultaneously [20, 21]. However, this technique lacks the ability to monitor product temperature.

Kasper et al. introduced an OFS based on Fiber Bragg Gratings to monitor product temperature and the end of primary drying. The OFS was shown to be significantly more sensitive and easier to handle compared to thermocouples. Further, they showed a better resolution and a faster response which even allows for the detection of physico-chemical events such as crystallization. Kasper et al. could also show that modifications of the OFS even enable a non-invasive temperature monitoring and end point determination [22].

TDLAS is another non-invasive method to monitor a freeze-drying cycle. This sensor simply requires optical access to the gas flow in the duct between the chamber and the condenser and can be implemented in freeze-dryers of various scales, which facilitates scale up. Gieseler et al. [23] have shown that the TDLAS technique is able to determine the water vapor concentration, gas flow velocity and the rate of water removal. The knowledge of the water vapor concentration enables the detection of the endpoint of primary and secondary drying [23]. Further work by Schneid et al. [24] describes the application of TDLAS to determine an average

sublimation rate, which can provide the vial heat transfer coefficient (K_v) and an average product temperature. Kuu et al. [25] further demonstrated the assessment of the product mass transfer resistance by TDLAS measurements and a pore diffusion model. However, it needs to be noted that it is not possible to retrofit the system into each freeze-dryer [23, 26].

Currently, only few methods allow detecting the end of secondary drying. These include methods based on pressure rise testing [3], MTM method [14], and electronic moisture sensors [5, 27]. Techniques such as sample thieves or single shelf closure systems enable the extraction of products directly from the freeze-drying process for the determination of the residual moisture at different time points [3].

A new and interesting approach to monitor T_p and critical end points is measuring the heat flux between shelf and vial(s). Heat flux sensors have been used in plastics-, automotive-, or solar energy industry [28], whereas the application as a monitoring and PAT tool in pharmaceutical freeze-drying has not been established yet. For heat flux measurement during freeze-drying, a heat flux sensor is used, which utilizes a thin foil type thermopile. A thermopile is an array of approximately 50-60 differential thermocouples connected in series that convert thermal energy into electrical energy. In a heat flux sensor, the thin foil type thermopile is bound to both sides of a known thermal barrier. The voltage output of each thermocouple of the thermopile is proportional to the temperature difference (ΔT) between the upper and the lower surface. In turn, ΔT is directly proportional to the heat flux through the sensor. Thus, the sensor needs to be placed in direct contact with the surface of interest, in our case the freeze-dryer shelf and the vial bottom. Generally, these sensors are able to measure heat flux resulting from conductive, convective, and radiation heat transfer [28]. As the sensor is placed between the vials and the shelf, it consequently measures mainly conduction and convection heat at that point.

The heat flux sensors evaluated within our study detect the ΔT between the shelf surface temperature (T_s) and the vial bottom temperature considered as product temperature (T_p). The measured temperature difference is transferred via the thickness of the sensor (0.18 mm) and

its thermal conductivity to an average amount of thermal energy that has been transferred per unit time per unit area. The area calculation is based on the area of the sensor. Thus, the heat flux sensor gives a direct reading in W/m^2. Throughout a freeze-drying cycle, the heat flux direction changes. During freezing, the heat flows from the warmer vial to the colder shelf surface, which results in a negative heat flux. During primary and secondary drying, heat flux is positive as long as heat flows from the shelf to the vials. This could also be used to determine the end of ice crystallization during freezing, because the generated exothermic heat warms the vial during ice formation, whereas the vial temperature approaches the T_s after the crystallization event [29]. Furthermore, during primary drying, when the vials reach T_s, heat flux approaches zero indicating the end of primary drying.

Moreover, heat flux measurements can provide important parameters for process development and control such as the vial heat transfer coefficient (K_v). K_v is influenced by different factors, such as vial type, geometry of the vial bottom and chamber pressure. Therefore, K_v needs to be determined for every setup of chamber pressure, shelf temperature and vial type [30]. Currently, gravimetrical approaches requiring time consuming weighing of numerous vials is typically used for K_v determination. Heat flux measurements could provide a fast, simple and non-invasive alternative. However, it should be noted that the vial heat transfer coefficient determined by heat flux measurement (K_v(heat flux)) differs from the K_v determined by gravimetrically measurements (K_v(gravimetrically)) and calculated as described by Pikal et al. [30], because the K_v(heat flux) comprises not for all heat transfer mechanisms in contrast to the K_v(gravimetrically). This can be explained by the sensors positioning below the vial. Heat supplied to the product by radiation effects is consequently not detected in completion. Therefore, the K_v(heat flux) is lower as the K_v(gravimetrically). This has been shown in previous work [31]. Additionally, mass flow per vial, mass flow of the entire batch, fraction of removed mass and the product resistance (R_p) could be assessed by heat flux measurements. Ultimately, from R_p, T_p at the sublimation interface could be calculated.

Besides process monitoring, the heat flux can also be used to control freeze-drying processes. For process control, the shelf temperature set point could be adjusted based on the measured heat flux in order to achieve maximum heat transfer while T_p is kept below the critical product temperature.

Our aim was to evaluate the performance and suitability of heat flux measurements for freeze-drying process monitoring under pharmaceutically relevant conditions. The heat flux data measured with the applied Accuflux™ sensors were compared to current state of the art techniques to monitor freeze-drying processes, such as comparative pressure measurement and TC readings for the end of primary drying. During secondary drying, the results from heat flux measurements were compared to product moisture determined by Karl Fischer titration and head space moisture analysis. Further, the accuracy of K_v(heat flux) for product temperature estimation was investigated by comparing the estimated product temperature with actual thermocouple readings.

V.3 MATERIALS AND METHODS

V.3.1 FORMULATIONS AND PRIMARY PACKAGING

Ph.Eur grade sucrose and bovine serum albumin (BSA) was purchased from Sigma-Aldrich (Munich, Germany). Sucrose solutions (5%, 20%, and 50% weight/volume (w/v) ratios) were prepared with highly purified water (Milli-Q integral water purification system, Merck Millipore, Hertfordshire, United Kingdom). BSA (10 mg/ml) was dissolved in a 10 mM phosphate buffer at pH 7.4 containing 5% sucrose as cryoprotectant. Prior to use, all formulations except the 50% sucrose solution were filtered through 0.22 µm PVDF membrane filters (Millipore, Schwalbach, Germany).

2R glass type I tubing vials and 10R tubing vials were kindly provided by MGlas AG (Münnerstadt, Germany). Rubber stoppers, 13 mm and 20 mm (Westar® RS, FluoroTec B2-40 coating) were kindly supplied by West Pharmaceutical Services (Eschweiler, Germany). For investigations on the 1st generation sensor 2R tubing vials with a filling volume of 1 ml were used. For evaluation of the 2nd generation sensor, 10R tubing vials were filled with 1, 3, 5 ml formulation depending on the experiment (details stated in each section).

V.3.2 FREEZE-DRYING EQUIPMENT AND PROCESS DESIGN

A pilot scale freeze-dryer (Millrock Magnum Series; 1.48 m^2) equipped with a Millrock FreezeBooster® for automatic controlled nucleation was used for the experiments. Three heat flux sensors (Accuflux™, Millrock Technology Inc., Kingston, NY, USA) are mounted on the middle shelf of the freeze-dryer (Figure 1B) and the corresponding control software (LyoPAT®, Millrock Technology Inc., Kingston, NY, USA) is installed.

Freeze-drying process parameters and freezing protocols by random (RN) or controlled nucleation (CN) are summarized in Table V-1. After freezing, the samples produced by both nucleation protocols were subjected to the same primary and secondary drying protocol. For

some experiments within this study, the standard drying protocol was varied, which is stated in the result section where applicable.

Table V-1: Freeze-drying protocol used for the experiments.

Process step	Controlled nucleation (CN)	Random nucleation (RN)
Equilibration	Equilibration at desired T_N (-5 °C) for 120 min	Equilibration at 2 °C for 120 min
Nucleation	Controlled at -5 °C	Random by shelf temperature decrease by 1 °C/min
Freezing	Decrease of shelf temperature to -50 °C (ramp 1 °C/min); hold for 120 min	
Primary drying	Shelf temperature: -25 °C (ramp 0.5 °C/min) Chamber pressure: 100 mTorr	
Secondary drying	Shelf temperature: 30 °C (ramp 0.1 °C/min) Chamber pressure: 100 mTorr	

The end of primary drying was determined by comparative pressure measurement, unless stated differently in the result section.

V.3.3 HEAT FLUX SENSORS

Accuflux™ heat flux sensors (Millrock Technology Inc., Kingston, NY, USA) of two different generations were used within this work. The 1st generation sensor measures 4 x 1.4 cm and has an external thermocouple mounted next to the sensor on the shelf to measure the shelf temperature (T-type Copper). The 2nd generation sensor measures 3.6 x 3 cm and is equipped with a built-in thermocouple to measure the shelf temperature (ANSI Type T). To improve a flat standing of the vials, approximately 2 cm of stainless-steel tape of the same thickness as the sensor (called “Scaffolding”) are mounted around the 2nd generation sensors (Figure V-1A). Both sensors are permanently fixed on the shelf with a conductive, silver filled epoxy (AI Technology Inc., Princeton, NJ, USA). The surface of the sensor, where the vials are placed on, is made of stainless-steel tape (total thickness of sensor and stainless-steel tape: 0.28 mm). The thermal resistance of the sensor (sensor thickness measures 0.18 mm) is 0.0013 $K/m^2/W$ and the heat capacity value is 29.8 $cal/m^2/K$. The sensor´s response time corresponds to 0.60 seconds.

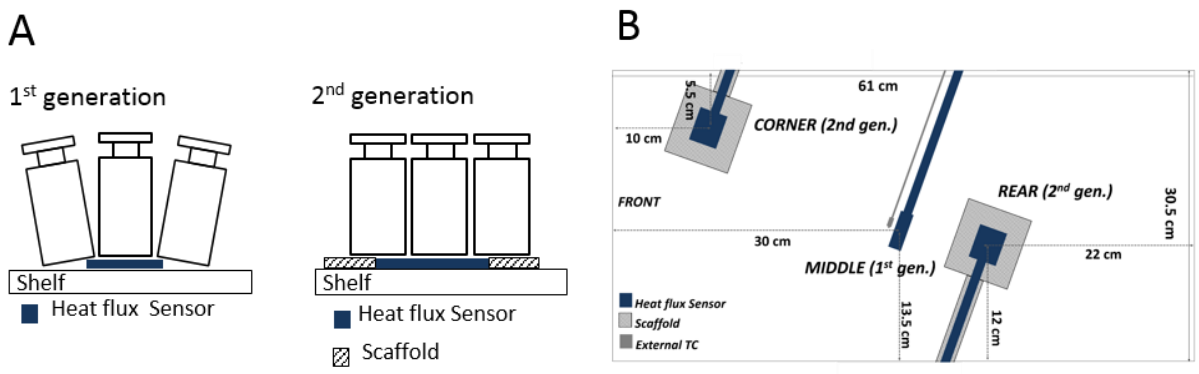

Figure V-1: (A) Schematic drawing of the heat flux sensor mounting; the 1st generation sensor lacks the scaffolding. In consequence, vials, which overhang, cannot be placed evenly. Scaffolding was added to the 2nd generation sensor, which ensures a better leveled vial position. (B) Schematic drawing of the freeze-dryer shelf, which the sensors are mounted on (drawing to scale).

The 1st generation sensor was mounted in the center of the shelf. One 2nd generation sensor was added right next to the 1st generation sensor in the center of the shelf. The other 2nd generation sensor was placed in the front left corner of the shelf. An overview about the positions of the different sensors on the shelf is provided by (Figure V-1B). All sensors were calibrated by the manufacturer (RdF corporation, Hudson, NH, USA). The measurement output data of the sensors was processed via the corresponding LyoPAT® software (Millrock Technology Inc., Kingston, NY, USA), which was part of the freeze-dryer controlling software.

V.3.4 DETERMINATION OF THE VIAL HEAT TRANSFER COEFFICIENT BY HEAT FLUX ($K_{V,}$ (HEAT FLUX))

The heat flux sensor can be used to calculate K_v(heat flux) according to Eq.1.

Eq. (1)
$$K_v = \frac{heat\ flux}{(T_s - T_p)}$$

where *heat flux* [W/m^2] and shelf temperature T_s [°C], are measured by the heat flux sensor and T_p [°C] is determined by TCs located in the vials on top of the sensor. It is important to note that Eq. (1) is only valid in the steady state phase of primary drying [30].

Ten T-type copper-constantan TCs (0.01 mm diameter; accuracy within 1 °C; Omega Engineering, Newport, CT, USA) were placed into the vials standing on the heat flux sensor and were used to measure T_p. T_s was determined by an external TC for the 1st generation sensor and by a built-in TC for the 2nd generation sensor.

V.3.5 PRODUCT TEMPERATURE ESTIMATION BY LYOPAT®

For T_p estimation, K_v is needed as a user input ($K_{v,user}$). Therefore, $K_{v,user}$ was determined in an identical pre-cycle according to Eq.(1) as the mean K_v over 20 h of steady state primary drying of the pre-cycle. $T_{p,est}$ was obtained by LyoPAT® according to Eq.(2).

Based on the knowledge of K_v, Eq. (1) can be transformed into Eq. (2) in order to calculate an estimated product temperature ($T_{p,est}$).

Eq. (2)
$$T_{p,est} = \frac{K_v * T_{s-heat\ flux}}{K_v}$$

V.3.6 PERFORMANCE CHECK OF HEAT FLUX SENSORS

For the one-vial performance checks, one 10R vial was filled with 9 ml of water at 0, 20, 30, 50, 70, and 90 °C was centrally placed on the sensor (shelf at room temperature 21 °C; not controlled). T_s (determined by heat flux sensor), T_p by TC and heat flux was recorded over five minutes (two data points per minute). This experiment was performed three times in order to investigate the sensor´s repeatability.

To analyze the repeatability and linear measurement range, the obtained heat flux data was plotted against $\Delta T(T_s\text{-}T_p)$. According to Eq 1, the resulting slope provides Kv(heat flux).

Additionally, the effect of moisture between shelf and vial was simulated, by dipping the vial into water to wet the outer surface of the vial bottom before it was placed on the center of the sensor. The heat flux results were compared to those obtained with a dry vial. Furthermore, a “rose” of seven 10R vials filled with 9 ml of ice water was shifted by 10 mm off center. The values generated

before and after the shift were compared. The effect of moisture was investigated on the 2nd generation sensor, whereas the impact of a vial shift on the sensor was evaluated on both sensors.

For repeatability tests, the performance of the heat flux measurement under process conditions using a partially filled shelf and a fully filled shelf was examined (each setup three times) for the 1st and the 2nd generation sensor. For both setups, the shelf was completely filled with vials in order to keep the vials in the correct position over the sensor. In case of the partially filled shelf, 150 2R vials (1st generation sensor) or 65 10R vials (2nd generation sensor) were filled with 1 ml and 3 ml of a 5% sucrose solution. A fully filled shelf corresponds to 772 2R vials and 332 10R vials, which results in a ratio of 20% for the partially filled shelves. The 5% sucrose solution was subjected to the random nucleation freezing and the standard drying protocol (Table V-1).

The applicability of heat flux measurements to (i) solutions of different solid content (5, 10, 20 and 50% sucrose in water (w/v)) and (ii) filling volumes (1, 3 and 5 ml of 5% sucrose solution) was studied with the 2nd generation sensor (10R vials) using the controlled nucleation and standard drying protocol (Table V-1).

V.3.7 SECONDARY DRYING KINETICS

One freeze-dryer shelf loaded with (i) 332 10R vials (3 ml of 5% sucrose solution) or (ii) 400 6R vials (3 ml of 10 mg/ml BSA solution) was subjected to the controlled nucleation and standard drying protocol (Table V-1). At set time points during secondary drying, the chamber was backfilled with dry nitrogen. The freeze-dryer door was opened, and selected vials were manually stoppered under nitrogen flush. At each time point, three samples from front, back and center of the shelf were taken. Subsequently, the chamber vacuum was reconditioned, and secondary drying was continued. Throughout secondary drying, the heat flux was monitored (rear sensor) and compared to the sample`s residual moisture content determined by Karl Fischer titration. The vials on the sensor were not moved throughout the study.

V.3.8 RESIDUAL MOISTURE DETERMINATION BY KARL FISCHER

Residual moisture of the freeze-dried product was determined by coulometric Karl Fischer titration with an Aqua 40.00 titrator (Analytik Jena, Jena, Germany) using a head-space module. Sample aliquots of approximately 20 mg were prepared in 2R vials (stoppered with rubber stoppers) under controlled residual humidity of less than 10% in a glove box. Blank values were obtained from empty vials treated identically. A system test was performed daily by measuring a pure water standard at 170 °C (Apura® water standard oven 1.0, Merck KGaA, Grafing, Munich).

V.3.9 HEADSPACE MOISTURE MEASUREMENT BY FREQUENCY MODULATED SPECTROSCOPY (FMS)

The partial pressure of water vapor in the vial headspace was measured using an FMS-1400 (Lighthouse Instruments, Charlottesville, VA, USA). Before usage the system was purged with 5 l/min nitrogen gas for at least 30 min to minimize background ambient moisture contribution to the signal. Prior to measurements, a two-point calibration followed by a five-point system suitability test was performed on a daily basis. The measurement time was set to 5 sec. Headspace moisture values are provided as the partial pressure of water vapor in mbar.

Sample vials were allowed to equilibrate to room temperature before the head space measurement was performed. As the FMS is a non-destructive method, the same vials were used for FMS and Karl Fischer analysis.

V.4 RESULTS

V.4.1 ONE-VIAL PERFORMANCE CHECK

First, the performance of the sensors with respect to repeatability, linear measurement range of $\Delta T(T_s\text{-}T_p)$ and robustness was tested.

To compare the repeatability of the 1st generation sensor with the 2nd generation sensor, the mean K_v(heat flux) over a 5 min measuring time and the corresponding relative (RSD) and absolute (STD) standard deviation were calculated. For the 1st generation sensor, a mean K_v(heat flux) of the three repeats of 33.4 W/m²*°C (RSD=8.1%; STD=2.7 W/m²*°C) was observed. The 2nd generation sensor showed improved repeatability with a measured K_v(heat flux) of 55.6 W/m²*°C (RSD=1.9%; STD=1.1 W/m²*°C). The difference in the measured K_v(heat flux) values of the two sensors can be attributed to the different sensor architecture (external thermocouple of the 1st generation sensor vs built-in thermocouple and additional scaffolding of the 2nd generation sensor), which contributes to an improved accuracy for the 2nd generation sensor.

Next, the performance of the sensor over a temperature range from 0 °C to 90 °C was examined. Both sensors showed a linear correlation (R^2=0.992) between the measured heat flux and $\Delta T(T_s\text{-}T_p)$ over the investigated temperature range (data not shown).

In a further scenario, moisture was introduced between the shelf and the vial to address the robustness of the sensor. This experiment was performed with the 2nd generation sensor, as all previous results showed a clear advantage of the 2nd generation sensor. The measured heat flux towards the wet vials (1115.4 W/m²) was almost double the heat flux of the dry vials (638.7 W/m²). The inserted TCs did not indicate a difference in T_p between the wet and dry vial.

Last, the robustness of heat flux measurements towards user influence was investigated. Therefore, it was simulated that the vials are not placed on the exact same spot but shifted by 10 mm towards the edge of the sensor. For the 1st generation sensor a change in mean heat

flux by 122.9 W/m^2 (717.1 W/m^2 vs 594.2 W/m^2) was detected. In contrast, for the 2nd generation sensor a change by only 6.8 W/m^2 (638.7 W/m^2 vs 631.9 W/m^2) was recognized.

V.4.2 PERFORMANCE CHECK UNDER PROCESS CONDITIONS

The repeatability of the heat flux measurements between different freeze-drying runs of the same protocol under partial and full filling conditions was tested (Figure V-2).

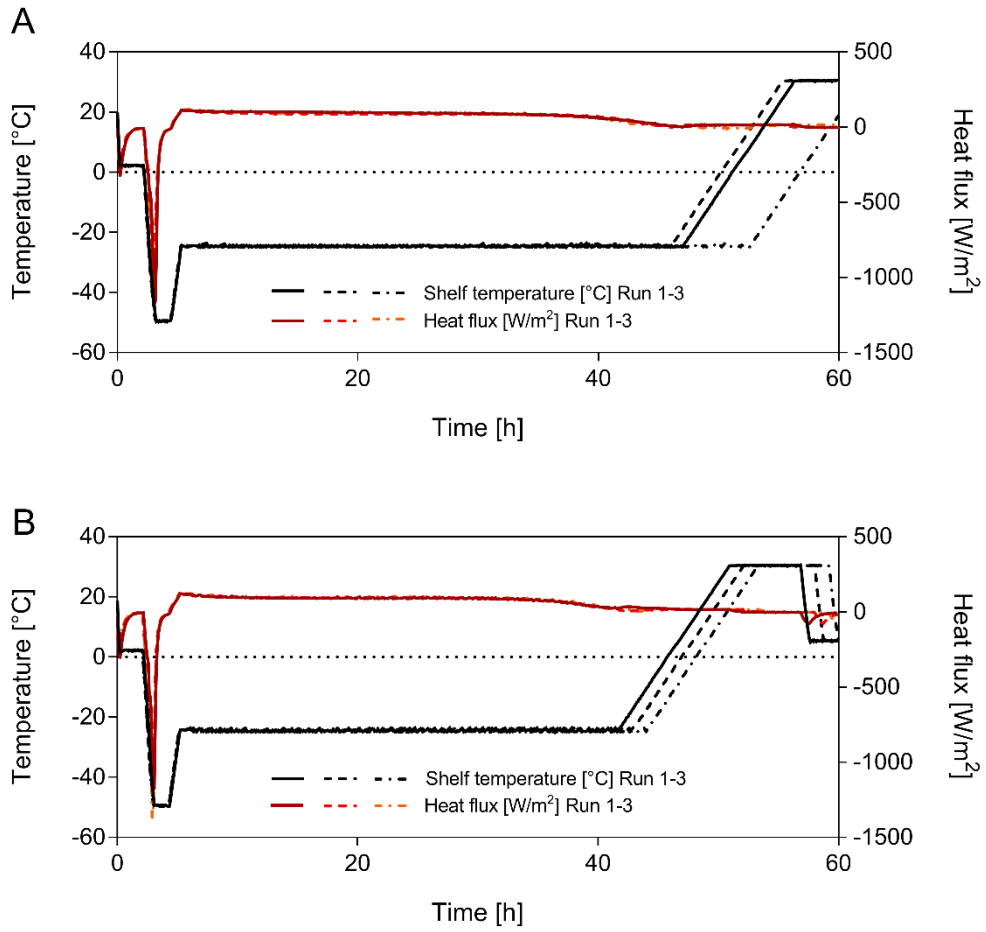

Figure V-2: Overlay of heat flux patterns of the 2nd generation sensor (n=3) during freeze-drying for fully loaded shelf (A) and partially loaded shelf (B). The repeatability of heat flux measurement was determined in three independent freeze-drying runs following the standard drying protocol after random nucleation.

The heat flux data were reproducible between the multiple experiments (n=3) performed using both partially and fully filled shelves. The mean heat flux of the three repeats (over 6 h of steady

state primary drying) was 98.2 W/m^2 (RSD=5.0%; STD=4.9 W/m^2) for the partially filled shelf and 98.0 W/m^2 (RSD=5.5%; STD=5.4 W/m^2) for the fully filled shelf.

The applicability of heat flux measurements for sucrose solutions of different concentrations and different vial filling volumes was tested, by comparing the mean heat flux and K_v(heat flux) value over 6 h of steady state primary drying (Figure V-3). A decrease in heat flux was observed with increasing sucrose concentration, as well as a linear correlation between the mean heat flux in steady state and the sucrose concentration (Figure V-3A). The mean K_v(heat flux) values of the 5, 10 and 20% sucrose solution fluctuate around 11.7 W/m^2*° (STD=0.9 W/m^2*°C) whereas the K_v(heat flux) of the 50% sucrose solution was remarkably lower (8.5 W/m^2*°C).

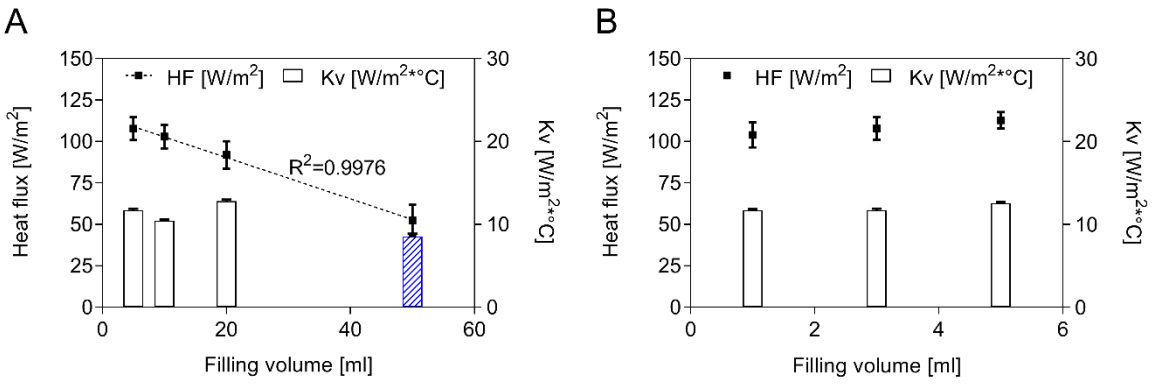

Figure V-3: (A) Heat flux measurements for different sucrose concentrations (10R vials; 3 ml filling volume). For the 50% sucrose solution no steady state could be reached and Eq. 1 is not valid, which is indicated by the blue striped column. (B) Heat flux measurements for different filling volumes (10R vials; 1, 3, 5 ml filling volume) of a 5% sucrose solution.

No change of the mean heat flux with increasing filling volumes was observed and a mean K_v(heat flux) of 11.9 W/m^2*°C (STD=0.4 W/m^2*°C) was measured (Figure V-3B).

V.4.3 MONITORING OF A FREEZE-DRYING PROCESS BY HEAT FLUX MEASUREMENTS

V.4.3.1 MONITORING OF THE FREEZING STEP

The heat flux was monitored during freezing by random and controlled nucleation of 10R vials with 3 ml of a 5% sucrose solution (Figure V-4A and 4B). Heat flux and T_p measured by TC decreased until nucleation occurred. For random nucleation, an irregular profile was observed by both heat flux and TC (Figure V-4A). For controlled nucleation, the heat flux and TC profile was more uniform in the moment of nucleation, as all vials on the sensor nucleated at the same time (Figure V-4B).

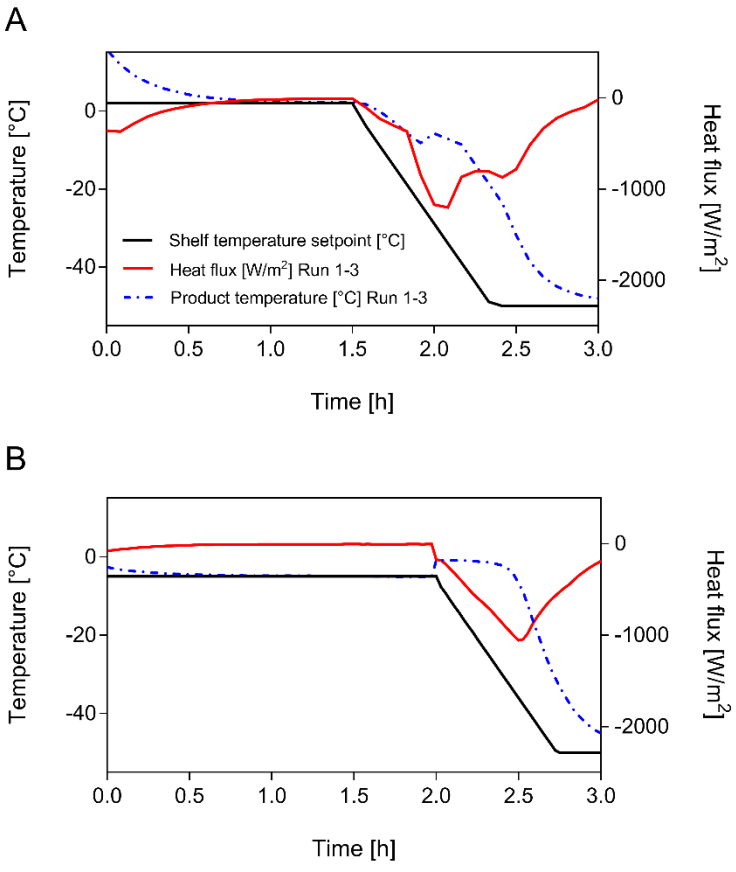

Figure V-4: Freezing with random nucleation (A) and controlled nucleation (B) (showing one example of n=3) of a 5% sucrose solution (10R vials; 3 ml filling volume).

V.4.3.2 MONITORING OF PRIMARY DRYING

The aim was to test the sensor´s ability to detect the end of primary drying compared to TC and comparative pressure measurement. Therefore, the heat flux data gained in the experiments shown in Figure V-3 were related to the corresponding T_p and comparative pressure measurement data at the time point, when heat flux reached zero. One example (5 % sucrose solution with a 3 ml filling volume in a 10R vial), is shown in Figure V-5.

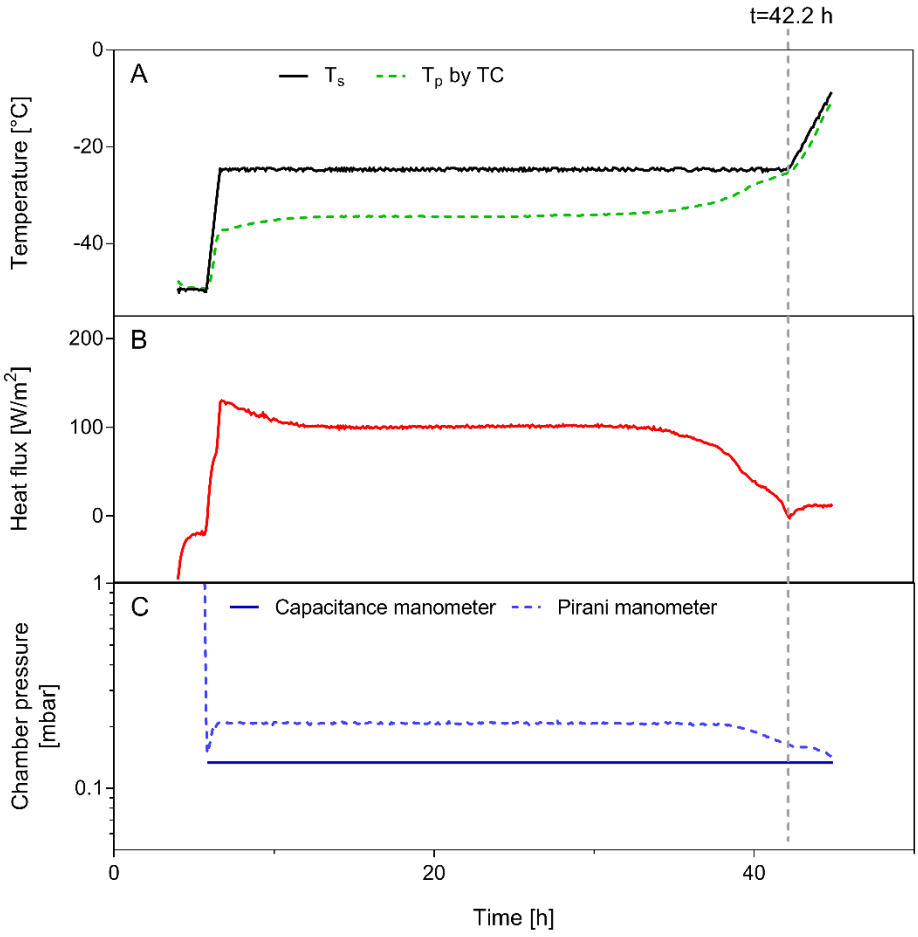

Figure V-5: Comparison of the end of primary drying determined via (A) thermocouples, (B) heat flux and (C) comparative pressure measurement of a 5% sucrose solution (10R vials; 3 ml filling volume).

In all cases, the end of primary drying determined by heat flux measurements was in accordance with the endpoint detected by TC, while comparative pressure measurement still indicated a pressure difference. For the provided example ΔT was 0.26 °C, which is below the accuracy specification of +/- 1 °C of the used TC, when heat flux reached zero (Figure V-5). The difference

in endpoint assessment between comparative pressure measurement and TC reading or heat flux measurement was expected as comparative pressure measurement accounts for the last few vials, which finish primary drying. In this context it should be clarified that the end of primary drying determined with the used methods does not indicate completion of sublimation. For heat flux or TC measurements that means that the heat transferred by the shelf after completion of sublimation is used to heat the container. When the container reaches the shelf temperature, the heat transfer lacks the driving force and approaches zero. In the case of comparative pressure measurement, the pressure ratio becomes equal to one when there is no water vapor in the chamber. However, ice sublimation could have been completed before as the concentration of water vapor in the chamber, after sublimation was completed, is a consequence of the fluid dynamics of the water. Taking this into account, for all methods sublimation most likely is completed prior to the determined end of primary drying time.

V.4.3.3 MONITORING OF SECONDARY DRYING

To investigate the sensor´s ability to indicate the end of secondary drying the heat flux in the course of secondary drying was compared to the residual moisture of the product (Figure V-6). The heat flux curves for both 5% sucrose (Figure V-6A) and 10 mg/ml BSA formulation (Figure V-6B) showed a steep decrease during the first 4 to 5 h of secondary drying. After that, the heat flux levelled off at negative values of about -2 W/m^2 for the 5% sucrose solution and at about -5 W/m^2 for 10 mg/ml BSA formulation. The residual moisture determined by Karl Fischer also showed a steep decrease in the initial phase of secondary drying followed by a plateau phase. Within the 5% sucrose solution experiment, the residual moisture decreased steeply from 2.3% to 0.8% in the first 6 h. In the next 8 h, the residual moisture changed only by 0.3%. For the 10 mg/ml BSA formulation, Karl Fischer measurements detected a steep decrease from 2.9% to 1.0% in residual moisture within the first 10 h of secondary drying, before the second phase was reached.

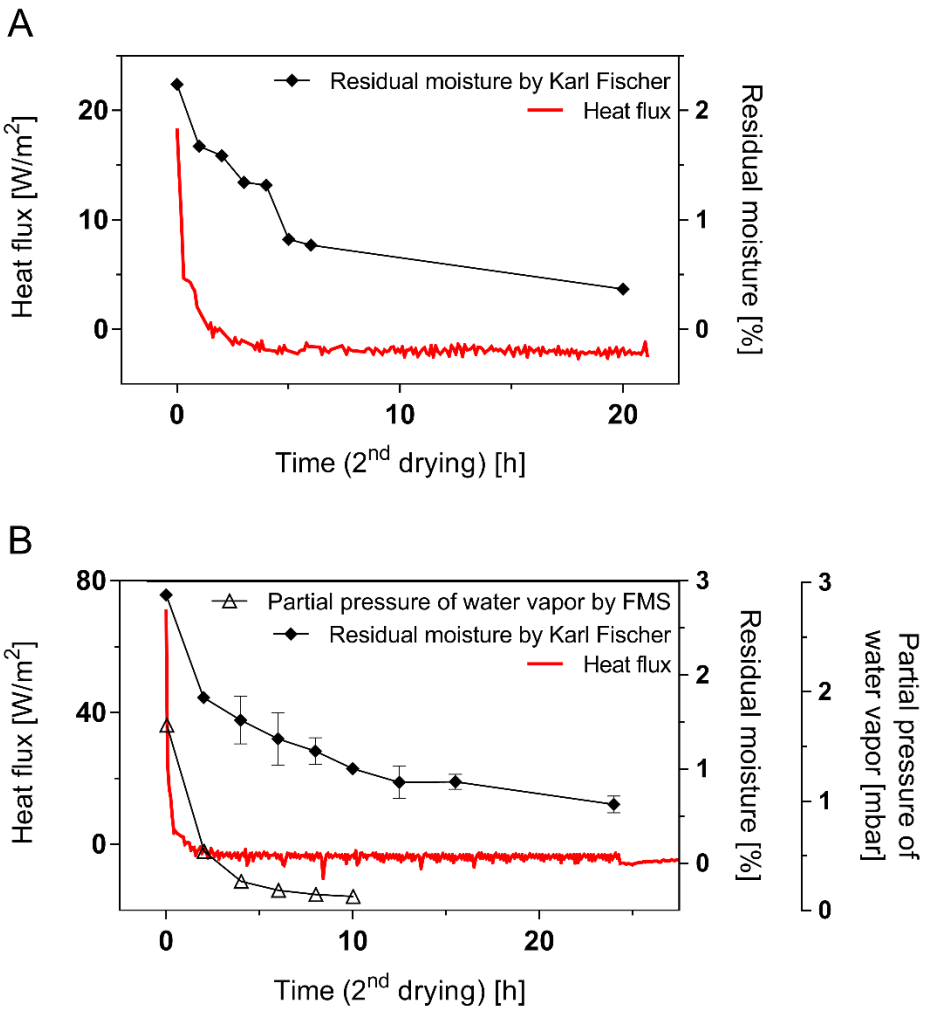

Figure V-6: (A) Heat flux of 5% sucrose solution (10R vials; 3 ml filling volume) measured during secondary drying, compared to residual moisture determined by Karl Fischer. (B) Heat flux of 10 mg/ml BSA formulation (10R vials; 3 ml filling volume) measured during secondary drying, compared to residual moisture determined by Karl Fischer and head space moisture analysis.

For the 10 mg/ml BSA formulation, additional headspace moisture measurements by FMS were performed. The partial pressure of water vapor in the vial head space, which corresponds to the headspace moisture decreased for the first 7 h of secondary drying before it reached a plateau at 0.15 mbar. Overall, it was not possible to reliably monitor the end of secondary drying by heat flux measurements, as the residual moisture still declined whereas heat flux has already reached a minimum level.

V.4.4 PRODUCT TEMPERATURE ESTIMATION BY LYOPAT

The aim of this experiment was to compare $T_{p,est}$ (based on $K_{v,user}$) with the product temperature determined by thermocouples (T_p(TC)). From the beginning until approximately 25 h of primary drying, $T_{p,est}$ and T_p(TC) are in good accordance (Figure V-7). Afterwards, T_p(TC) showed a steeper increase than $T_{p,est}$. The end of primary drying was indicated by both methods at 40.5 h.

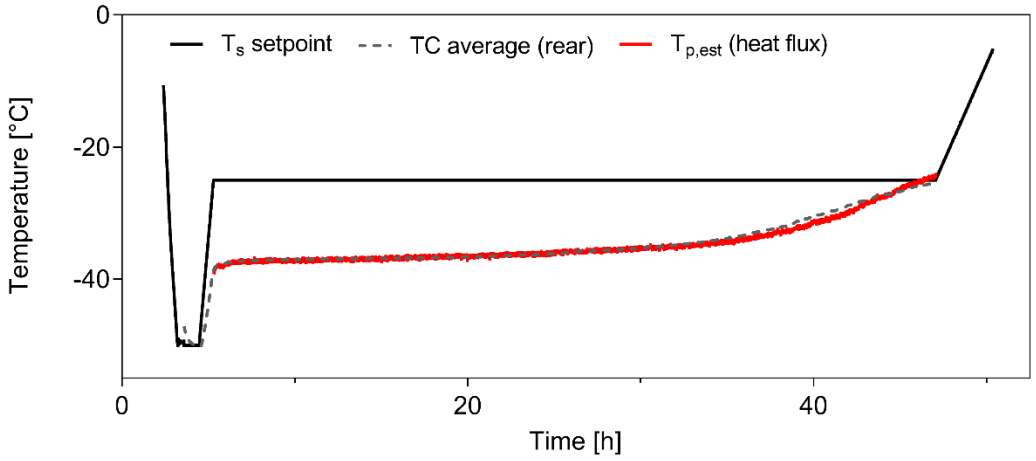

Figure V-7: Noninvasive T_p monitoring during primary drying based on heat flux measurements in comparison to T_p monitoring by TC readings of a 5% sucrose solution (10R vials; 3 ml filling volume).

V.5 DISCUSSION

V.5.1 ONE-VIAL PERFORMANCE CHECK

The one-vial performance check showed that for accurate and repeatable heat flux measurements a flat placement of the vials on and across the sensor´s edges is crucial (Figure V-1A). The scaffold around the actual 2nd generation sensor provided the necessary even stand for the vials to assure repeatable and accurate heat flux measurements.

Further, moisture between the sensor and the vials was found to strongly impact heat flux measurements, because the higher thermal conductivity of water, compared with air, results in higher heat flux values. T_p by TC is not affected by moisture between shelf and vial. Nevertheless, the moisture effect on heat flux measurements should be kept in mind when applied e.g. for freeze-drying cycles with loading on pre-cooled shelves, as the water condensing on the shelf during loading may lead to a higher heat flux value. However, under typical process conditions, the condensed water will have been sublimed by the time the process reaches the steady state of primary drying and the K_v determination would also be accurate in this case. During the performance check, we experienced that the mounting of the sensor was robust against manual cleaning with 70% isopropanol and water. Careful loading of vials to the shelf is required as the sharp borders of the tray could loosen the sensor. Robustness towards sterilization (e.g. steam or H_2O_2) was not investigated in this study. In addition, both sensors were able to measure the heat flux reliably and linearly over a range of ΔT from 20 to-50 °C, which is relevant for pharmaceutical freeze-drying processes.

V.5.2 PERFORMANCE CHECK UNDER PROCESS CONDITIONS

The 2nd generation sensor measured the heat flux repeatable and independent of the shelf filling degree. This is important as it enables process development with partially filled shelves, which, in turn, may reduce material and time.

During the application of heat flux measurements to different product concentrations, the sensor showed the expected decrease in heat flux as the higher product resistance (R_p) at higher product concentrations (i.e. higher solids content) leads to lower sublimation rates and therefore lower heat flux values [32]. The corresponding K_v values for the 5%, 10% and 20% sucrose solution were independent of the sucrose concentration and stayed constant during the pseudo-steady state of primary drying. The K_v value obtained for the 50% sucrose solution was remarkably lower. It can be assumed that this extremely high solids content caused a very low sublimation rate. Therefore, the heat supplied by the shelf and the heat needed for sublimation was not in balance, which results in a warming of the product. Consequently, no pseudo-steady state was reached, and Eq. 1 was not valid, which resulted in the deviation of the K_v value. An error in heat flux measurement could be excluded as the heat flux measured for the 50% sucrose solution met the linear correlation between measured heat flux and product concentration. Within the application of the sensor to different filling volumes, heat flux measurements also showed reliable results. Generally, a decrease in heat flux with increasing filling volume is expected, as the dry layer thickness directly correlates with the R_p [33]. As we compared the means over the first 6 h of primary drying, we assumed that no difference between the filling volumes will be obvious at this early stage of primary drying, which was confirmed by the experimental data (no statistically relevant difference) (Figure V-3B).

V.5.3 MONITORING OF A FREEZE-DRYING CYCLE BY HEAT FLUX MEASUREMENTS

The ability to detect the nucleation event of individual vials during the freezing step was comparable between heat flux measurements and TCs. Heat flux measurements provide further insights into freezing kinetics. At the moment of nucleation, the sensor showed an interrupted steep decrease in heat flux (Figure V-4). In the following phase of crystal growth and solidification, no information is provided by TCs, whereas heat flux measurements indicate the end of ice crystallization based on the end of latent heat production by a change in heat flux direction. The lack of the latent heat production causes the product temperature to approach the cooler shelf temperature, thus ΔT(Ts-Tp) decreases and finally, heat flux reaches 0, which determines the end of freezing. The heat flux progress of controlled nucleated samples differed markedly from the pattern of random nucleated samples. From the irregular pattern of the random nucleated samples, it could be concluded that the vials showed heterogeneous freezing kinetics. In contrast, with controlled nucleation all vials in contact with the sensor followed the same freezing kinetics. From the difference in pattern, one can also distinguish between controlled nucleation and random nucleation during freezing, additionally to the thermal information the sensor provides. Recent work of Wang et al. has shown that primary (ice nucleation) and secondary (water and solute) crystallization of a 5% NaCl solution was successfully detected by heat flux measurements [34].

In primary drying, the focus was to compare the sensor´s ability to detect the end of primary drying with TCs or comparative pressure measurement, respectively. The heat flux sensor data agreed with those obtained using TCs. With respect to batch representation, some consideration should be taken into account. For progress into the secondary drying step, it is critical that primary drying has finished for all vials. As the sensor monitors only a few vials, it is crucial to mount the sensor on the coldest spot of the freeze-dryer shelf, where the vials dry slowest. This is comparable to TCs. However, the sensor is non-invasive and therefore no influence of the sensor on freezing needs to be suspected. It would be recommended to use

more than one sensor to also monitor the warmest spot of the shelf to assure that T_c is not exceeded. Further, a larger sensor could help to improve batch representation of the endpoint detection. Comparative pressure measurement was found to still provide one of the easiest and safest method for a batch representative detection of the endpoint of primary drying. However, it lacks the ability to monitor the product temperature. In conclusion, heat flux measurements are a valuable tool to determine an average endpoint of primary drying, however, techniques that include the last few vials, such as comparative pressure measurement, should be preferred for monitoring the end of primary dying that drives the decision to progress into secondary drying.

During secondary drying, heat flux measurements could not detect the small amount of desorption heat and could not indicate the progress of drying as for example by monitoring the residual moisture content. The heat flux already levelled off, whereas the residual moisture determined by Karl Fischer or via headspace moisture further decreased (Figure V-6).

V.5.4 PRODUCT TEMPERATURE ESTIMATION

The possibility to directly measure the heat flux and thus K_v and from this calculate $T_{p,est}$, clearly distinguishes heat flux measurements from a simple temperature monitoring tool. To estimate the product temperature, K_v needs to be determined in a pre-cycle during the pseudo-steady state of primary drying (no need to fully complete the pre-cycle) using TCs to measure T_p. In this work, an overall good accordance between $T_{p,est}$ and T_p by TC was shown (Figure V-7). Towards the end of primary drying, a minor deviation between product temperatures determined by the different approaches was observed. This might be caused by several reasons. On the one hand, it is not possible to place a TC in the way that it has contact to the ice until the very last moment. The TC will lose the contact at some point, which results in an increase of the measured T_p. On the other hand, the $K_{v,user}$ is kept constant throughout the process to calculate $T_{p,est}$. However, it is known that the correlation between K_v and heat flux is only valid during pseudo-steady state (Eq.1). Towards the end of primary drying the pseudo-steady state is no longer given. Therefore, K_v would change, which is not considered in $T_{p,est}$ as the $K_{v,user}$ is pre-set for this experiment. With ΔT(Ts-Tp) approaching zero, the difference between $T_{p,\,est}$ and T_p(TC) levels off. The accuracy of the K_v determination by heat flux measurements was not investigated in this study. In previous work, the authors showed that due to the sensor´s position below the vials, the sensor does not detect all of the heat from radiation [31]. Further studies are ongoing to investigate these phenomena.

V.6 CONCLUSION

Our systematic evaluation proofed that heat flux measurements are a reliable and promising new tool suitable for freeze-drying process monitoring. Heat flux measurement is a non-invasive alternative to TCs, for monitoring selected vials. With the current set-up, the technique is not able to monitor a whole batch. As the sensors can be mounted tightly on the shelf, no manual handling is required that offers the potential for an application in production. The application of heat flux measurements is suitable for container systems that are in direct contact with the sensor surface, e.g. vials. One limitation is the usage of the technique for monitoring of secondary drying, because the small amount of desorption heat is below the limit of detection of the sensor. Overall, the direct measurement of the transferred heat, compared to the simple temperature measurement of thermocouples, enables to gain more insights in the freezing process and renews process development by using energy transfer as a control parameter.

V.7 REFERENCES

[1] Patel, S.M., Doen, T., and Pikal, M.J., *Determination of End Point of Primary Drying in Freeze-Drying Process Control.* AAPS PharmSciTech, 2010. 11(1): p. 73-84.

[2] Jameel, F. and Searles, J., *Development and Optimization of the Freeze-Drying Processes*, in *Formulation and Process Development Strategies for Manufacturing Biopharmaceuticals*. 2010, John Wiley & Sons, Inc. p. 763-796.10.1002/9780470595886.ch30.

[3] Presser, I., *Innovative online Messverfahren zur Optimierung von Gefriertrocknungsprozessen*. 2003, LMU Munich.

[4] Wiggenhorn, M., Presser, I., and Winter, G., *The current state of PAT in freeze-drying.* American Pharmaceutical Review, 2005. 8: p. 38-44.

[5] Roy, M.L. and Pikal, M.J., *Process Control in Freeze Drying: Determination of the End Point of Sublimation Drying by an Electronic Moisture Sensor.* PDA J. Pharm. Sci. Technol., 1989. 43(2): p. 60-66.

[6] Tang, X. and Pikal, M., *Design of Freeze-Drying Processes for Pharmaceuticals: Practical Advice.* Pharm. Res., 2004. 21(2): p. 191-200.

[7] Bosca, S., Barresi, A.A., and Fissore, D., *Use of a soft sensor for the fast estimation of dried cake resistance during a freeze-drying cycle.* Int. J. Pharm., 2013. 451(1-2): p. 23-33.

[8] Nail, S.L. and Johnson, W., *Methodology for in-process determination of residual water in freeze-dried products.* Dev. Biol. Stand., 1992. 74: p. 137-50; dicussion 150-1.

[9] Willemer, H., *Measurements of temperatures, ice evaporation rates and residual moisture contents in freeze-drying.* Dev. Biol. Stand., 1992. 74: p. 123-34; discussion 135-6.

[10] Neumann, M.K., *Steuerungsverfahren einer Gefriertrocknung und Vorrichtung zu seiner Ausfuehrung A control method of a freeze-drying and device for its execution*. 1958, Google Patents.

[11] Oetjen, G.W., et al., *Method for controlling a freeze drying process*. 2000, Google Patents.

[12] Milton, N., et al., *Evaluation of manometric temperature measurement as a method of monitoring product temperature during lyophilization.* PDA J. Pharm. Sci. Technol., 1997. 51(1): p. 7-16.

[13] Tang, X., Nail, S.L., and Pikal, M.J., *Evaluation of manometric temperature measurement, a process analytical technology tool for freeze-drying: part I, product temperature measurement.* AAPS PharmSciTech, 2006. 7(1): p. E14.

[14] Tang, X.C., Nail, S.L., and Pikal, M.J., *Freeze-drying process design by manometric temperature measurement: design of a smart freeze-dryer.* Pharm. Res., 2005. 22(4): p. 685-700.

[15] Tang, X.C., Nail, S.L., and Pikal, M.J., *Evaluation of manometric temperature measurement (MTM), a process analytical technology tool in freeze drying, part III: heat and mass transfer measurement.* AAPS PharmSciTech, 2006. 7(4): p. 97.

[16] Chouvenc, P., et al., *Optimization of the Freeze-Drying Cycle: A New Model for Pressure Rise Analysis.* Drying Technology, 2004. 22(7): p. 1577-1601.

[17] Velardi, S.A., Rasetto, V., and Barresi, A.A., *Dynamic Parameters Estimation Method: Advanced Manometric Temperature Measurement Approach for Freeze-Drying Monitoring of Pharmaceutical Solutions.* Ind. Eng. Chem. Res., 2008. 47(21): p. 8445-8457.

[18] Fissore, D., Pisano, R., and Barresi, A.A., *On the Methods Based on the Pressure Rise Test for Monitoring a Freeze-Drying Process.* Drying Technology, 2010. 29(1): p. 73-90.

[19] Bosca, S., Barresi, A.A., and Fissore, D., *Use of soft sensors to monitor a pharmaceuticals freeze-drying process in vials.* Pharm. Dev. Technol., 2014. 19(2): p. 148-59.

[20] Jennings, T.A., *Residual gas analysis and vacuum freeze drying.* J. Parenter. Drug Assoc., 1980. 34(1): p. 62-9.
[21] Connelly, J.P. and Welch, J.V., *Monitor lyophilization with mass spectrometer gas analysis.* J. Parenter. Sci. Technol., 1993. 47(2): p. 70-5.
[22] Kasper, J.C., et al., *Implementation and evaluation of an optical fiber system as novel process monitoring tool during lyophilization*, in *Eur. J. Pharm. Biopharm.* 2013. p. 449-459.
[23] Gieseler, H., et al., *Evaluation of tunable diode laser absorption spectroscopy for in-process water vapor mass flux measurements during freeze drying.* J. Pharm. Sci., 2007. 96(7): p. 1776-93.
[24] Schneid, S.C., et al., *Non-invasive product temperature determination during primary drying using tunable diode laser absorption spectroscopy.* J. Pharm. Sci., 2009. 98(9): p. 3406-18.
[25] Kuu, W.Y., et al., *Product mass transfer resistance directly determined during freeze-drying cycle runs using tunable diode laser absorption spectroscopy (TDLAS) and pore diffusion model.* Pharm. Dev. Technol., 2010. 16(4): p. 343-357.
[26] Rey, L. and May, J.C., *Freeze Drying/Lyophilization of Pharmaceutical and Biological Products*. 3rd ed. Vol. 206. 2010, London, UK: Informa Healthcare.
[27] Bardat, A., et al., *Moisture measurement: a new method for monitoring freeze-drying cycles.* J. Parenter. Sci. Technol., 1993. 47(6): p. 293-9.
[28] RdF Corporation. *Simplified Heat Flow Measurement*. 2003 [cited October 8th, 2014]; Available from: http://www.rdfcorp.com/anotes/pa-hfs/pa-hfs_pf.html.
[29] Thompson, T.N. and Millrock Technology Inc., *LyoPAT(TM): real-time monitoring and control of the freezing and primary drying stages during freeze-drying for improved product quality and reduced cycle times.* American Pharmaceutical Review, 2013. 2013.
[30] Pikal, M.J., Roy, M.L., and Shah, S., *Mass and heat transfer in vial freeze-drying of pharmaceuticals: Role of the vial.* J. Pharm. Sci., 1984. 73(9): p. 1224--1237.
[31] Konrad, I., et al. *Determination of mass transfer (dm) and vial heat transfer coefficients (Kv) by heat flux measurements during freeze drying.* in *AAPS Annual Meeting and Exposition*. 2015. Orlando, Fla.
[32] Pikal, M.J., *Use of laboratory data in freeze drying process design: heat and mass transfer coefficients and the computer simulation of freeze drying.* J. Parenter. Sci. Technol., 1985. 39(3): p. 115--39.
[33] Johnson, R.E., et al., *Use of manometric temperature measurements (MTM) to characterize the freeze-drying behavior of amorphous protein formulations.* J. Pharm. Sci., 2010. 99(6): p. 2863-73.
[34] Wang, Q., et al., *Monitoring secondary (solute+water) crystallization by DSC, synchrotron X-ray diffraction, and in vials using heat flux transducer*. 2016: Breckenridge.

CHAPTER VI

VI. FINAL SUMMARY AND OUTLOOK

The goal of product development is, besides developing a stable formulation, to establish robust manufacturing processes to consistently produce high quality products. With the FDA`s cGMP initiative and the introduction of QbD, researchers focused on a thorough process understanding and control. This also includes the development of PAT tools to ensure process monitoring during production or to improve process understanding. In this context, two innovative technologies, controlled nucleation and heat flux measurement, gained interest in the field of freeze-drying. The aim of this thesis was to evaluate, in case of controlled nucleation, its potential to improve product quality, process control, and efficiency, and in case of heat flux measurements, its potential as a new PAT tool.

A general introduction into the principles of QbD and the investigated techniques, CN and heat flux measurements is provided in **Chapter I**.

The objective of **Chapter II** was to evaluate the combination of controlled nucleation with aggressive primary drying for highly concentrated protein formulations and the effect of this combination on product properties. By this combination, CN and an aggressive lyo cycle PD time was drastically reduced, independent of the application of CN. Product characteristics, such as cake appearance, morphology, pore size, SSA and RM were comparable between conservative and aggressive PD lyo cycles. Furthermore, the positive effect of CN on reconstitution time reduction was detected after conservative and aggressive PD lyo cycles. Thus, this positive effect of CN on reconstitution time is a robust observation and does not depend on the drying protocol.

In **Chapter III**, the main objective of this thesis, the potential of CN for improving other product quality attributes, such as the physico-chemical stability of protein therapeutics, was evaluated. The performed stability studies exhibited that CN did neither have a positive nor a negative effect on mAb stability compared to RN. Besides that, it was observed that the applied CN protocol and not only T_N determined the SSA of the final product. Furthermore, it was demonstrated that polysorbate promotes the crystallization of sucrose in lyophilized products stored at elevated temperatures.

In **Chapter IV**, two key challenges for the practical application of CN were addressed: First, how to monitor if CN was successfully performed in all vials of a batch and second, if it is necessary to apply the same CN method in development and production scale. Additionally, based on the conclusions of Chapter III, impact factors, such as nucleation protocol, T_N, formulation composition or protein concentration, on the SSA of the final product were assessed. Regarding the first challenge, frequency modulated spectroscopy (FMS) was successfully evaluated as a monitoring tool to non-destructively measure nucleation success on a high-throughput basis. As FMS enables to determine the partial pressure of water vapor as a surrogate for residual moisture, the measured data was used to assess inter-vial batch homogeneity during freeze-drying (the freeze-drying process was stopped shortly after primary drying) and of the final product. Hereby, an improved inter-vial batch homogeneity after primary drying for CN samples was detected, but these advantages in homogeneity were no longer present in the final product. The fact that CN improved batch homogeneity during primary drying supports the hypothesis that CN could facilitate scale-up, however, this was not investigated within this work and has not yet been studied. In context of the question, if it is necessary to apply the same CN method within the different scales, it was shown that three ice fog CN methods, VERISEQ® system, FreezeBooster® and Geidobler et al., resulted in similar product quality attributes with only minor differences in RM of the lyophilized product. In conclusion, applying different ice fog CN methods in development and production scale would most likely not change the product properties much. Finally, the observations of Chapter III that T_N is not the only determining factor for ice morphology (and consequently SSA) were confirmed. Besides T_N, the fact whether a CN method or a random freezing protocol was applied and the used formulation (sugar) impacted the SSA. Consequently, for practical application, it should be considered that a higher T_N does not necessarily lead to additional primary drying time reduction but poses a higher risk for not-controlled nucleated products compared to a T_N that safely assures 100% controlled nucleation of the product vials.

Chapter V represents the second part of this thesis and provides the evaluation of heat flux measurements as a new PAT tool to improve monitoring and process understanding of freeze-drying cycles. Compared to state-of-the art thermocouples, heat flux measurements are non-invasive and easier in handling. Furthermore, they provide additional information, which can be used to calculate critical process parameters. However, heat flux measurements are not a batch representative technique and the fact that they are only suitable for container systems being in direct contact with the sensor surface, e.g. vials, poses a limitation. Moreover, the technique was not suitable for monitoring secondary drying, because the small amount of desorption heat is below the limit of detection of the sensor. Overall, the direct measurement of the transferred heat improves process development by using energy transfer as a control parameter. From the study presented in Chapter V, it was concluded that heat flux measurements are a reliable and promising monitoring tool for freeze-drying processes.

When putting the findings of this thesis into the context of QbD, CN could not enhance QbD approaches for freeze-drying in all aspects. The principles of QbD comprise the improvement of product quality or assurance of product quality by controlled and robust processes. This thesis showed that CN did not directly improve product quality with respect to mAb stability or inter-vial batch homogeneity of the final product. Solely, for special products, it was shown to shorten reconstitution times. However, the improved inter-vial batch homogeneity during primary drying and the robustness of the techniques, shown by the fact that different ice fog CN methods resulted in comparable product quality attributes, could supports CN`s suitability for the QbD concept.

Additionally, heat flux measurements, which were shown to be a valuable PAT tool, could support QbD approaches for freeze-drying. Besides monitoring of critical endpoints, e.g. freezing or primary drying, heat flux measurements provide critical process parameters. The creation of a design space for a freeze-drying product by the application of heat flux measurements would be of great interest to further integrate the cGMP initiative into freeze-dried products and thus, should be investigated further. Overall, it should be considered that the

complexity of the freeze-drying process reveals that a single tool would not be able to control and monitor all aspects of this multi-step process. By combining e.g. CN with heat flux measurements and thermocouple readings, or TDLAS, it would be possible to develop, control and transfer robust freeze-drying processes that assure product quality at every stage of development.

CHAPTER VII

VII. Addendum

VII.1 LIST OF ABBREVIATIONS

BET	Brunauer, Emmett and Teller Theory
BRT	Barometric temperature measurement
BSA	Bovine serum albumin
BTM	Barometric temperature measurement
CMC	Critical micelle concentration
CN	Controlled nucleation
DLS	Dynamic light scattering
DPE	Dynamic parameters estimation
DSC	Differential scanning calorimetry
FDM	Freeze-drying microscopy
FMS	Frequency modulated spectroscopy
HMW	High(er) molecular weight species
HP-SEC	High performance size exclusion chromatography
KF	Karl Fischer titration
K_v	vial heat transfer coefficient
$K_{v,user}$	vial heat transfer coefficient as user input
LC	Lyo cycle
LDH	Lactate dehydrogenase
mAb	Monoclonal antibody
MFI	Micro-Flow Imaging
MS	Mass spectrometry
MTM	Manometric temperature measurement
OFS	Optical fiber system
PAT	Process analytical technology
p_c	Chamber pressure
PD	Primary drying
PDI	Polydispersity index
PES	Polyethersulfone membrane
PRA	Pressure rise analysis
PRT	Pressure rise test
PS	Polysorbate
PVDF	Polyvinylidenfluorid membrane

R2	Correlation coefficient
RM	Residual moisture
RN	Random nucleation
R_p	Product resistance
RSD	Relative standard deviation
RTD	Resistance temperature detectors
SDS	Sodium dodecyl sulfate polyacrylamide gel electrophoresis
SD	Secondary drying
SEM	Scanning electron microscopy
SSA	Specific surface area
STD	Standard deviation
TC	Thermocouples
TDLAS	Tunable diode laser absorption spectroscopy
TFF	Tangential flow filtration
T_g	Glass transition temperature of the lyophilized product
$T_g`$	Glass transition temperature of the frozen product
T_N	(Ice) nucleation temperature
T_p	Product temperature
$T_{p,est}$	Estimated product temperature
T_s	Shelf temperature
XRD	X-ray powder diffraction

VII.2 LIST OF FIGURES

VII.3 LIST OF TABLES

VII.4 PRESENTATIONS AND PUBLICATIONS

VII.4.1 PUBLICATIONS

Vollrath, I., Friess, W., Freitag, A., Hawe, A., Winter, G.,
Comparison of ice fog methods and monitoring of controlled nucleation success after freeze-drying. Manuscript submitted to the International Journal of Pharmaceutics, 2018.

Vollrath, I., Friess, W., Freitag, A., Hawe, A., Winter, G.,
Does controlled nucleation impact the properties and stability of lyophilized monoclonal antibody formulations? European Journal of Pharmaceutics and Biopharmaceutics, 2018. 129: p. 134-144.

Vollrath, I., Pauli, V., Friess, W., Freitag, A., Hawe, A., Winter, G.,
*Evaluation of Heat Flux Measurement as a New Process Analytical Technology Monitoring Tool in Freeze Drying***.** Journal of Pharmaceutical Sciences, 2017. 106(5): p. 1249-1257.

Geidobler*, R., Konrad*, I., Winter, G.,
Can controlled ice nucleation improve freeze-drying of highly-concentrated protein formulations? Journal of Pharmaceutical Sciences, 2013. 102(11): p. 3915-9.
*these authors contributed equally to this work

VII.4.2 ORAL PRESENTATIONS

Vollrath I.,

Innovative techniques for lyophilization – Controlled nucleation and heat flux measurements.
2nd Annual Pharmaceutical Lyophilisation Summit, 2018, Vienna, Austria

Konrad I., Pauli V., Friess W., Freitag A., Hawe A., Winter G.,

Heat flux measurements as a new PAT tool in freeze drying.
CHI´s 15th Annual Peptalk, 2016, San Diego, CA, USA

Konrad I., Geidobler G., Freitag A., Friess W., Hawe A., Winter G.,

A critical eye on controlled nucleation during Lyophilization.
7th International Congress on Pharmaceutical Engineering (ICPE), 2014, Graz, Austria

Konrad I., Geidobler G., Freitag A., Friess W., Hawe A., Winter G.,

Controlled ice nucleation followed by aggressive primary drying during lyophilization of highly concentrated protein formulations.
9th PBP World Meeting, 2014, Lisbon, Portugal

VII.4.3 POSTER PRESENTATIONS

Konrad I., Pauli V., Benz L., Friess W., Hawe A., Freitag A., Winter G.,
Determination of mass transfer (dm) and vial heat transfer coefficients (Kv) by heat flux measurements during freeze drying.
AAPS Annual Meeting and Exposition, 2015, Orlando, FL, USA.

Konrad I., Pauli V., Benz L., Friess W., Hawe A., Freitag A., Winter G.,
Heat flux measurements as a new PAT Tool in freeze drying.
AAPS Annual Meeting and Exposition, 2015, Orlando, FL, USA.

Konrad I., Geidobler G., Winter G.,
The impact of Controlled Nucleation on Freeze Drying of Highly Concentrated Protein Formulations.
Freeze Drying of Pharmaceuticals and Biologicals, 2014, Garmisch-Partenkirchen, Germany.

Konrad I., Geidobler G., Freitag A., Bosch T., Friess W., Hawe A., Winter G.,

Controlled Nucleation Combined with Aggressive Primary Drying during Lyophilization of Highly Concentrated Protein Formulations.
Freeze Drying of Pharmaceuticals and Biologicals, 2014, Garmisch-Partenkirchen, Germany.

Konrad I., Geidobler G., Freitag A., Bosch T., Friess W., Hawe A., Winter G.,

Controlled ice nucleation followed by aggressive primary drying during lyophilization of highly concentrated protein formulations.
National Biotechnology Conference (NBC), 2014, San Diego, CA, USA.

Konrad I., Geidobler G., Wiggenhorn M., Bosch T., Hawe A., Winter G.,
Controlled ice nucleation for freeze-drying – Just fashion or real progress?
AAPS Annual Meeting and Exposition, 2013, San Antonio, TX, USA**.**

CHAPTER VIII

VIII. APPENDIX

VIII.1 SUPPLEMENTARY MATERIAL FOR CHAPTER II

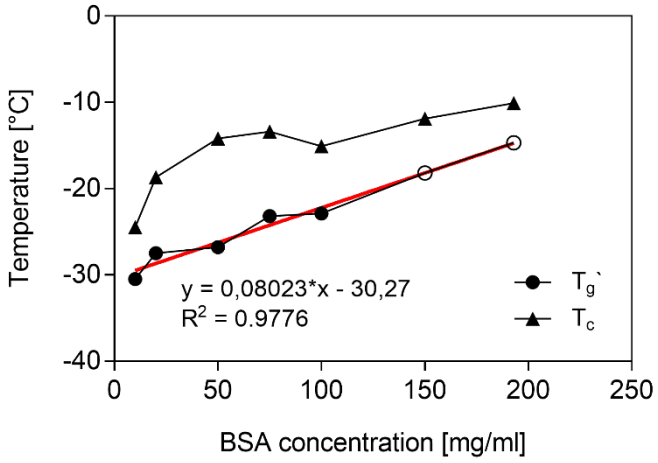

Figure VIII-1: T_c and $T_g`$ values of the different BSA concentrations. Extrapolated $T_g`$ values for 150 mg/ml and 200 mg/ml BSA are indicated by open circles.

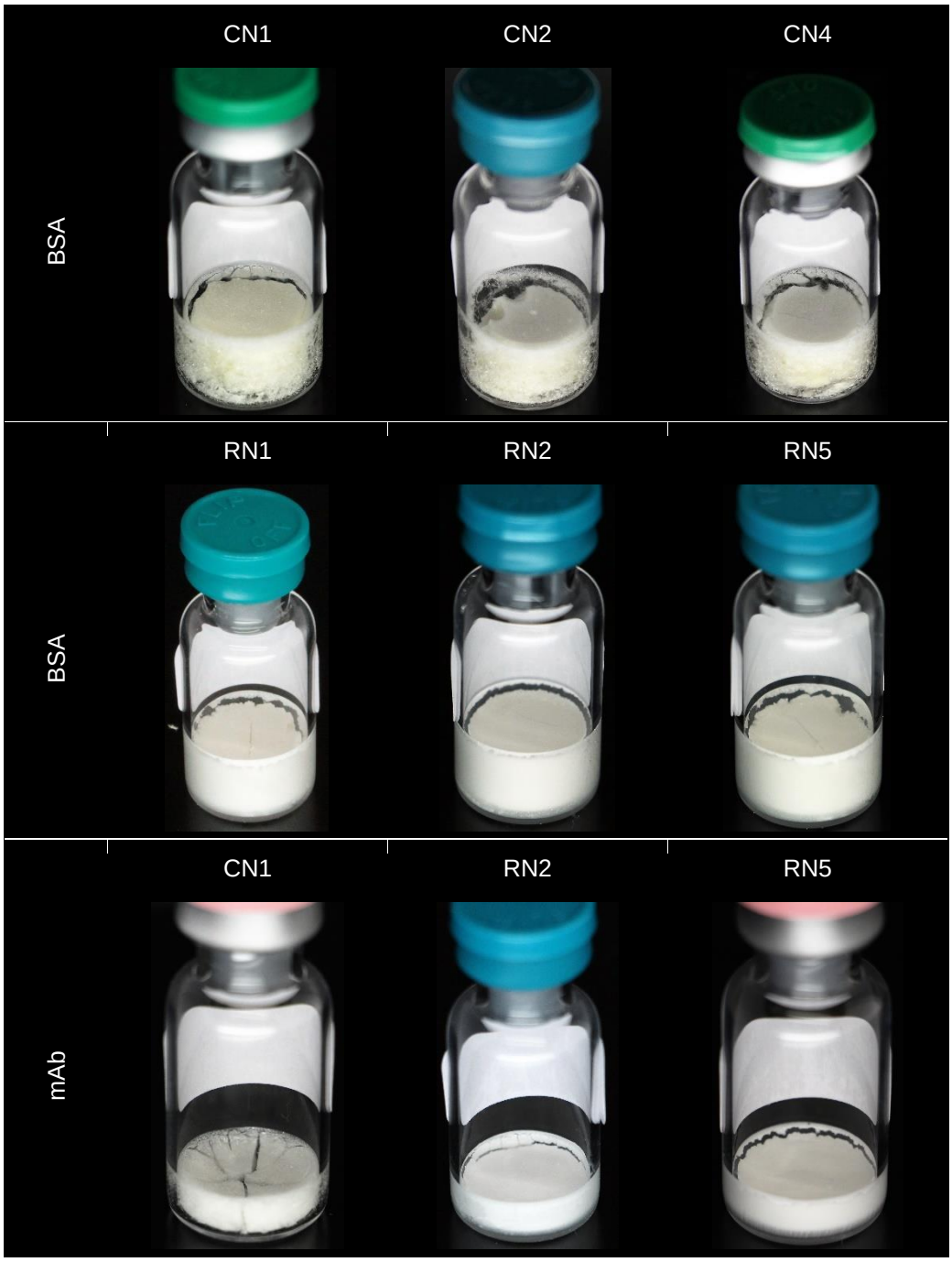

Figure VIII-2: Examples of photographs of BSA and mAb lyophilizates processed by different lyo cycles.

VIII.2 SUPPLEMENTARY MATERIAL FOR CHAPTER III

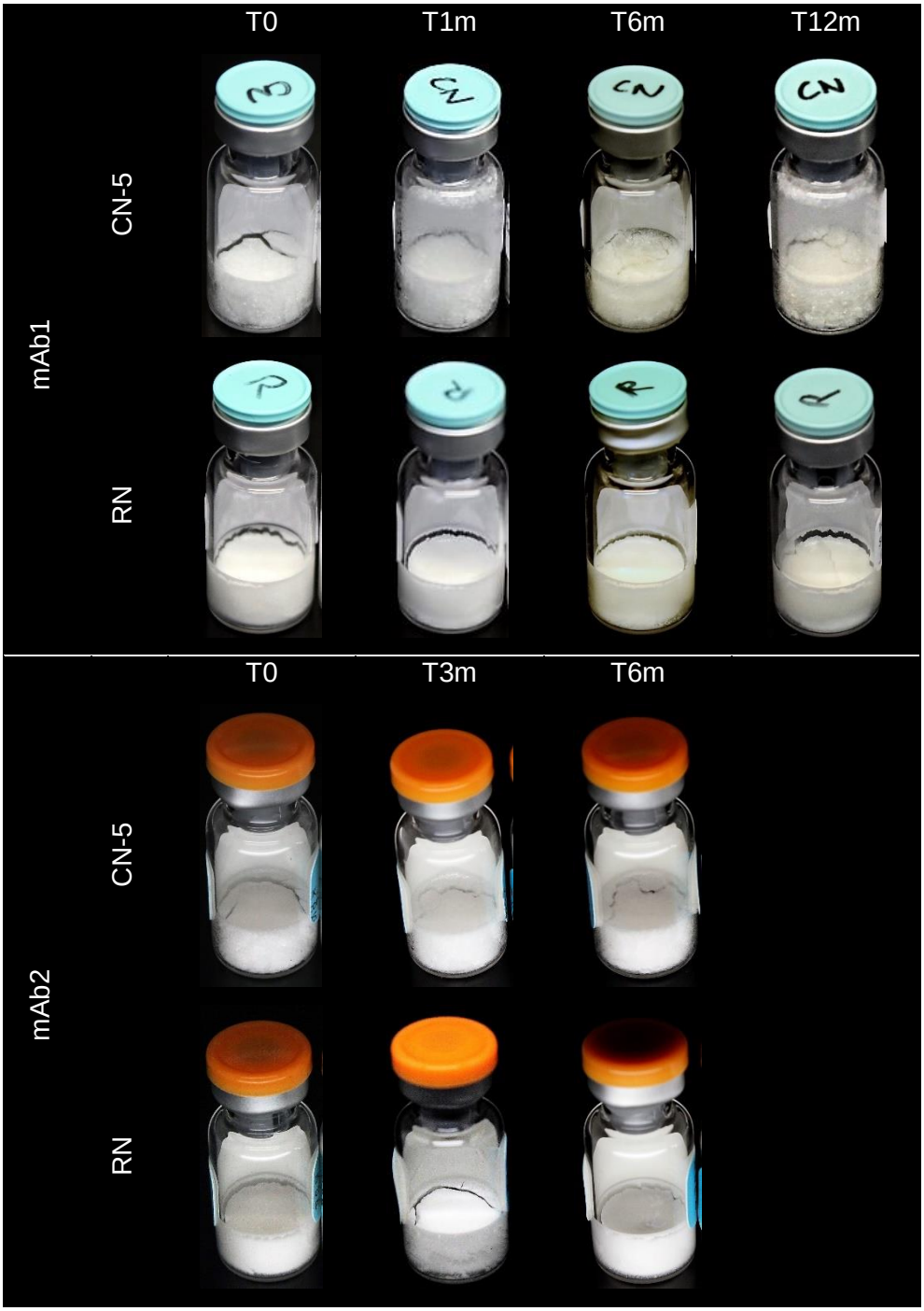

Figure VIII-3: Photographs of mAb1 and mAb2 lyophilizates taken at all time points of the high concentration study (storage at 40 °C/75% r.H.).

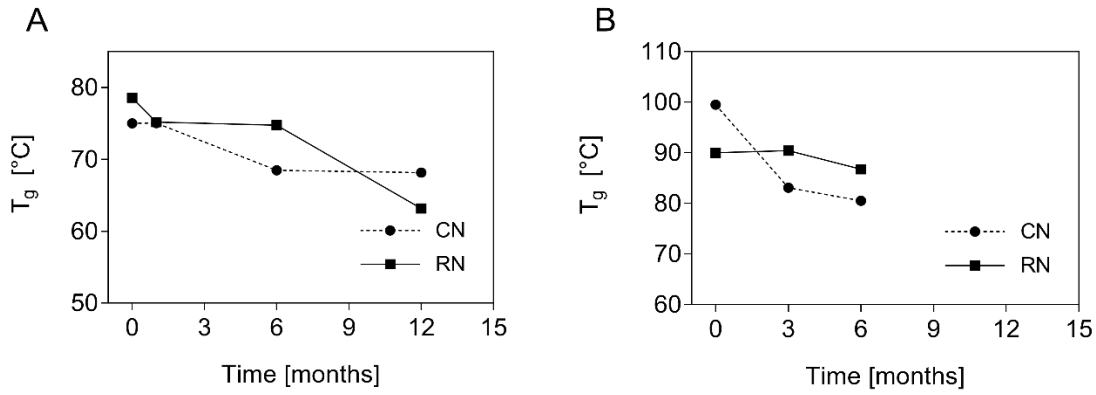

Figure VIII-4: T_g over storage time for (A) mAb1 and (B) mAb2 of the high concentration study.

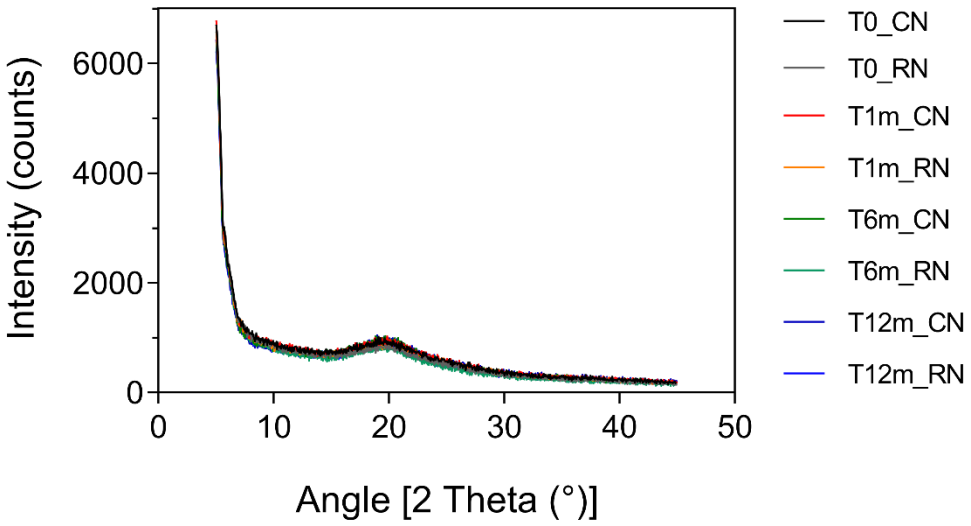

Figure VIII-5: Overlay of XRD-refractograms of mAb1 CN and mAb1 RN samples at all timepoints.

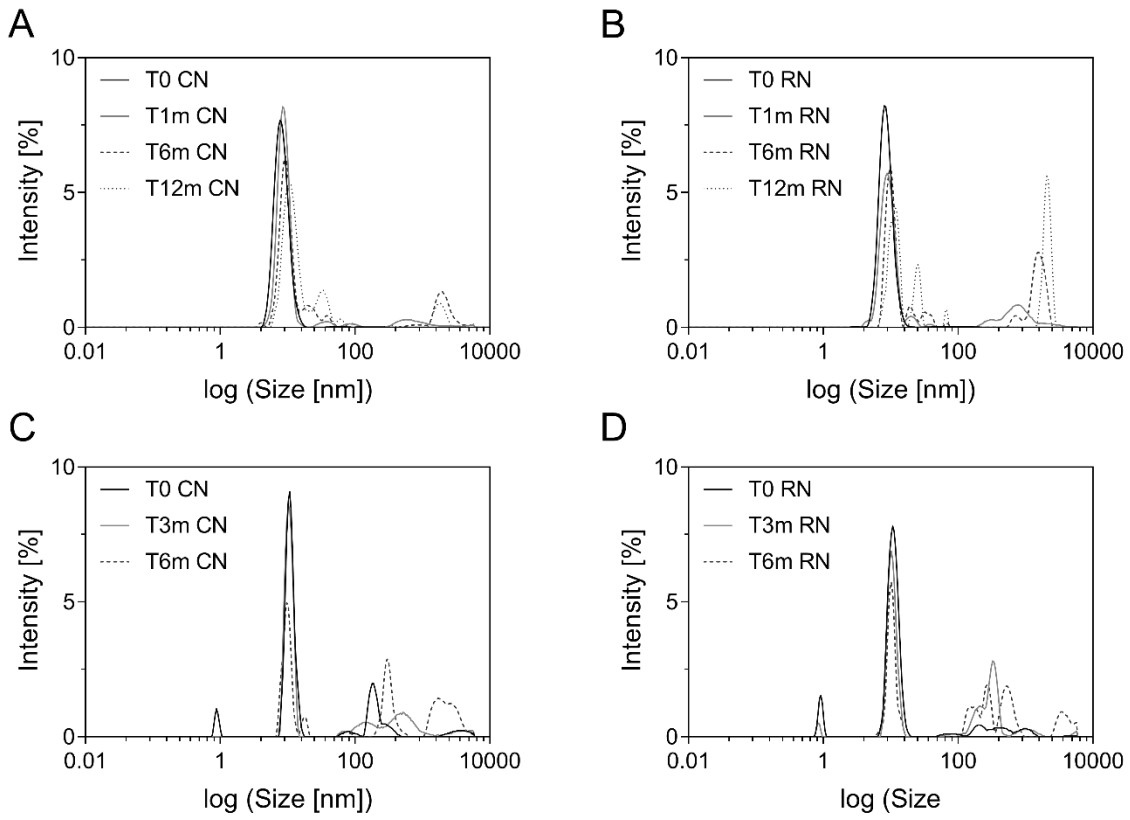

Figure VIII-6: Size distribution based on intensity detection of the high concentration study. (A) mAb1 CN, (B) mAb1 RN, (C) mAb2 CN and (D) mAb2 RN.

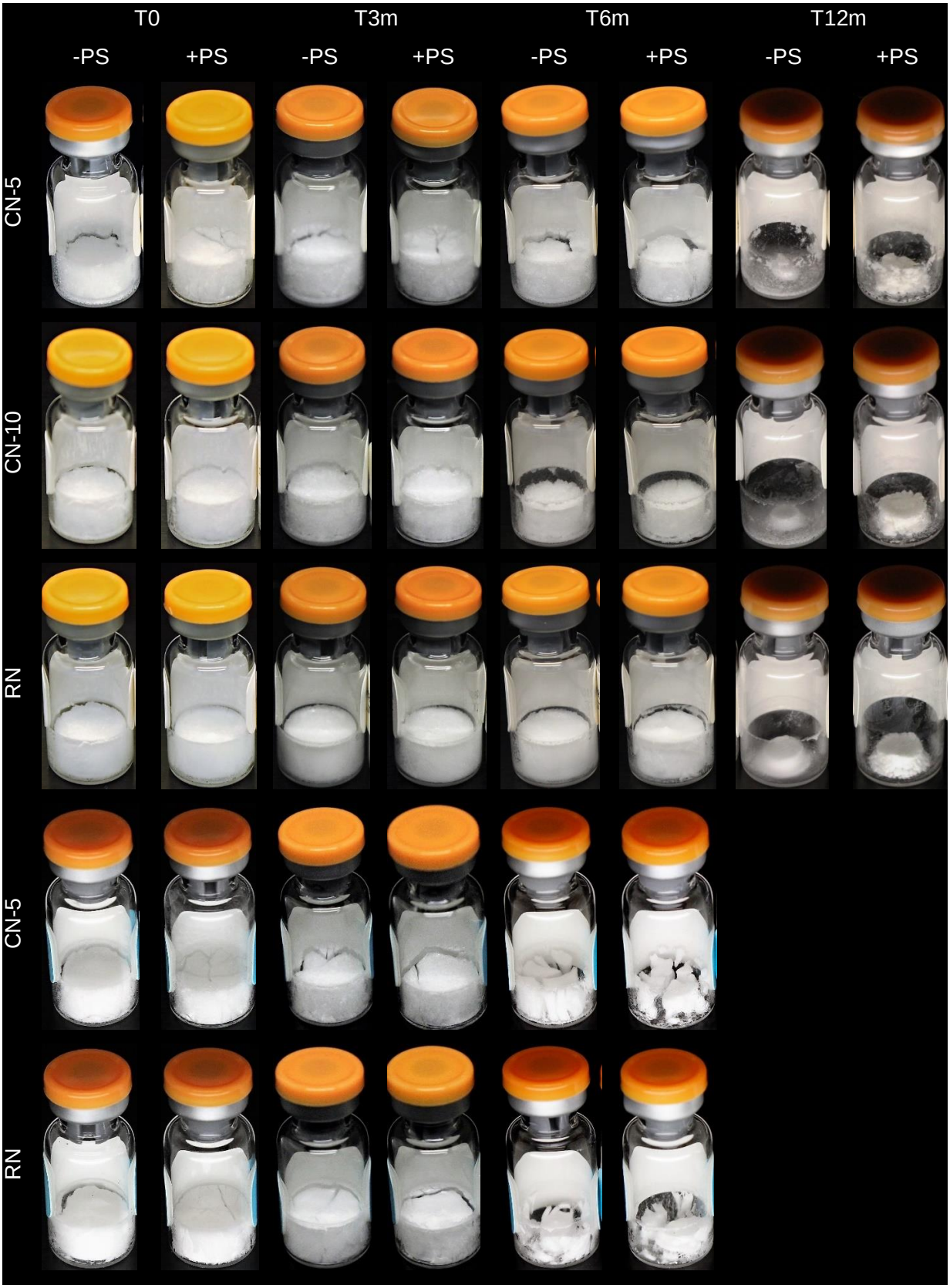

Figure VIII-7: Photographs of mab1 and mab2 lyophilizates taken at all time points of the low concentration study (storage at 40 °C/75% r.H.).

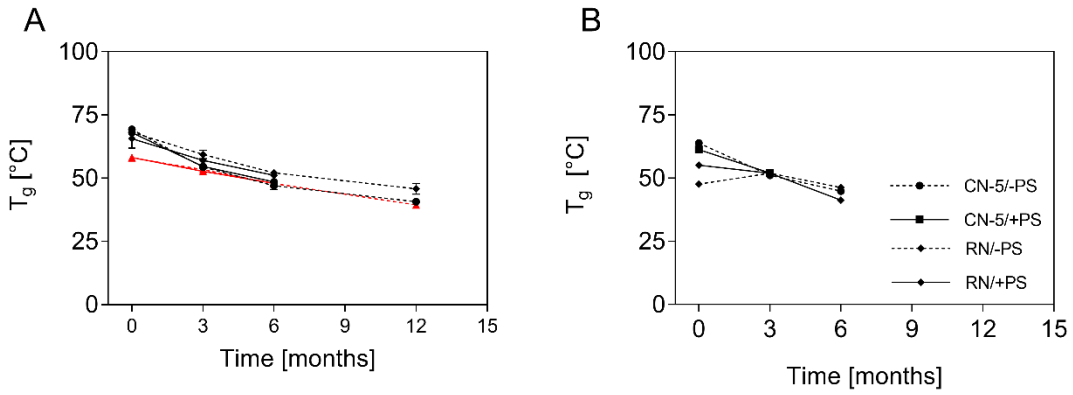

Figure VIII-8: T_g over storage time for (A) mAb1 and (B) mAb2 of the low concentration study.

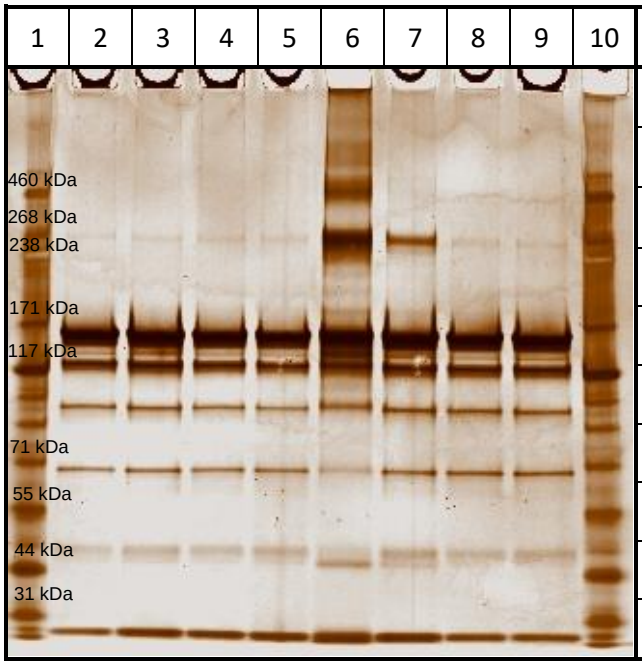

No.	Sample name
1	MW Marker
2	T3m_CN_PS
3	T3m_RN_PS
4	T3m_CN
5	T3m_RN
6	T7m_CN_PS
7	T7m_RN_PS
8	T7m_CN
9	T7m_RN
10	MW Marker

Figure VIII-9: SDS-page under non-reducing conditions of mAb2 T3m and T7m samples.

No.	Sample name
1	MW Marker
2	T3m_CN_PS
3	T3m_RN_PS
4	T3m_CN
5	T3m_RN
6	T7m_CN_PS
7	T7m_RN_PS
8	T7m_CN
9	T7m_RN
10	MW Marker

Figure VIII-10: SDS-page under reducing conditions of mAb2 T3m and T7m samples.

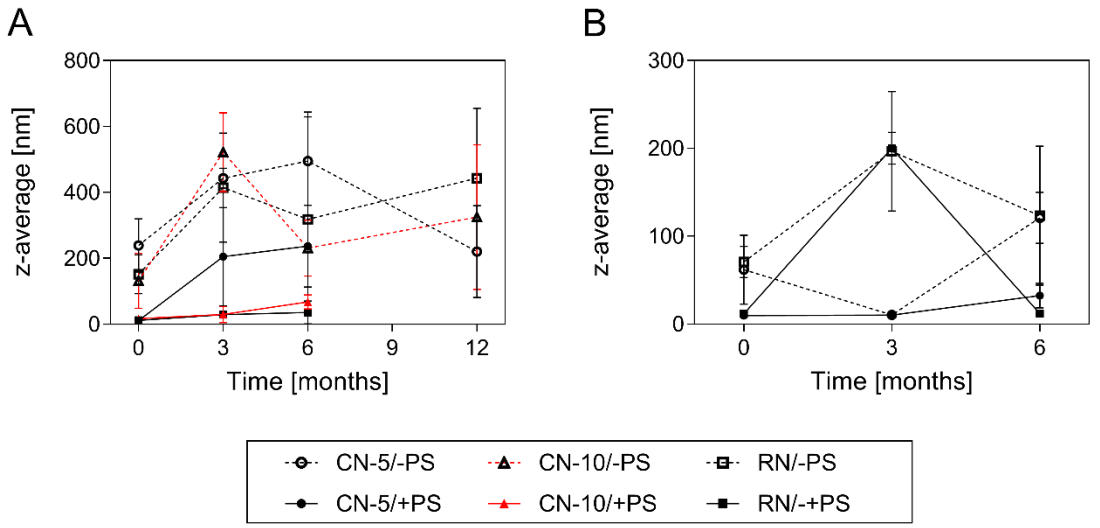

Figure VIII-11: z-average of CN and RN samples of (A) mAb1 and (B) mAb2 low concentration study over storage time.

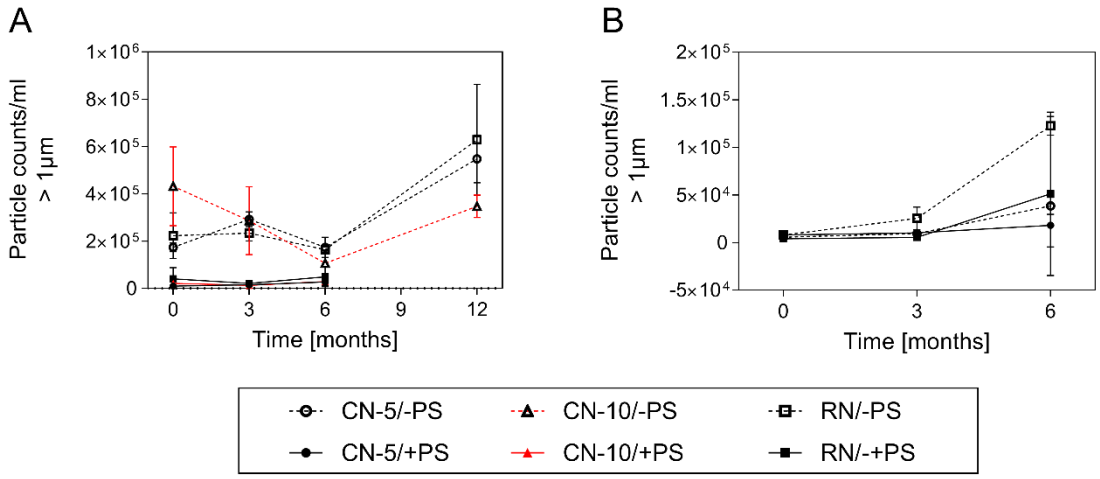

Figure VIII-12: Cumulative particle counts of particles larger 1 µm for (A) mAb1 low concentration and (B) mAb2 low concentration over storage time.

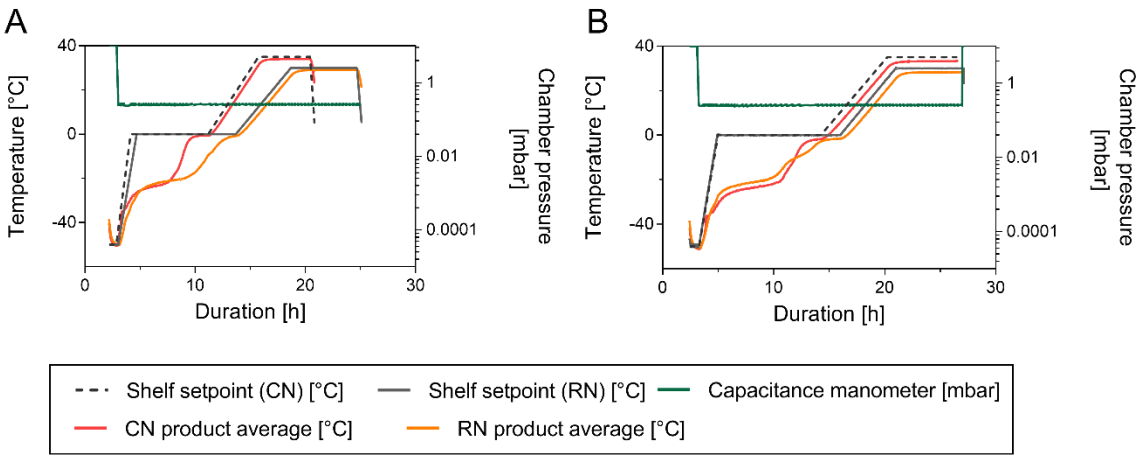

Figure VIII-13: Freeze-drying process documentation: Shelf setpoint, product temperature and pressure traces over process duration. (A) mAb1 high concentration study CN and RN process. (B) mAb2 high concentration study CN and RN process.

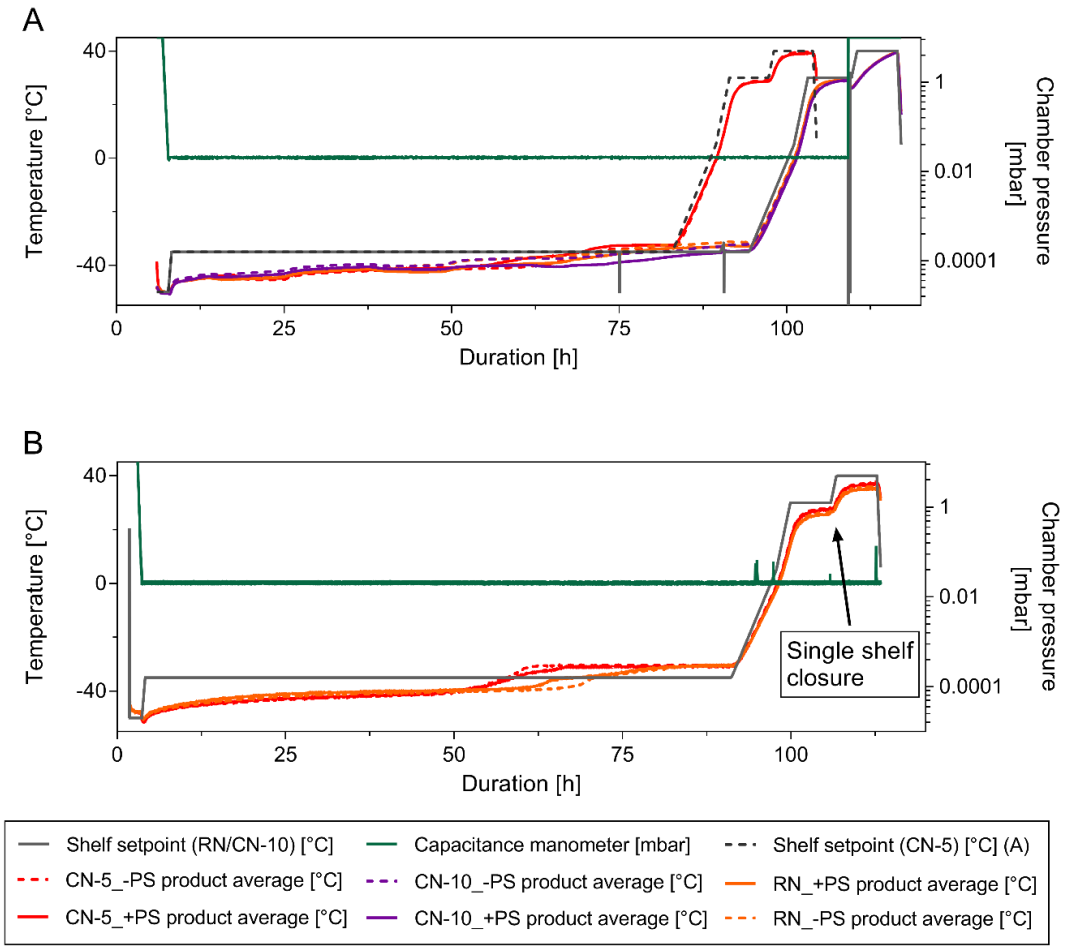

Figure VIII-14: Shelf temperature setpoint, product temperature and chamber pressure traces of low concentration study CN and RN process for (A) mAb1 and (B) mAb2.

Table VIII-1: Overview of primary drying duration in hours of all studies and processes. The time when the shelf temperature reached the set primary drying temperature until the thermocouples indicated the end of primary drying, was considered as primary drying duration.

	Duration primary drying in [h]					
Study	CN-5 -PS	CN-5 +PS	CN-10 -PS	CN-10 +PS	RN -PS	RN +PS
mAb1 high conc	6.8	---	---	---	9.4	---
mAb2 high conc	---	10.0	---	---	---	11.7
mAb1 low conc	61.8	59.1	66.0	77.7	61.5	65.9
mAb2 low conc	52.7	53.5	---	---	60.4	65.7

VIII.3 SUPPLEMENTARY MATERIAL FOR CHAPTER IV

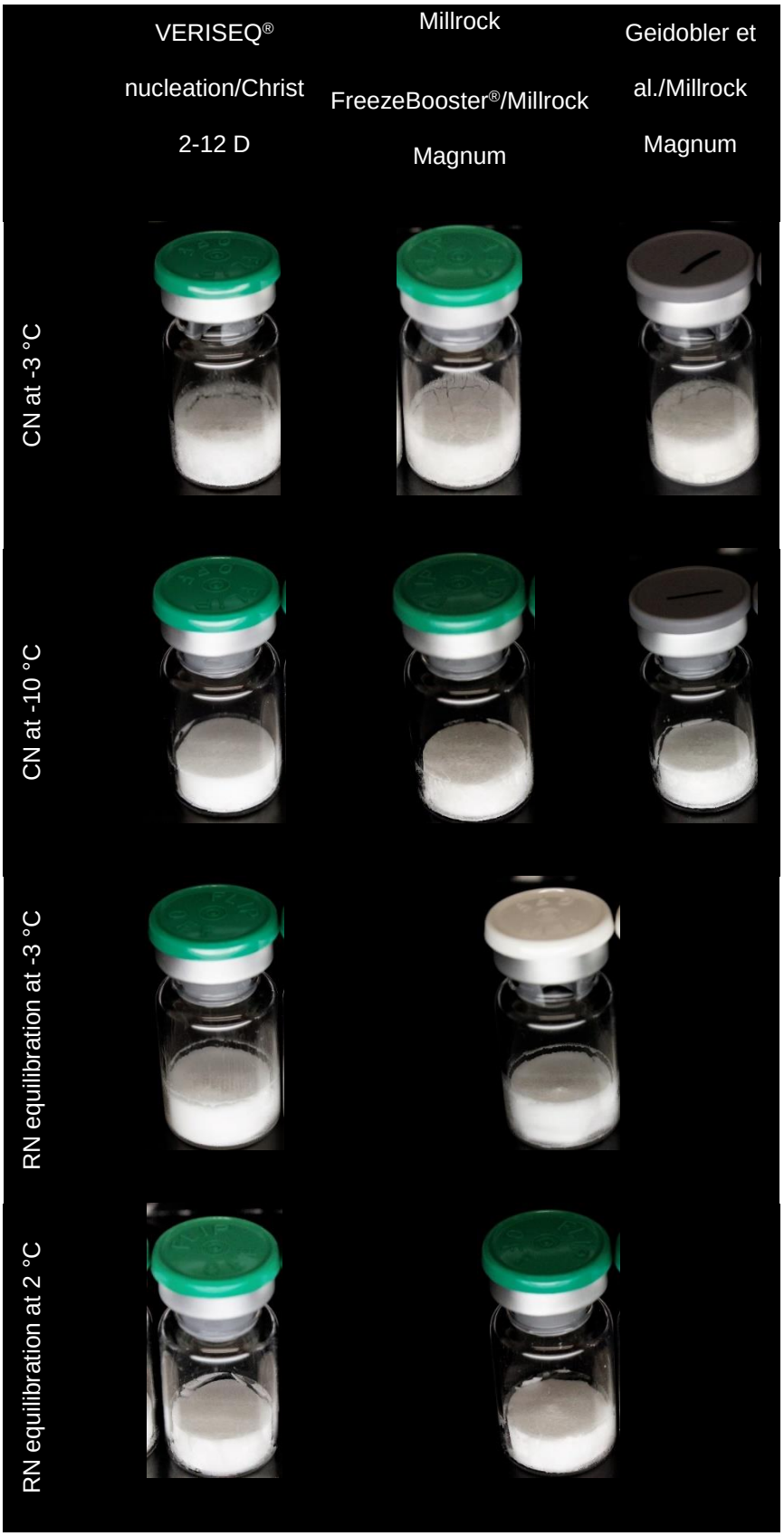

Figure VIII-15: Optical evaluation of all freeze-drying runs of the sucrose formulation

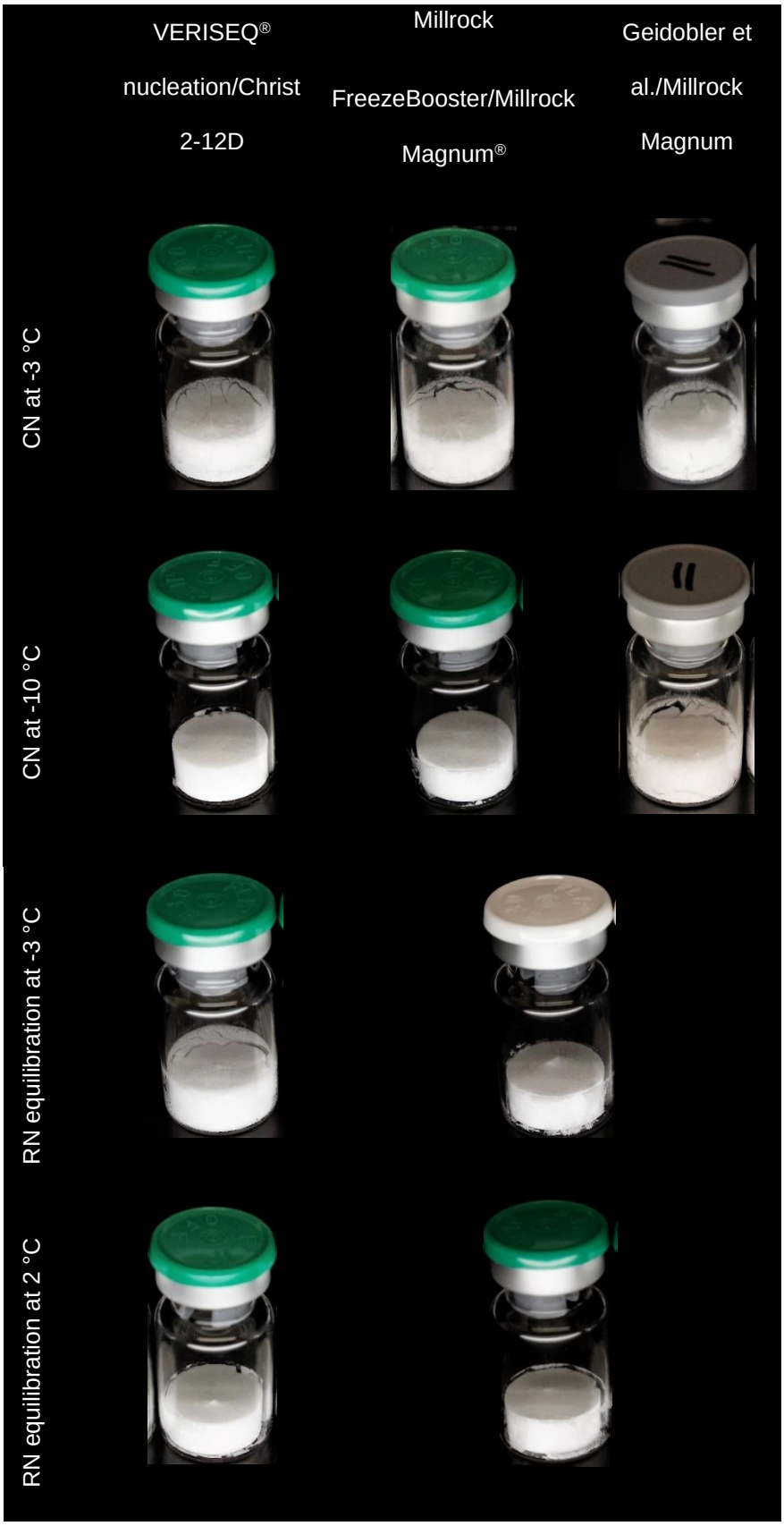

Figure VIII-16: Optical evaluation of all freeze-drying runs of the trehalose formulation.